Reduced Navigation Data:

Optimizing the Galileo I/NAV Navigation Message for a Fast First Fix

Master thesis- S.H. Lamers

TU Delft

Reduced Navigation Data:
Optimizing the Galileo I/NAV Navigation Message for a Fast First Fix

Master thesis

by

S.H. Lamers

to obtain the degree of Master of Science
at Delft University of Technology,
to be defended publicly on Friday February 1, 2019 at 03:00 pm.

Student number:	4239369	
Project duration:	June 27, 2018 – February 1, 2019	
Thesis committee:	Prof.dr. L.L.A. Vermeersen,	Delft University of Technology, chair
	Dr. ir. W. van der Wal,	Delft University of Technology, supervisor
	Dr. ir. A.A. Verhagen,	Delft University of Technology, committee member
	Dr. J. T. Curran,	Apple, external supervisor

An electronic version of this thesis will be made available at `http://repository.tudelft.nl/`.

TU Delft

Preface & Acknowledgements

When looking for a research topic, it was important to me that it would be relevant for the majority of people on Earth. I wanted to spend nine months researching something in space that could actually make a difference in people's daily lives on this planet. With a combination of effort and luck, I ended up researching how to optimize the Galileo signal for a fast first fix. Since GNSS technology is used by billions of people every single day, relevance was something I no longer had to worry about. Now it was up to me, what was I going to contribute to this field of knowledge?

After finishing my literature study, I could not wait to start designing, testing and finding out what the results of my research would be. Reality has trumped my expectations. Doing research is definitely full of surprises, both welcomed and unwanted. Nine months ago I would have never imagined that my research would actually have potential, that an expert like Oliver Montenbruck (whom I cited over a thousand times) would take the time to call with me and that I would be speaking to a patent attorney. In contrast, nine months ago I would also have never imagined that I would forget to multiply by the speed of light in my code, that I would manually download a year of broadcast ephemerides, and that I would spend days researching topics that were in hindsight not relevant to include at all. It turns out, both ups and downs are part of doing your thesis research.

What I did imagine, or maybe knew, nine months ago, but is now all the more clear, is that nothing of this would have been possible without my two intelligent, dedicated and inspiring supervisors: Dr. ir. W. van der Wal and Dr. J. T. Curran. I would like to thank both of them for their time and dedication and hope that you have enjoyed our meetings and this thesis adventure as much as I did. Your support has been of indescribable value.

Furthermore, I would like to acknowledge the contribution of Dr. ir. D. Dirkx to this research. He provided some valuable insights among other on astrodynamics and the propagation of the equations of motion in the starting phase of this research. Moreover, I'd like to thank Dr. O. Montenbruck. Our personal conversations resulted in a tipping point in the research: providing the crucial advice, when I seemed to be stuck.

My thesis adventure might have come to an end, but we are definitely not done yet. I am excited to continue working on the publication of an article with my supervisors and hopefully presenting this at the annual European Navigation Conference in Warsaw. For now I hope you enjoy reading this thesis and maybe, really really maybe, you some day not only read about it but actually determine your position with it.

Sanne Lamers
Amsterdam, January 2019

Contents

List of Figures

List of Tables

List of Abbreviations

bps bits per second.

CED clock correction and ephemeris data.

CRC cyclic redundancy check.

DOY day-of-year.

ECEF Earth-centered, Earth-fixed.

ESA European Space Agency.

FEC forward error correction.

GNSS Global Navigation Satellite System.

GPS Global Positioning System.

GST GNSS time reference.

HPE horizontal position error.

ICD Interface Control Document.

LVLH local vertical, local horizontal.

OECD Organisation for Economic Cooperation and Development.

OOB out-of-band.

PVT position-velocity-time.

RAC radial, along-track, cross-track.

rms root mean square.

RTC real-time clock.

SISRE signal-in-space ranging error.

SVID Space Vehicle Identification.

TOW time of week.

TTFF time to first fix.

TTFFD TTFF-data.

USD United States Dollar.

1

Introduction

1.1. Context

In May 2000, the Global Positioning System (GPS) commercial era was opened by announcing the end of selective availability. Selective availability was the intentional degradation of the GPS civilian signal. Until then the accurate GPS signal was restricted to military purposes only. By ending this limitation, the GPS civilian signal accuracy improved by a tenfold: a turning point for GPS towards becoming a global utility (Braunschvig et al. 2003). Since then the Global Navigation Satellite System (GNSS) market has experienced major growth. Where in 2000 the Organisation for Economic Cooperation and Development (OECD) estimated the total GNSS market size to be about 8 billion United States Dollar (USD) (OECD 2000), by 2015 the size had increased thirteen-fold to about 105 billion USD [1] (European GNSS Agency 2017). In the future, GNSS is expected to grow further. This trend of market penetration is reflected in Figure 1.1, showing the amount of GNSS devices per capita in 2014 and a 2023 estimation. By 2020 there will be as many GNSS devices in the world as there are people, making GNSS a key technology in the average person's life (European GNSS Agency 2017).

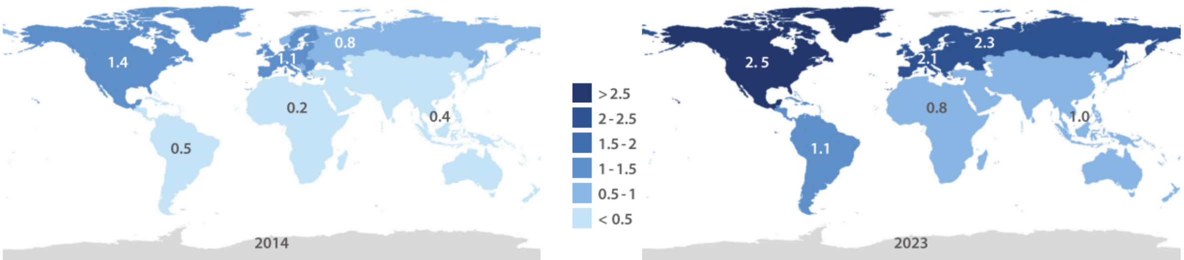

Figure 1.1: The amount of GNSS devices per capita in 2014 and estimated in 2023 (European GNSS Agency 2015)

1.2. Motivation

GNSS provides users with position, velocity and timing information by processing signals broadcast by satellites. As indicated, GNSS has moved from military restricted application to ubiquitous usage. The increase in applications has resulted in a wider range of user requirements. Yet, despite meeting completely divergent needs, all GNSS applications make use of more or less the same input GNSS signals (European GNSS Agency 2017). This seemingly sub-optimal situation gave rise to the idea of optimizing the GNSS signal for a specific requirement. As could be expected with such a key technology, the signal had been optimized before. Other GNSSs like the Chinese Beidou or the European Galileo, learned from the design choices made for the GPS legacy signal (Bhatta 2010). Moreover, GPS itself is undergoing modernization as well, soon providing three additional improved civil signals (Betz et al. 2006). Apart from changes in the signal, many developments

[1] Using the average 2015 Euro to USD exchange rate of 1.11 (Statista 2018)

took place on the receiver side. Innovations were applied using among others smarter signal acquisition algorithms, differential positioning and out-of-band (OOB) assistance (Kaplan and Hegarty 2005) (Teunissen and Montenbruck 2017).

Yet, according to European Space Agency (ESA) expert Curran (2018) most of the past and ongoing developments focus on improving GNSS accuracy. This research instead builds upon the idea that some users are willing to accept an (initially) degraded accuracy for a faster position fix (Anghileri et al. 2012). This is often the case when there is limited navigation data stored in the receiver and occurs when turning on a mobile phone or sport watch to use a location-based service (Schiller and Voisard 2004) Peng (2008), driving out of a parking garage with a navigational device or activating a search & rescue beacon in case of an emergency (Affens et al. 2011). Whether it is out of impatience or serious distress, to the user every second counts. Moreover, these users care more about directly setting a certain action into motion, rather than waiting until a sub-meter level of accuracy is acquired. This research therefore focuses on decreasing the time to first fix (TTFF) of a receiver at the expense of position accuracy. In effect, the position accuracy is only initially degraded, since the receiver can use the original GNSS signal to improve the position accuracy after obtaining a fast first fix.

1.3. Research aim

The TTFF is a measure of how quickly after activation a first position can be computed within the required accuracy bounds (European GNSS Agency 2017). This study considers a situation which resembles a so-called cold start. Since the definition between the commonly used terms cold, warm and hot start differ from author to author, we make the situation of the receiver explicit. At activation, the receiver only has an in-memory almanac and an estimation of time held by the real-time clock (RTC). In this case, the most dominant contribution to the TTFF is the time to retrieve the first fix data from the navigation message, which we call the TTFF-data (TTFFD) (Paonni et al. 2010). Moreover, the contribution of the TTFFD is crucial as it cannot be reduced by improving receiver technology (Anghileri et al. 2012). After all, the receiver has no influence on the content of the broadcast navigation message nor at what speed it is broadcast. The first fix data consists of the clock correction and ephemeris data (CED) and a GNSS time reference (GST), which are used as follows. To compute a position fix, the receiver must make range measurements to at least four satellites, and determine the positions of these satellites. These range measurements require the extraction of a "transmit-time" from the message, which takes the form of the GST. Determination of the satellite positions then further requires the extraction of the CED.

The TTFFD is affected by many factors among which: the data transmission rate, the size of the first fix data, the location and repetition rate of the first fix data within the navigation message and the message robustness (Anghileri et al. 2012). The relation between these factors and the TTFFD is explained in Appendix B.1. This research specifically aims to decrease the TTFFD by reducing the size of the CED, which is the largest component of the first fix data and currently the delaying factor in obtaining a position fix. In literature we find several studies that focus on reducing or improving the CED. In a patent by Grelier and Ries (2016) it is proposed to select the most dominant positioning parameters and only broadcast those. Trautenberg (2013) discusses a method to replace the portion of each parameter that is redundant for adhering to the accuracy requirements with additional position information to improve performance. Anghileri et al. (2012) reduce the size of the CED of the GPS legacy navigation message by applying truncation. This research combines this last effort with two new reduction strategies: the relative expression of the CED parameters with respect to matching parameters in the almanac and the absorption of CED parameters by leveraging redundancy in the user algorithm.

As was mentioned previously, it is not only the size but also the location and repetition rate of the CED that finally determines the TTFFD and thus the TTFF. Therefore, we not only aim to reduce the size of the CED, we also consider the integration of this reduced set in the existing Galileo I/NAV message. The data transmission rate is not considered, because it is unlikely to change within the current Galileo system. The I/NAV message is specifically attractive since it has already allocated space for future developments in the form of spare and reserved bit fields (European GNSS Open Service 2016). When only using these fields, backward compatibility is maintained. In this case, legacy users can continue using their old receiver for positioning, and only those wishing to benefit from the faster fix should acquire a receiver with an updated algorithm.

The I/NAV message structure, content and opportunities for integration are detailed in Appendix A. This research's outcome, a reduced CED, could be broadcast by the Galileo satellites immediately, since no changes in the Galileo hardware or infrastructure are required. Alternatively, the proposed reduction strategies can be considered for the next generation of Galileo satellites.

As is pointed out by Anghileri et al. (2012) there are alternative ways to decrease the TTFFD. A common approach is downloading an extended ephemeris through an out-of-band channel every few days. The receiver then only needs to read a time reference and no longer has to wait until the entire broadcast navigation message is read (Garin 2009). Over the years, the performance of such extended ephemerides has improved significantly (Chan et al. 2018). Baseband Technologies (2018) now has a patent pending for an extended ephemeris with a 28-day validity at 65 m signal-in-space ranging error (SISRE) (68^{th}-percentile). The distinguishing factor of this research is, however, that the receiver standalone capability is maintained. The decrease in TTFFD is achieved completely autonomously. This is important to applications that due to their remote use cannot rely on having access to an out-of-band channel such as search & rescue beacons (Affens et al. 2011), freight management (He et al. 2009), wildlife tracking (Forin-Wiart et al. 2015) and stolen good trackers (Bensky 2016). In many countries this also applies to mobile phones, since there is no full cellular coverage outside urban areas. Moreover, maintaining autonomy is important from a safety, privacy and redundancy related point of view. There are situations in which one does not want to depend on commercial out-of-band GNSS services for positioning. Next to this, the use of an extended ephemeris requires the receiver to have two radio communication systems, one for the satellite channel and one for the out-of-band channel, resulting in a higher energy consumption.

Finally, a reduction of the CED not only decreases the TTFF, it also has the potential to improve the availability. If we reduce the size of the CED and increase its repetition rate, the impact of a bit error is expected to become smaller. Moreover, the chances of reading a full ephemeris increase. In addition, the time the user receiver has to be on to read the CED is likely to decrease. Assuming this on-time is proportional to the power usage, a reduced CED is very interesting to low-power applications that do not require a high accuracy, such as freight management, wildlife tracking and stolen goods trackers. For these applications a sub-meter level accuracy is not necessary, neither does every second count, it is battery life that is crucial. A container at sea needs to be tracked for months, a wild animal cannot be caught every other week and you do not want to worry about charging your bicycle tracker. Overall, a reduced CED thus has the potential to provide a multitude of advantages.

1.4. Research questions

Based on the research aim described in the previous section: "decrease the TTFFD by reducing the size of the CED and integrating this reduced set in the existing Galileo I/NAV message while maintaining backward compatibility", the following research questions have been identified:

What is the optimal size of the CED in terms of TTFFD and position accuracy of a GNSS receiver when integrating this reduced set into the Galileo I/NAV message while maintaining backward compatibility?

1. How much can the size of the CED be reduced by expressing broadcast CED parameters relative to the matching almanac parameters?

2. How much can the size of the CED be reduced by absorbing broadcast CED parameters through redundancies in the user algorithm?

3. Given the size of the reduced CED, which division of the total number of bits over the individual parameters yields the highest position accuracy?

4. How does the size of the reduced CED translate to the TTFFD when integrating this reduced set into the I/NAV navigation message while maintaining backward compatibility?

5. What is the effect of broadcasting the reduced CED within the I/NAV message on the receiver's availability and on-time?

1.5. Thesis outline

The outline of this thesis diverges from what is common practice as it is split up in an article, conclusions & recommendations and several appendices. We have chosen for this uncommon split to accelerate the process of writing an article and submitting it to a scientific journal. The article contains the most essential information of this research and is written such that it can be submitted separately. Therefore, part of its content overlaps with this introduction, the conclusions & recommendations and the information given in the appendices. Paragraphs in the article that refer to ESA expert Dr. J.T. Curran are not part of this thesis research but are nevertheless important to include in the article to sketch a complete picture. The reason to include appendices is two-folded. First, a scientific article has another purpose than a thesis. Some appendices thus provide information that is of secondary importance in an article, but essential to include in a thesis. Second, it is likely that readers of this thesis do not have the same knowledge of the research topic as readers of a dedicated journal. Other appendices therefore serve to provide additional background to those readers.

Bearing this in mind, the thesis is outlined as follows. Chapter 2 presents the article including an abstract, introduction, the applied reduction strategies, the simulation process & data sets, the results and a summary and conclusions. Next, Chapter 3 provides a more extensive version of the conclusions by directly answering the research questions and also provides a list of recommendations. Subsequently, the appendices are included in the following order. Appendix A discusses the content and characteristics of the Galileo I/NAV navigation message. Thereafter, Appendix B explains three central measures of performance: the TTFF, size of the CED and SISRE. Appendix C then describes the verification of this research. Lastly, Appendix D presents additional results that were not included in the article, but are nevertheless of interest.

2

Scientific article

Abstract

This research focuses on GNSS users interested in a faster position fix in a situation where the receiver holds limited data. This occurs when turning on a mobile phone or sport watch to use a location-based service, driving out of a parking garage with a navigational device or activating a search & rescue beacon. In these cases, users care more about directly setting a certain action into motion, than waiting until a sub-meter level of accuracy is acquired. For this purpose, we aim to decrease the time to first fix (TTFF) of a receiver at the expense of position accuracy by focusing on its most dominant component: the time to read the first fix data, i.e. the TTFFD. In turn, the TTFFD is decreased by reducing the size of the clock correction and ephemeris data (CED) and integrating this reduced set into the existing Galileo I/NAV message while maintaining backward compatibility. Three reduction strategies are presented to reduce the size of the CED. First, the expression of the CED parameters relative to the matching almanac parameters, which requires downloading the most recent almanac. Second, the absorption of the clock and ephemeris time reference into related parameters by leveraging redundancies in the user algorithm. Third, the truncation of the CED parameters, where the optimal parameter bit allocation per CED size is determined by means of a Monte Carlo simulation. Subsequently, the optimal reduced set is integrated in the existing Galileo I/NAV message, since it is not only size but also the location and repetition rate of the reduced CED in the navigation message that determine the final decrease in TTFFD.

A simulation is developed where the three reduction strategies are combined and applied to one year of Galileo navigation messages and almanacs starting from October 2017. The current I/NAV message has a size of 428 bits and an average TTFFD of 25.4 seconds. The relative expression of the CED parameters, the absorption of the clock time reference and ephemeris time reference yield a 76, 15 and 10 bit reduction respectively, without a significant decrease in position accuracy expressed as the signal-in-space ranging error (SISRE). The reduction in size that can be realized by truncation results from a trade-off with the maximum acceptable level of SISRE. When combining all three reduction strategies a 296 bit, i.e. 69%, size reduction can be realized at a SISRE level of 10.04 meters, yielding a 132 bit CED. 66% of the size reduction is in this case achieved by parameter truncation. To maintain backward compatibility, the spare and reserved bits of the I/NAV message are used to integrate the reduced set. This finally results in an average TTFFD of 6 seconds, which is a decrease of almost 20 seconds. With the reduced CED the user gains full independence of out-of-band channels for the computation of a fast position fix. In addition, it decreases the impact of bit errors on the TTFF and increases the chance of receiving an error free set of first fix data. Moreover, the reduced CED is not only of interest to fast fix applications that desire a decrease in waiting time. Positioning based on the reduced set also decreases the time the receiver has to be "on" to read the navigation data and consequently the receiver's power usage. This leads to a second type of applications that benefits from the reduced CED: low-power applications that do not require a high accuracy, such as freight management, wildlife tracking and stolen goods trackers. To conclude, the constructed reduced CED provides multiple advantages for a wide range of GNSS users and should therefore be considered as a purpose for the spare and reserved bits of the Galileo I/NAV message.

2.1. Introduction

Nowadays there are countless GNSS applications and consequently a wide range of user requirements. Where much focus in GNSS development lies on improving position accuracy, this research builds upon the idea that some users are willing to accept an (initially) degraded accuracy for a faster position fix (Anghileri et al. 2012). This often occurs when there is limited navigation data stored in the receiver, such as when turning on a mobile phone or sport watch to use a location-based service (Schiller and Voisard 2004) Peng (2008), driving out of a parking garage with a navigational device or activating a search & rescue beacon (Affens et al. 2011). In all these cases, whether it is out of impatience or serious distress, to the user every second counts. Moreover, these users care more about directly setting a certain action into motion, rather than waiting until a submeter level of accuracy is acquired. This research therefore focuses on decreasing the time to first fix (TTFF) of a receiver at the expense of position accuracy. In effect, the position accuracy is only initially degraded, since the receiver can use the original GNSS signal to improve the accuracy after obtaining a fast first fix.

The TTFF is a measure of how quickly after activation a first position can be computed within the required accuracy bounds (European GNSS Agency 2017). This study considers a situation which resembles a so-called cold start. Since the definition between the commonly used terms cold, warm and hot start differ from author to author, we make the situation of the receiver explicit. At activation, the receiver only has an in-memory almanac and an estimation of time held by the real-time clock (RTC). In this case, the most dominant contribution to the TTFF is the time to retrieve the first fix data from the navigation message, which we call the TTFF-data (TTFFD) (Paonni et al. 2010). The first fix data consists of the clock correction and ephemeris data (CED) and a GNSS time reference (GST). Moreover, this contribution is crucial as it cannot be reduced by improving receiver technology (Anghileri et al. 2012).

The TTFFD is affected by many factors among which: the data transmission rate, the size of the first fix data, the location and repetition rate of the first fix data within the navigation message and the message robustness (Anghileri et al. 2012). The relation between these factors and the TTFFD is explained in Appendix B.1. This paper specifically aims to decrease the TTFF by reducing the size of the CED, which is the largest component of the first fix data and currently the delaying factor in obtaining a position fix. In literature we find several studies that focus on reducing or improving the CED. In a patent by Grelier and Ries (2016) it is proposed to select the most dominant positioning parameters and only broadcast those. Trautenberg (2013) discusses a method to replace the portion of each parameter that is redundant for adhering to the accuracy requirements with additional position information to improve performance. Anghileri et al. (2012) reduce the size of the CED of the GPS navigation message by applying truncation. This research combines this last effort with two new reduction strategies: the relative expression of the CED parameters with respect to matching parameters in the almanac and the absorption of CED parameters by leveraging redundancy in the user algorithm.

As was mentioned previously, it is not only the size but also the location and repetition rate of the CED within the navigation message that finally determine the TTFFD and thus the TTFF. Therefore, we not only aim to reduce the size of the CED, we also consider the integration of this reduced set in the existing Galileo I/NAV message. The data transmission rate is not considered, because it is unlikely to change within the current Galileo system. The I/NAV message is specifically attractive since it has already allocated space for future developments in the form of spare and reserved bit fields (European GNSS Open Service 2016). When only using these fields, backward compatibility is maintained. In this case, legacy users can continue using their old receiver for positioning, and only those wishing to benefit from the faster fix should acquire a receiver with an updated algorithm. The considered Galileo CED consists of the Kepler parameters, harmonic coefficients and clock correction parameters presented in Table 2.1. The I/NAV message structure, content and opportunities for integration are described in more detail in Appendix A. This research's outcome, a reduced CED, could be broadcast by the Galileo satellites immediately, since no changes in the Galileo hardware or infrastructure are required. Alternatively, the proposed reduction strategies can be considered for the next generation of Galileo satellites.

As is pointed out by Anghileri et al. (2012) there are alternative ways to decrease the TTFFD. A common approach is downloading an extended ephemeris through an out-of-band channel every few days. Then the receiver only needs to read a time reference and no longer has to wait until the entire broadcast navigation message is read (Garin 2009). Over the years, the performance of such extended ephemerides has improved significantly (Chan et al. 2018). Baseband Technologies (2018) now has a patent pending for an extended ephemeris with a 28-day validity at 65 m SISRE (68^{th} percentile). The distinguishing factor of this research is, however, that the receiver standalone capability is maintained. The decrease in TTFF is achieved autonomously. This is important to applications that due to their remote use cannot rely on having access to an out-of-band channel such as search & rescue beacons (Affens et al. 2011), freight management (He et al. 2009), wildlife tracking (Forin-Wiart et al. 2015) and stolen good trackers (Bensky 2016). In many countries this also applies to mobile phones, since there is no full cellular coverage outside urban areas. Moreover, maintaining autonomy is important from a safety, privacy and redundancy point of view. There are situations in which one does not want to depend on commercial out-of-band GNSS services for positioning. Next to this, the use of an extended ephemeris requires the receiver to have two radio communication systems, one for the satellite channel and one for the out-of-band channel, resulting in a higher energy consumption.

Finally, a reduction of the CED not only decreases the TTFF, it also has the potential to improve availability. If we reduce the size of the CED and increase its repetition rate, the impact of a bit error is expected to become smaller. In addition, the chances of reading a full ephemeris increase. Moreover, the time the user receiver has to be "on" to read the CED is likely to decrease. Assuming this on-time is proportional to the power usage, a reduced CED is interesting to low-power applications that do not require a high accuracy, such as freight management, wildlife tracking and stolen goods trackers. For these applications a sub-meter level accuracy is unnecessary, neither does every second count, it is battery life that is crucial. A container at sea needs to be tracked for months, a wild animal cannot be caught every other week and you do not want to worry about charging your bicycle tracker. Overall, a reduced CED has the potential to provide a multitude of advantages.

The remainder of this paper is structured as follows. Section 2.2 outlines the concepts used for CED reduction. It describes the individual reduction strategies and the integration of the reduced set in the I/NAV navigation message. Next, Section 2.3 describes the simulation process and the data sets that were used in this research. Section 2.4 then presents and discusses the results with regards to the effectiveness of the reduction strategies, the optimization of the reduced set and the characteristics of the reduced set. Finally, Section 2.5 wraps up with a summary and conclusions.

2.2. Concepts for CED reduction

This research aims to decrease the TTFF by reducing the size of the clock correction and ephemeris data. Three reduction strategies are explored: the relative expression of CED parameters with respect to the matching almanac parameters, the absorption of CED parameters and the increase in scale factor of CED parameters. Next to these three reduction strategies, this Section also discusses the integration of the constructed reduced set into the Galileo I/NAV message.

To explain, the size of the CED is the sum of the individual bit allocations per parameter. The CED is broadcast by the Galileo satellites in a fixed-point binary representation (Anghileri et al. 2012). In this format the number of bits allocated per parameter depends on three factors: the range, scale factor and signedness, where the scale factor corresponds to the resolution of a parameter (Parhami 1999). The computation of the CED size is described in Appendix B.2. The number of bits transmitted per parameter finally determines the level of accuracy, here expressed as the signal-in-space ranging error (SISRE), with which the user can determine its position.

2.2.1. Relative expression of the CED parameters

Reducing a parameter's range can have great impact on the final position accuracy. Yet, the strategy proposed here, allows for a range and thus size reduction without increasing SISRE. The idea is to leverage the fact that the CED and almanac have parameters in common. The almanac is broadcast together with the CED by GNSS satellites. Its parameters can be used to calculate a rough estimate of the satellites' positions and originally aided satellite acquisition. In total the almanac and CED have nine matching parameters: $\sqrt{a}$, e, i_0, Ω_0, ω, m_0, $\dot{\Omega}$, a_{f0} and a_{f1}.

It is suspected that a substantial part of the CED and almanac parameters overlap. If this is the case, a set of relative CED parameters with decreased range can be constructed by expressing the CED parameters with respect to the matching almanac parameters. The constructed relative set can be broadcast by the GNSS satellites. In the receiver the relative parameters are added to the almanac parameters to recover the full

Table 2.1: CED parameter definitions (European GNSS Open Service 2016)

Symbol	Parameter
m_0	Mean anomaly at reference time
Δn	Mean motion difference from computed value
e	Eccentricity
$\sqrt{a}$	Square root of the semi-major axis
Ω_0	Longitude of ascending node of orbit plane at weekly epoch
i_0	Inclination angle at reference time
ω	Argument of perigee
$\dot{\Omega}$	Rate of right ascension
i_{dot}	Rate of inclination angle
C_{uc}	Amplitude of the cosine harmonic correction term to the argument of latitude
C_{us}	Amplitude of the sine harmonic correction term to the argument of latitude
C_{rc}	Amplitude of the cosine harmonic correction term to the orbit radius
C_{rs}	Amplitude of the sine harmonic correction term to the orbit radius
C_{ic}	Amplitude of the cosine harmonic correction term to the angle of inclination
C_{is}	Amplitude of the sine harmonic correction term to the angle of inclination
t_{oe}	Ephemeris reference time
a_{f0}	SV clock bias correction coefficient
a_{f1}	SV clock drift correction coefficient
a_{f2}	SV clock drift rate correction coefficient
t_{0c}	Clock reference time

CED. Based on this full set the receiver computes a position solution. This strategy yields the desired reduction in size at broadcast, while maintaining an equal accuracy for determining the final position solution.

To position based on the relative CED, the user must be able to identify the almanac to which the parameters are referenced. Simulation shows that if the receiver uses an expired almanac issue as a reference, the accuracy is heavily degraded. SISRE increases to the 100 km level which is unacceptable. To see whether this accuracy degradation may be overcome by propagating the parameters of an expired almanac issue, we analyze the variations of the almanac parameters of satellite E04 over time, as is illustrated in Figure 2.1. It shows the variation pattern of the majority of the almanac parameters is unpredictable. This makes it difficult to reliably propagate the parameters over a long period of time with a simple algorithm that has limited computational costs. Therefore, it is paramount that the receiver always downloads the right reference almanac. In addition, Figure 2.1 explains the high sensitivity of SISRE to the use of expired almanac issues. For most parameters the difference between sequential almanac issues are substantial. Positioning based on an expired almanac therefore yields completely different results.

We propose two options for almanac identification. The first minimizes the number of bits used, the second minimizes the number of almanac downloads. In the identification process the space vehicle identifier (SVID) does not have to be included as the receiver tunes in on a satellite signal and thereby knows from which satellite it originates. Both options require an almanac marker in the form of a day-of-year (DOY) marker. 9 bits are necessary to define each day of the year uniquely. Yet, we can decrease this number by making use of two characteristics. First, the upload interval of the almanac alternates between 3 and 4 days. Second, the relative CED is based on the most recent almanac issue. Therefore, we can conclude that any almanac downloaded more than 4 days ago can no longer be used for positioning.

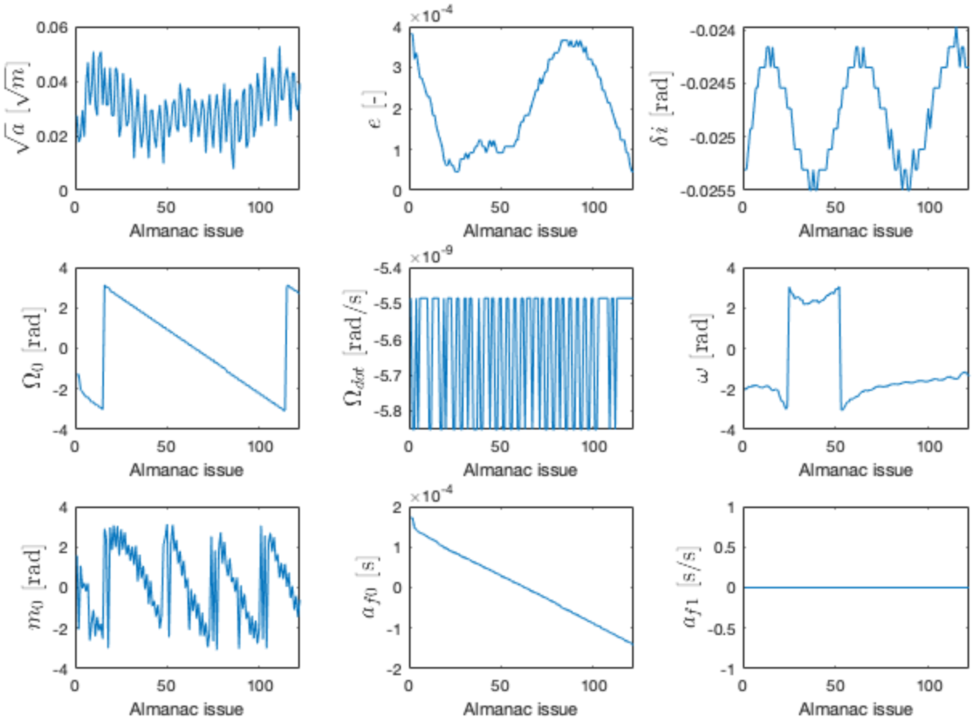

Figure 2.1: Variation over time of the almanac parameters for SVID E04

Based on this, the first identification option uses a 3 bit (modulus 8) DOY-marker and reloads the almanac if the last almanac download was over 3 days ago. The second option uses a 4 bit DOY-marker and only has to reload the almanac if it is older than 4 days. In addition, the following rules apply. If the almanac marker is more recent than the download day, the almanac must be reloaded. If the almanac marker is equal to the download day, the almanac must be only be reloaded the first time this occurs that day. After this reload took place, the receiver can continue positioning if the marker is equal to the download day. If the download day is more recent than the almanac marker, the receiver can continue positioning. To conclude, the 3 bit marker minimizes the number of bits used. The 4 bit marker fully exploits the upload interval and minimizes the number of almanac downloads. It depends on the positioning requirements which option is more attractive.

2.2.2. Absorption of the CED parameters

A second strategy that is explored to decrease the size of the CED is the absorption of parameters. Based on the user algorithm, as outlined by the European GNSS Open Service (2016) in the Galileo interface control document (ICD), we found that the clock reference time, t_{0c}, and the ephemeris reference time, t_{0e}, do not have to be broadcast individually but can be absorbed into the parameters they affect. In principle, the absorption of a parameter should realize a reduction in size without increasing SISRE. If full decoupling of the absorbed parameter from the variable parameters in the equation is not possible, this is no longer the case. It must then be decided if the neglect of the coupled terms is acceptable with regards to the SISRE contribution.

Absorption of the clock time reference, $\mathbf{t_{0c}}$

Based on the equation for the computation of the clock correction, Δ_{SV}, this paragraph shows how the clock time reference, t_{0c}, can be absorbed in the clock bias correction coefficient, a_{f0}:

$$\Delta_{SV} = a_{f0} + a_{f1}[t - t_{0c}] + a_{f2}[t - t_{0c}]^2 + \Delta_{tr} \tag{2.1}$$

where

$$\Delta_{tr} = Fea^{1/2}\sin(E) \tag{2.2}$$

Here F is a constant with value -4.442807309e-10 s/m$^{1/2}$, e the eccentricity, a the semi-major axis and E the eccentric anomaly. We rewrite equation 2.1 such that we can decouple the variable time of interest t from t_{0c}.

$$\Delta_{SV} = a_{f0} + a_{f1}[t] - a_{f1}[t_{0c}] + a_{f2}[t^2] - a_{f2}[2tt_{0c}] + a_{f2}[t_{0c}]^2 + \Delta_{tr} \tag{2.3}$$

From this equation it becomes clear that decoupling is only possible to certain extent. In the fifth term, t and t_{0c} cannot be separated. To fully absorb t_{0c} we must therefore assume a_{f2} is negligibly small. The error caused by this assumption is absorbed in the error budget corresponding to t_{0c} absorption. We then obtain the following equation:

$$\Delta_{SV} = a_{f0,absorb} + a_{f1}[t] + \Delta_{tr} \tag{2.4}$$

where

$$a_{f0,absorb} = a_{f0} - a_{f1}[t_{0c}] \tag{2.5}$$

Having absorbed t_{0c}, it no longer has to be broadcast, directly saving 14 bits. The impact on the range of a_{f0} and SISRE is described in Section 2.4.

Absorption and shift of the ephemeris time reference, t_{0e}

A similar strategy can be applied to absorb the ephemeris time reference, t_{0e}, in the mean anomaly, m_0, the inclination, i_0, and the longitude of the ascending node, Ω_0. In the user algorithm t_{0e} occurs in:

$$t_k = t - t_{0e}^* \tag{2.6}$$

Subsequently, t_k and t_{0e} occur in:

$$M = m_0 + nt_k \tag{2.7}$$

$$i = i_0 + \delta i + i_{dot} t_k \tag{2.8}$$

$$\Omega = \Omega_0 + [\dot{\Omega} - \omega_e] t_k - \omega_e t_{0e} \tag{2.9}$$

The asterisk in equation 2.6 refers to the fact that week rollovers should be taken into account. This means t_k is not always simply t minus t_{0e}, but is formulated as follows:

$$\text{if} \quad t - t_{0e} > 302400 \quad \text{then} \quad t_k = t - t_{0e} - 604800 \tag{2.10}$$

$$\text{if} \quad t - t_{0e} < -302400 \quad \text{then} \quad t_k = t - t_{0e} + 604800 \tag{2.11}$$

$$\text{else} \quad t_k = t - t_{0e} \tag{2.12}$$

For this reason the equation for M in fact looks like:

$$M = m_0 + n(t - t_{0e} + \text{rollover}) \tag{2.13}$$

Where the rollover is either 0, 604800 or -604800. The rollover term cannot be fully absorbed since it depends on t, which is variable. Yet, when neglecting the rollover term this leads to a hundreds of kilometer level SISRE. This accuracy degradation is unacceptable, so just absorbing t_{0e} is not an option.

An additional shift in time is proposed instead. Rather than referring the time of interest to the beginning of the Galileo week, it is referred to the beginning of each I/NAV frame. Here, the assumption is made that the receiver can determine the time at the beginning of each 720 second frame to within some tens of milliseconds, based on the time estimate held by the RTC (U-blox 2018). According to Curran (2018), this assumption is justified as follows: a receiver typically has a 32 kHz crystal oscillator RTC. This RTC holds the time with an accuracy of 5 to 20 parts per million (ppm). Given the trend towards improved accuracy (Maxim Integrated 2019) (Abracon 2019) and factory-calibration (STMicroelectronics 2018), we assume a value of 5 ppm, i.e. a deviation of about 0.5 seconds per day.

In addition, the described receiver retrieves an almanac periodically over some communication network. While doing so, it is possible to also avail of some type of time assistance. One such example might be the standard network time protocol (NTP) (Network Time Foundation 2018). This would allow the receiver to re-align its RTC to UTC with a typical accuracy of some tens of milliseconds. After this alignment the RTC time estimation starts to deviate at the given rate. Assuming that the deviation of time has a Gaussian distribution and leveraging the fact that we download an almanac at least every three or four days, the 3 sigma time error, dT, is about ± 1.5 seconds for a 3-day interval and about ± 2 seconds in case of a 4-day download interval.

Once the receiver reads the first page from a satellite, it can start to deduce a more accurate time estimate. We know that the start of each page is aligned with the beginning of a second and that each page has a 1 bit even/odd marker. Based on this information the receiver can determine the fractional bit of time exactly and the integer bit of time with a ± 2N second ambiguity, where N is an integer. In addition to this time estimation, the receiver can also make a rough estimation of the locations of all satellites based on the almanac it holds and make a good guess of how long the signal took to travel from the satellite. When combining this information with the RTC time estimation, we can resolve time if dT is below 2 seconds, which is indeed the case at a maximum almanac download interval of 4 days. Subsequently, the time to the beginning of the frame can be determined by taking the modulus of 720, corresponding to the duration of a frame.

For redundancy we add a reduced time of week (TOW) header in case dT passes 2 seconds, for example when the RTC wanders or if the almanac download is delayed. The conventional TOW-header represents the seconds passed within the Galileo week and occupies 20 bits. We use a reduced version that communicates the seconds passed within a frame, which vary between 0 and 720. Moreover, the receiver knows whether it is reading an even or odd page. With this knowledge, the size of the header can be reduced by modulating to only even numbers, 0 to 350, translating to a 9 bit header. Based on this TOW-header the time can be resolved when dT exceeds 2 seconds. However, this does increase the average TTFFD since the receiver needs to read additional pages. If dT is below 2 seconds, the header can be used to cross-validate the resolved time. The integration of these additional TOW-headers in the navigation message is discussed in Section 2.2.4.

Knowing the time at the beginning of each frame, the absorption and shift of t_{0e} is as follows:

$$M = m_0 + nt_k = m_0 + n(t - t_{0e} + \text{rollover}) = m_0 + nt - nt_{0e} + n * \text{rollover} \tag{2.14}$$

Subsequently, t is split up:

$$t = t_{frame} + \Delta t_{frame} \tag{2.15}$$

Where t_{frame} is the time corresponding to the number of full I/NAV frames that have passed since the beginning of Galileo week multiplied by the duration of a frame: 720 seconds, and Δt_{frame} represents the seconds passed in the current I/NAV frame. Then,

$$M = m_0 + nt_{frame} + n\Delta t_{frame} - nt_{0e} + n * \text{rollover} \tag{2.16}$$

Where all parameters not including t_{frame} can be absorbed:

$$m_{0absorb,shift} = m_0 + nt_{frame} - nt_{0e} + n * \text{rollover} \tag{2.17}$$

Again the rollover term would pose a problem as it depends on the variable t. Yet, because of the shift we know the value of t up to 720 seconds for each broadcast. At the creation of each reduced set it is therefore already known if a rollover term applies to the range in which t falls.

The procedure is repeated for the absorption of t_{0e} into i_0 and Ω_0. Absorbing t_{0e} saves 14 bits by not having to broadcast it. The impact on range and SISRE is presented in Section 2.4. To conclude, it is emphasized that the shifted model does demand a navigation message upload interval of 720 seconds, which is shorter than the current average upload interval. However, this should not pose any problems when using a real-time or batch upload strategy (Curran 2018).

2.2.3. Increasing the scale factor of the CED parameters

The strategy to reduce the number of bits by increasing the scale factor, i.e. reducing the parameter resolution, differs from the other strategies since it trades-off size for position accuracy. This strategy is also called truncation and is applied as follows. For transmission in the navigation message the real valued CED parameters are converted to a fixed-point binary form. This form represents the parameters as an integer multiplied by a scale factor. For the CED parameters this scale factor is generally a specific power of 2. To truncate the parameters a method is used as described by Anghileri et al. (2012). They explain that to reduce, for example, the size of the eccentricity e, the scale factor should be increased with the desired amount of factors of two. So to decrease the eccentricity from 32 to 22 bits, the scale factor should increase from 2^{-33} to 2^{-23}. The same methodology can be applied to the other CED parameters.

By varying the level of truncation and thus bit allocation per parameter, SISRE changes. Since each parameter has a different influence on SISRE and perhaps a correlation to each other, we apply the following optimization strategy to find the optimal bit allocation for a given CED size. First, we plot SISRE versus various levels of truncation per parameter with respect to a constant reference set. These so-called variation profiles give information about the sensitivity of SISRE to the bit allocation of each parameter. Subsequently, the reference set is also varied to see if there exist parameter correlations. Lastly, two types of Monte Carlo simulations are run. In the first, the search space is limited by using bounded allocation ranges. These ranges can be deduced from the variation profiles that indicate the bit allocations where SISRE becomes less sensitive. The second simulation targets size and leaves the parameter allocation completely random to make sure we do not oversee unexpected correlations. Subsection 2.2.4 discusses which sizes are of specific interest. Finally, the optimal sets are selected based on the combination of the results of both simulations.

2.2.4. Integration in the I/NAV navigation message

As was mentioned previously, the TTFFD does not only depend on the size of the first fix data, it also depends on its location and repetition rate within the navigation message. To maintain backward compatibility, we choose to integrate the reduced CED in the spare and reserved bits of the existing Galileo I/NAV message that are specifically meant for future development. However, this does put a constraint on the availability of bits. There are basically four types of fields in the I/NAV message that are potentially available for use: reserved 1, reserved 2, spare and additional reserved fields that are named reserved extra. The reserved 1 and 2 fields provide a bandwidth of respectively 40 and 8 bits every 2 seconds, whereas, the spare and reserved extra fields are more randomly spread over the message. This is detailed in Appendix A.

Based on the division of the fields over the message, we simulate how the TTFFD responds to a variation in the size of the reduced CED while using different combinations of fields. This simulation assumes that the CED message blocks from different uploads can be used interchangeably. Moreover, it assumes that the reduced CED is broadcast constantly in a set sequence and that the receiver therefore knows what information it is reading. This way the message blocks have a repeating order, but do not have a set location within the subframe. In Figure 2.2 the computed TTFFD profiles are illustrated for combinations of reserved 1 and an additional bit field. The reserved 1 + 2 and the reserved 1 + 2 + extra curve are identical. The figure clearly shows the TTFFD's step wise behaviour. For example, when only using the reserved 1 field, an average TTFFD of 8 seconds is achieved for a reduced CED size of both 121 and 160 bits. Since TTFFD is invariant over this range, we define the TTFFD target size as the size that yields the lowest SISRE, i.e. the largest size.

We recall that not only the CED is part of the first fix data, the GST is as well. The GST is encoded in the form of a TOW-header, which represents the seconds passed within the week. In the current navigation message this header has a maximum repetition interval of 20 seconds compared to 30 seconds for the CED and therefore has no major impact on the TTFFD. However, if we manage to decrease the repetition rate of the CED to 6 seconds, this changes. To realize an average TTFFD of 6 seconds, the repetition interval of the TOW should be equal to (or less than) that of the CED.

As was explained in Section 2.2.2 the receiver can resolve the time within some tens of milliseconds based on the almanac, the time held by the RTC (accurate to within 2 seconds), and observation of the page-boundaries of the navigation message. Therefore, the full TOW-header does not necessarily have to be read. If, however, the RTC wanders beyond 2 seconds, the additional TOW-headers might be required to resolve the time-ambiguity. As such, it is proposed to provide a TOW repetition rate that is always equal to that of the CED, thereby providing additional service to poorly synchronized receivers, and proving an additional level of redundancy to receivers that are well synchronized.

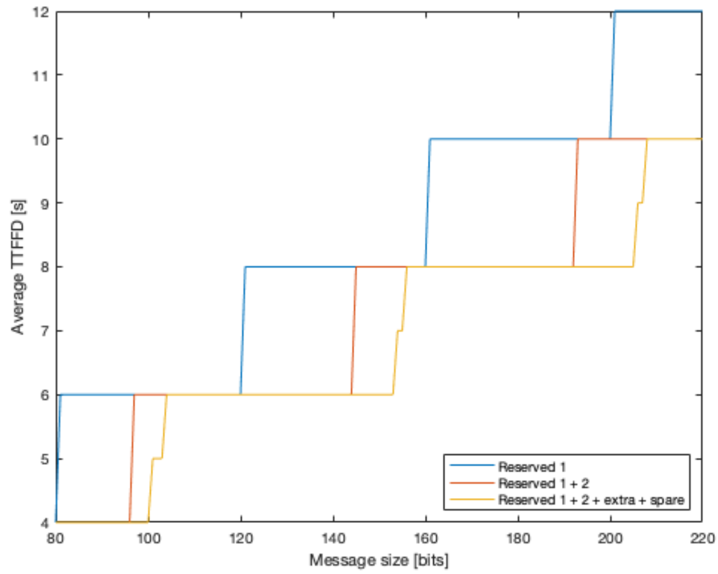

Figure 2.2: Average TTFFD versus message size for different combinations of available fields

The inclusion of these additional 9 bit headers requires extra space. Moreover, the header cannot be divided into smaller parts as it indicates a specific moment in time. Therefore we can either use the reserved extra fields or we include the headers in the reduced CED itself, making it epoch independent. The first option is most attractive for an 8 second TTFFD. The header could then be included at epoch 12 and 19. The second option is more feasible for a 6 second target TTFFD, otherwise the CED and TOW compete for the use of the reserved extra fields.

Based on the TTFFD profiles in Figure 2.2, the inclusion of a 9 bit TOW-header and a 3 bit almanac marker, several TTFFD target sizes are computed. These target sizes are presented in Table 2.2. In all cases the reserved 1 field is included since it provides an essential amount of bits. The most interesting target sizes are the ones that either only use the reserved 1 field or the reserved 1 and 2 fields. This way there is still room in the message for other developments. On the other end of the spectrum, the sizes that use all the fields are also of interest, since these yield the best performance in terms of TTFFD and SISRE. The sizes marked with an asterisk are less realistic since the same fields are assigned to include both CED and TOW, which might not fit. The target sizes that are of particular interest are in bold and further discussed in Section 2.4.

Table 2.2: TTFFD target sizes for different combinations of available fields, average TTFFD and TOW inclusion

Fields used versus maximum size [bits]	**TTFFD - 6 seconds**		**TTFFD - 8 seconds**	
	TOW included	TOW not included	TOW included	TOW not included
Reserved 1	**108**	**117**	**148**	**157**
Reserved 1 + 2	**132**	141*	**180**	**189**
Reserved 1 + Spare	114	123*	156	165
Reserved 1 + Extra	108	117*	148	157*
Reserved 1 + 2 + Spare	138	147*	188	197
Reserved 1 + 2 + Extra	132	141*	180	189*
Reserved 1 + Extra + Spare	117	126*	161	170*
Reserved 1 + 2 + Extra + Spare	**141**	150*	**192**	202*

*Target size is less realistic since the same bit fields are assigned to include both CED and TOW.

2.3. Simulation process & data sets

A simulation is developed to construct reduced sets based on historical data and analyze the performance in terms of position accuracy. This Section discusses the simulation process, what algorithms and in which order are applied and finally how the performance of the output is measured. Next, it discusses the data sets that were used in this research and the cleaning steps that were executed.

2.3.1. Simulation process

The broadcast navigation messages form the simulation's input and are considered as the original CED. The navigation messages thus serve as the "true" orbit. The three reduction strategies can be applied separately to the input set, but it is expected that the biggest reduction in size is achieved when they are combined. The three strategies are applied to the original CED in the following order. First the original CED parameters are expressed relative to the matching almanac parameters. Next, both the relative parameters and the original non-overlapping parameters are truncated to the indicated level. Thereafter, t_{0c} absorption and t_{0e} absorption and shift are applied. Here one should be careful that the absorption is executed with the full yet truncated values of a_{f1} and $\dot{\Omega}$, and not with the relative values. After conversion to binary form, the parameters have reached the state in which they are transmitted. It are these parameter values based on which the new parameter ranges are determined. These ranges are combined with the applied scale factors to compute the total number of bits per parameter.

For the computation of the positioning solution, the receiver can only use information that is available at the time of interest. In the simulation we therefore use the most recent but past broadcast navigation message compared to the time of interest. Which navigation message is most recent is determined based on the transmission time. This approach is deemed more realistic than selecting messages based on the time of ephemeris, since the t_{0e} is not necessarily in line with the time of broadcast (Montenbruck et al. 2018). For the construction of the relative CED, the procedure is similar. Here the most recent almanac update with respect to the transmission time of the original navigation message is used.

In the receiver, the relative parameters are recovered to their full state by adding the matching almanac values. Based on these parameters the state vector at the time of interest is computed. Next, the position error vector is constructed by subtracting the original state vector from the reduced state vector. This position error vector is then transformed from the Earth-centered, Earth-fixed (ECEF) frame to the radial, along-track, cross-track (RAC) frame relative to the original state vector. Together with the error in the clock offset this forms the input for the final SISRE computation. Appendix B.3 describes the transformation and computation in more detail.

SISRE accounts for the accuracy of the navigation message, including ephemeris and satellite clock errors (Warren and Raquet 2003). Montenbruck et al. (2015) point out SISRE is a key performance indicator for the comparison of different GNSSs and also serves the purpose of this research to compare the accuracy of the reduced CED with the original CED. This paper uses the definition of SISRE as outlined by Montenbruck et al. (2018):

$$SISRE = \sqrt{(w_R * R - \Delta cdt)^2 + w_{A,C}^2 (A^2 + C^2)} \tag{2.18}$$

Here w_R and $w_{A,C}$ are constellation-specific weight factors. For Galileo they are found to be $w_R = 0.98$ and $w_{A,C}^2 = 1/61$ (Montenbruck et al. 2015). R, A and C represent the radial, along-track and cross-track components of the position error vector. Lastly, Δcdt denotes the error in the broadcast clock offset multiplied by the speed of light. This computation is applied to each combination of time of interest and CED, yielding a SISRE value per epoch. The root-mean-square (rms) of all SISRE values delivers the final SISRE result. The verification of the various components of the simulation is presented in Appendix C.

It is emphasized that this paper uses SISRE as a relative measure of accuracy. It expresses the accuracy of the reduced set with respect to the original set which corresponds to a SISRE of 0 m. In reality this is not the case. According to Montenbruck et al. (2018) the 2017 rms SISRE value for the Galileo original broadcast ephemeris is at the 0.2 m level with respect to the precise orbit, which serves as the "true" orbit here. However, as we aim to trade-off accuracy for TTFF, the computed relative SISRE values are expected to be at least one order of magnitude larger than the 0.2 m level. The contribution of the original set is therefore deemed negligible.

With regards to position accuracy it is not SISRE but the horizontal position error (HPE) that is finally most important to the user. The HPE can be approximated as follows (Montenbruck et al. 2018):

$$HPE = HDOP * \sqrt{SISRE^2 + UEE^2} \tag{2.19}$$

Here UEE is the user equipment error and HDOP the horizontal dilution of precision. According to Curran (2018) the UEE is on average below 1 meter, but even in extreme cases it is negligible compared to the SISRE levels in this research. HDOP has improved a lot over the past couple of years as more and more GNSS satellites were launched. For Galileo HDOP is around 1.3 (Teunissen and Montenbruck 2017). It is expected to improve to values below 1 as the constellation expands or if multiple GNSSs are used simultaneously for positioning. For now we therefore assume an HDOP value of 1, making the HPE performance neither better nor worse. If we neglect the UEE and assume an HDOP of 1, we can view the HPE as approximately equal to the computed SISRE in the remainder of this article.

2.3.2. Broadcast navigation messages

As was mentioned previously, the historical broadcast navigation messages form the input to the simulation process. Since the actual broadcast navigation messages are not publicly available, the daily navigation files obtained and published by stations of the IGS (Dow et al. 2009) through the Multi-GNSS experiment (MGEX) are used as the original navigation messages (Montenbruck et al. 2014). These receiver independent exchange format (RINEX) files contain orbit, clock and auxiliary data required for the receiver to compute a navigation solution (WG and RTCM-SC104 2015). In addition, a field with the transmission time is added to communicate the time at which the data were broadcast by the satellite. In particular, we make use of the "BRDM" RINEX 3 navigation data product as was suggested by Montenbruck et al. (2018). This research uses a year of BRDM Galileo navigation files dating from 01-10-2017 until 30-09-2018. A year of data represents the changes in the constellation adequately. Moreover, we have chosen to limit the analysis to the most recent year of data possible at the time, since the performance of the broadcast navigation messages has improved over the last couple of years (Montenbruck et al. 2015, 2018). It is therefore expected that the most recent set delivers an outcome that best represents the current situation.

The following data preparation steps have been applied to the broadcast navigation messages to construct the final input data set:

1. All broadcast navigation messages flagged as unhealthy are removed.

2. Double records are removed by filtering out navigation messages with an equal SVID, Galileo week number and transmission time.

3. Navigation messages with unknown transmission times, marked with 0.9999e9, are filtered out. Furthermore, navigation messages where the transmission time does not fall within the possible time range are excluded.

2.3.3. Almanac data

The second historical data set that serves as an input to the simulation are the Galileo almanacs. The almanacs broadcast by the Galileo satellites are published by the European GNSS Service Centre on their website (European GNSS Service Centre 2018). Over the past year the almanac updates for operational satellites have in general been at alternating between 3 and 4 days. For the construction of the reduced sets only the almanacs dating from 01-10-2017 to 30-09-2018 are used.

This research studies the variance over time of all almanacs between 21-11-2014 and 19-10-2018 to make sure they can be used for relative expression. 10 out of 15 active satellites were found to show anomalies in at least one of the following almanac parameters: Ω_0, $\dot{\Omega}$, a_{f0} or a_{f1}. The nature of these anomalies is illustrated based on satellite E05. As can be seen in Figure 2.3, the almanac of satellite E05 shows anomalous peaks at almanac issue 113 for parameters: $\dot{\Omega}$, a_{f0} and a_{f1}, while the other parameters remain smooth over the course of all almanac issues. These peaks do not coincide with a Notice Advisory to Galileo Users (NAGU), nor is the almanac signal health status flagged as unhealthy. Moreover, the anomalies in the almanacs of other satellites do not occur on the same issue date.

To confirm whether these peaks are actually anomalous, two methods are used. First it is checked whether these peaks also occur in the ephemeris parameters. If the satellite would have made an unexpected manoeuvre that is reflected in the almanac, the parameter peaks should also show up in the ephemeris. However, this is not the case. Where the almanac parameters present peaks, the ephemeris parameters remain smooth. Secondly, we check if the anomalies in the almanac parameters indeed correspond to anomalies in the computed position and are not compensated by other other parameters. This is indeed the case. When positioning based on almanac 113, the position error shows an anomaly at the exact same instance. Since the almanac peaks are confirmed anomalous, we do not construct ephemerides relative to these almanacs. Table 2.3 gives an overview of the almanacs per satellite that contain anomalies. Appendix D shows the variation of the almanac parameters for all active Galileo satellites.

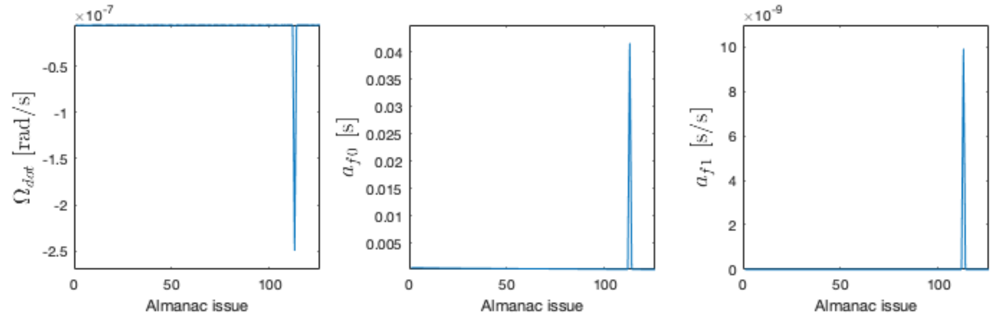

Figure 2.3: Variation of anomalous almanac parameters $\dot{\Omega}$, a_{f0} and a_{f1} for SVID E05

Table 2.3: Anomalous almanac issues per satellite

Satellite	Almanac issue
E02	103, 127
E03	104
E05	113
E09	20, 22, 23, 40, 46, 51, 140, 158
E11	22, 23, 208, 214, 221, 227,229,365
E12	130, 199, 202, 207, 213, 220, 223, 226, 334, 294
E19	306
E24	48, 49, 56, 60, 74, 76, 77 ,78, 150,151, 152
E26	11, 279, 154, 208, 227
E30	83,84

2.4. Results & discussion

This Section presents and discusses the research outcomes. First, the effectiveness of the individual reduction strategies is discussed. Next, the simulation results and the constructed optimal sets are presented. Lastly, the characteristics of the reduced set are described in terms of bit allocation, TTFFD, availability and on-time.

2.4.1. Effectiveness of the reduction strategies

We assess the effectiveness of the individual reduction strategies in terms of size reduction and SISRE contribution. The first reduction strategy, expressing the CED parameters relative to the matching almanac parameters, reduces the size with 76 bits from 428 to 352. Including the required 3 bit almanac marker, this results in a 73 bit net reduction without an increase in SISRE. It is emphasized that this decrease is computed based on the maximum absolute range the parameter has taken on in one year of ephemeris data. No safety margin is applied. When using the reduced set in practice, it is recommended to consider the extent to which an off-nominal orbit should be represented and how this translates to the required parameter ranges.

The second reduction strategy, absorbing t_{0c} and t_{0e}, yields the following results. The absorption of t_{0c} directly saves 14 bits and, moreover, leads to a 1 bit range decrease of a_{f0}. In total a saving of 15 bits is realized by the absorption of t_{0c}. In terms of accuracy, the absorption of t_{0c} corresponds to a SISRE of 0.01 m. This small error is due to the neglect of a_{f2}. Absorbing t_{0e} likewise saves 14 bits. In parallel, the range of Ω_0 increases with 4 bits. The ranges of the other parameters remain equal. This results in a net decrease of 10 bits. The SISRE contribution of t_{0e} absorption and shift is negligible.

The effectiveness of the third reduction strategy, parameter truncation, is assessed based on parameter variation profiles. These profiles show SISRE versus the number of bits allocated to a specific parameter, while the bit allocation to the other parameters is kept constant. As a reference set we have chosen to keep all parameters in full resolution, except for a_{f2} which is assigned zero bits. Without taking a_{f2} into account, we can make a fair comparison between the variation profiles of three selected simulation scenarios: without absorption, with only t_{0c} absorption and with both t_{0c} and t_{0e} absorption. This comparison allows us to see if SISRE is sensitive to different combinations of reduction strategies, or that all simulation scenarios provide the same SISRE.

Figure 2.4 shows the variation profiles of all CED parameters split up into sensitivity categories. It illustrates SISRE is most sensitive to the bit allocation of m_0, Ω_0 and ω. This can be explained by the fact that these are all quickly changing angular parameters that vary over their entire range: $-\pi$ to π. On the other end of the spectrum, SISRE is least sensitive to the bit allocation of $\dot{\Omega}$, i_{dot}, a_{f1}, a_{f2}, C_{uc}, C_{us} C_{ic} and C_{is}. The first four of which are all higher order parameters, logically having less influence than their first order counterparts. The last four have limited effect in radial direction, which is the direction SISRE is measured in. The remaining parameters: $\sqrt{a}$, e, i_0, C_{rc}, C_{rs}, and a_{f0} have an average influence on SISRE. Of these parameters, SISRE is clearly most sensitive to the bit allocation of a_{f0}.

Though the sensitivity of SISRE to the variation of the bit allocation differs per parameter, a general trend can be noticed: the more bits are allocated to a parameter, the lower SISRE and thus the better the accuracy. The presented variation profiles are exactly the same for all three simulation scenarios, proving that for the same bit allocation, all scenarios yield an equal SISRE. Therefore, we can optimize the bit allocation for one simulation scenario and apply the optimal allocation to all three combinations of reduction strategies. We choose to optimize based on the third simulation scenario since this gives us the smallest starting size irrespective of truncation.

The discussed variation profiles are based on a reference set where all parameters are in full resolution except for a_{f2}. If the parameters are fully independent, these variation profiles should have the same shape for any reference set making it straightforward to determine the global optimum per size. Yet, if a form of parameter correlation exists, one should be careful for local optima in the optimization. To search for parameter correlations, we have created variation profiles for the same parameter while changing reference sets. The first correlation we found is illustrated in Figure 2.5. It shows the variation profiles of C_{rc} and C_{rs} for reference sets with a changing bit allocation to a_{f0}. In both figures it is clear the shape of the curves changes for different allocations to a_{f0}, implying that C_{rc} and C_{rs} are correlated with a_{f0}. We can see that if a_{f0} is not in full resolution, SISRE increases as the amount of bits allocated to C_{rc} or C_{rs} passes a certain level. This relation is opposite to the C_{rc} and C_{rs} variation profiles for the full reference set or a set where the bit allocation to other CED parameters was decreased. Due to the existence of parameter correlations, it is important to try out many different allocations to increase the chance of finding a global instead of a local minimum per size. So instead of trying to find all parameter correlations, we leverage the randomness of the Monte Carlo simulation.

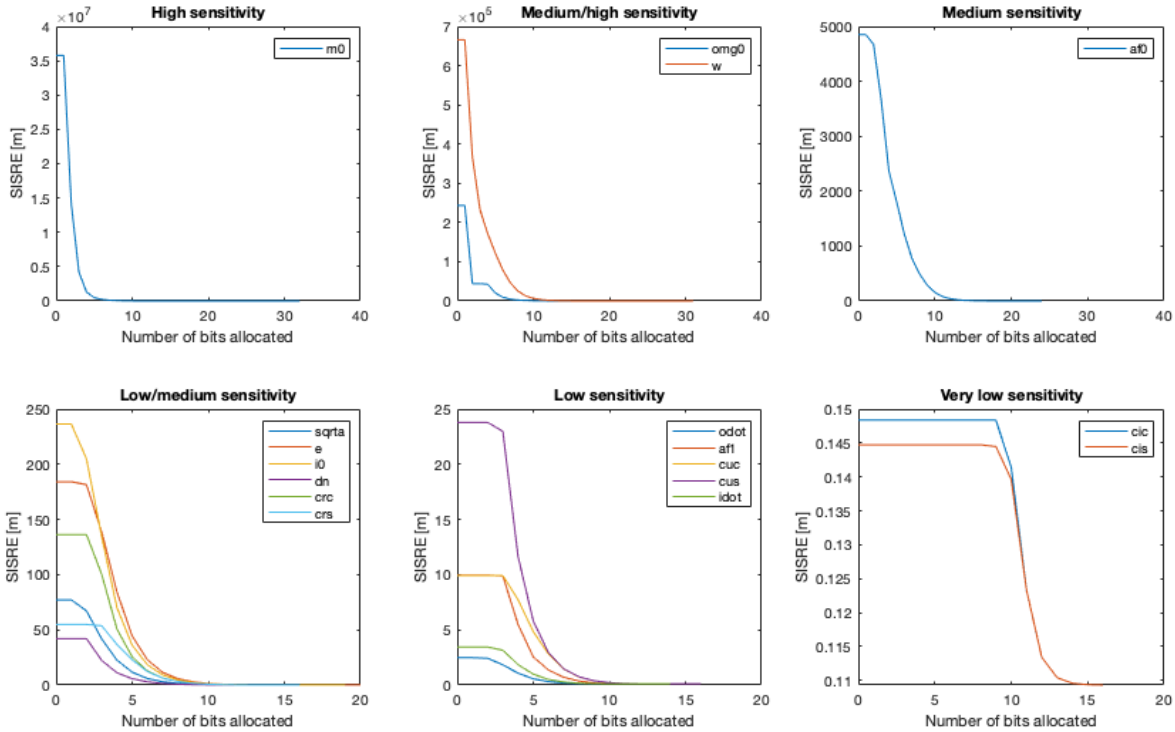

Figure 2.4: Variation profiles illustrating the sensitivity of SISRE to the variation of bit allocation per parameter

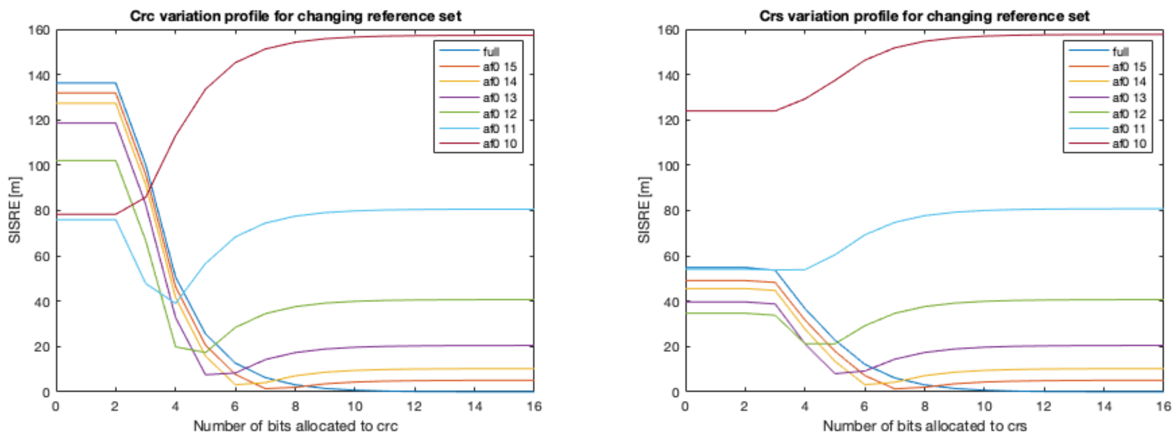

Figure 2.5: Variation profiles of C_{rc} and C_{rs} for different a_{f0} reference sets illustrating the sensitivity of SISRE to the variation of bit allocation per parameter

2.4.2. Optimization of the reduced set

As was mentioned previously, we perform a Monte Carlo simulation for the third simulation scenario: the combination of all three reduction strategies where both t_{0c} and t_{0e} absorption are applied, to obtain the optimal set per CED size. For each size, there is a multitude of ways to divide the bits over the different parameters. The division corresponding to the lowest SISRE is deemed to be the optimal set. To avoid overfitting the model on our specific data set, we have divided the input data set into a train and test set with an 80/20 split. The difference in SISRE between the train set and the test set is consistently below 1 m. This reinforces the assumption that the reduced set is not only optimal for the train data but that its characteristics are universal and that it has the same effect on another set of Galileo I/NAV navigation messages.

Figure 2.6 shows a scatter plot of the CED size versus SISRE based on the aggregated output of all Monte Carlo simulations. The optimal reduced sets are connected with an orange line. As expected, SISRE decreases with an increasing number of bits. A trade-off should thus be made between SISRE and size, i.e. accuracy and TTFF. The identified TTFFD target sizes in Section 2.2.4 aid in making this trade-off. The computed optimal sets in between these target sizes provide only an improvement in SISRE and not in the TTFFD. Table 2.4 shows the TTFFD target size and SISRE of the optimal set for a selection of combinations of TTFFD, fields used and TOW inclusion. The full list of optimal sets per CED size is provided in Appendix D. Depending on the desired TTFFD, the fields that are available and the required accuracy; a reduced set can be selected from this list. For the analysis of the reduced set characteristics in the next Subsection, we select the 132 bit set that includes TOW and delivers a 6 second average TTFFD while only using reserved fields 1 and 2.

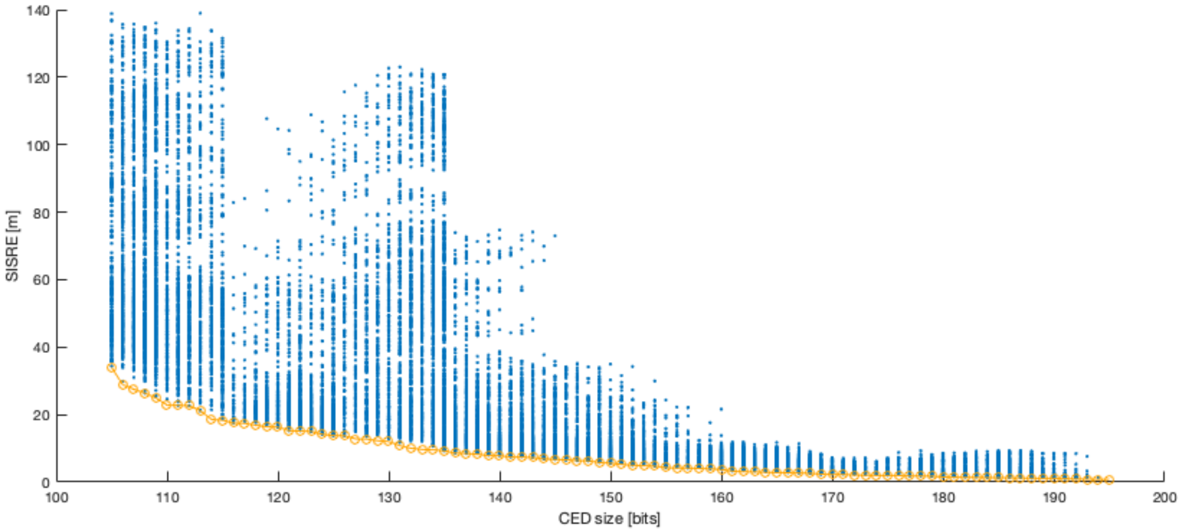

Figure 2.6: Scatter plot of SISRE versus the CED size ranging from 105 until 195 bits for a varying bit allocation per parameter

Table 2.4: TTFFD target sizes and the corresponding SISRE of the optimal set for a selection of combinations of TTFFD, fields used and TOW inclusion

Average TTFFD	**Fields used**	**TOW inclusion**	**TTFFD target size [bits]**	**SISRE [m]**
6 seconds	reserved 1	yes	108	26.35
	reserved 1	no	117	17.40
	reserved 1 + 2	yes	132	10.04
	reserved 1 + 2 + extra + spare	yes	141	7.44
8 seconds	reserved 1	yes	148	6.33
	reserved 1	no	157	4.15
	reserved 1 + 2	yes	180	1.51
	reserved 1 + 2	no	189	1.13
	reserved 1 + 2 + extra + spare	yes	192	0.91

2.4.3. Characteristics of the reduced set

This Section elaborates on the characteristics of the reduced set. The previously selected optimal set serves as an example for further analysis. This set is 132 bits in size, delivers a SISRE of 10.04 meters and with a repetition rate of 6 seconds yields an average TTFFD of 6 seconds. The division of bits over the different parameters and their scale factors are shown in comparison to the original set in Table 2.5. The difference in scale factors indicates the level of truncation that is applied. The remainder of the reduction in number of bits is realized by range decrease. Next, Figure 2.7 shows a curve of the TTFFD versus the epoch of the first available symbol for the reduced set and the original I/NAV message. The dashed lines represent the average values. With 6 seconds the TTFFD of the reduced message is almost 20 seconds smaller than the original average of 25.4 seconds (Anghileri et al. 2013).

Table 2.5: Comparison of clock correction and ephemeris parameters of the Galileo I/NAV message (European GNSS Open Service 2016) and the reduced set

	Number of bits/Scale factor			
Parameter	Galileo I/NAV		Reduced set	
m_0	32	2^{-31}	23	2^{-22}
Δn	16	2^{-43}	6	2^{-33}
e	32	2^{-33}	8	2^{-21}
$\sqrt{a}$	32	2^{-19}	5	2^{-9}
Ω_0	32	2^{-31}	18	2^{-21}
i_0	32	2^{-31}	9	2^{-21}
ω	32	2^{-31}	22	2^{-22}
$\dot{\Omega}$	24	2^{-43}	0	-
i_{dot}	14	2^{-43}	0	-
C_{uc}	16	2^{-29}	6	2^{-19}
C_{us}	16	2^{-29}	7	2^{-20}
C_{rc}	16	2^{-5}	6	2^{5}
C_{rs}	16	2^{-5}	6	2^{5}
C_{ic}	16	2^{-29}	0	-
C_{is}	16	2^{-29}	0	-
t_{0e}	14	60	0	-
a_{f0}	31	2^{-34}	13	2^{-23}
a_{f1}	21	2^{-46}	0	-
a_{f2}	6	2^{-59}	0	-
t_{0c}	14	60	0	-
Total	**428**		**132**	

The presented TTFFD curves assume error free data. In reality, a receiver discards the entire data block when a bit error is present (Anghileri et al. 2013). This means the receiver has to wait the length of an entire subframe before it can read the necessary data again. The impact of this waiting time is five times as large at the original repetition rate of 30 seconds, than at the reduced repetition rate of 6 seconds. Moreover, at an equal bit error rate, the chance of receiving an error free CED increases as the size decreases. To illustrate, if we name the bit error rate per page p_{page} and assume these bit errors are independent of each other, then the probability of receiving an error free ephemeris is defined by p_{full}:

$$p_{full} = 1 - (1 - p_{page})^N \tag{2.20}$$

Where N is the total number of pages that represents a full ephemeris. In the original scenario a full ephemeris consists of 15 pages, in the reduced scenario these are only 3. Figure 2.8 shows the ephemeris error probability at a varying bit error rate per page in the original and the reduced scenario. It demonstrates that the error probability is always lower for the reduced set, except at a p_{page} of 0 and 1. A third and last remark to be made about the chance on receiving a full ephemeris regards an obstructed scenario like in an urban canyon or under foliage. The reduced size of the ephemeris has a positive impact on the chance to receive a full ephemeris in a low signal-to-noise environment.

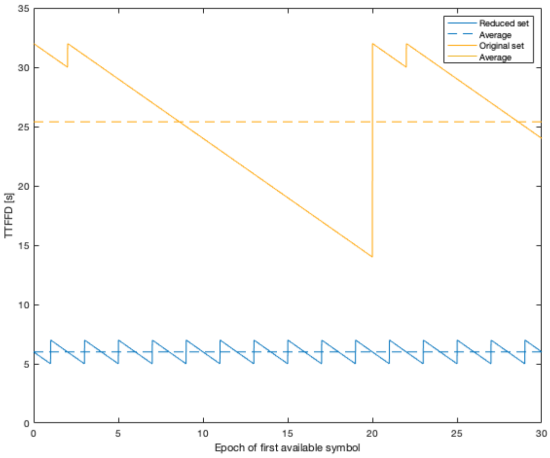

Figure 2.7: TTFFD in case of error free data for the Galileo I/NAV message (Anghileri et al. 2013) and the reduced set

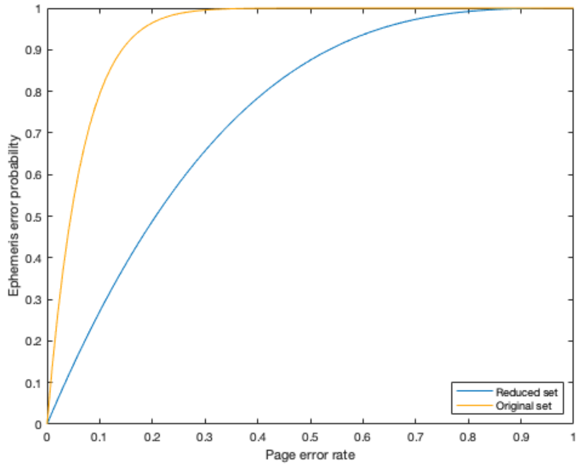

Figure 2.8: Error probability for receiving a full ephemeris in case of the original I/NAV message and the reduced set

The last characteristic to consider is the required on-time. The on-time is defined as the time the receiver has to be "on" to receive first fix data. Fast fix applications that require a high position accuracy can determine their fast, but less accurate first fix based on the reduced CED and can then continue reading the entire navigation message to improve their accuracy based on the full CED. In this case, the position accuracy is only initially degraded. Yet, applications that do not require a high position accuracy can choose to only use the reduced set for positioning and remain at the provided accuracy level. In this case, the receiver on-time is decreased since the receiver can go into a power saving mode as soon as the required data is read.

We distinguish two situations to compute the on-time for. On the one hand, the proposed reduced set can be used for complete standalone positioning. We then assume that the receiver starts without any data. On the other hand, one can also imagine a situation in which a receiver has an internet connection every two days, and in between has to position autonomously. The internet connection can then be used to download the almanac. Here we assume the receiver has an in-memory almanac and an estimation of time held by the RTC.

It takes 12 minutes, or 720 seconds, to read the almanac data. Per week there are two almanac issues broadcast, so the almanac should at least be read twice. The average TTFFD for the original I/NAV message is 25.4 seconds and 6 seconds for the reduced set. Based on these numbers, the on-time is computed while varying the number of times the receiver reads the first fix data. Figure 2.9 shows the difference between the original set, the standalone reduced set and the reduced set with an internet connection every two days. One can see the connected reduced set always performs better. The standalone reduced set has a lower on-time from reading the first fix data 75 times per week or more. This corresponds to a reading interval of 135 minutes, which is a little over two hours.

If we assume the on-time translates to a decrease in power usage of a receiver, the reduced CED becomes not only interesting for fast fix applications desiring to decrease their waiting time but also for low-power applications that do not require a high accuracy, such as freight management (He et al. 2009), wildlife tracking (Forin-Wiart et al. 2015) and stolen goods trackers (Bensky 2016). The internet of things is another segment that is focused on low-power applications and provides huge market potential (European GNSS Agency 2017).

On a critical note, it is emphasized that in reality it is not necessary to read all first fix data to compute a new position. The CED parameters can be read once every validity period which is about two hours or at each new upload which is about every 10 minutes for Galileo. Only the TOW-header has to be read at each positioning epoch. Here it is important to keep in mind that the repetition interval for the TOW-header is significantly lower for the original message than for the reduced message. Overall, there are many configurations possible. Figure 2.9 merely serves as an example to show the possible impact on on-time.

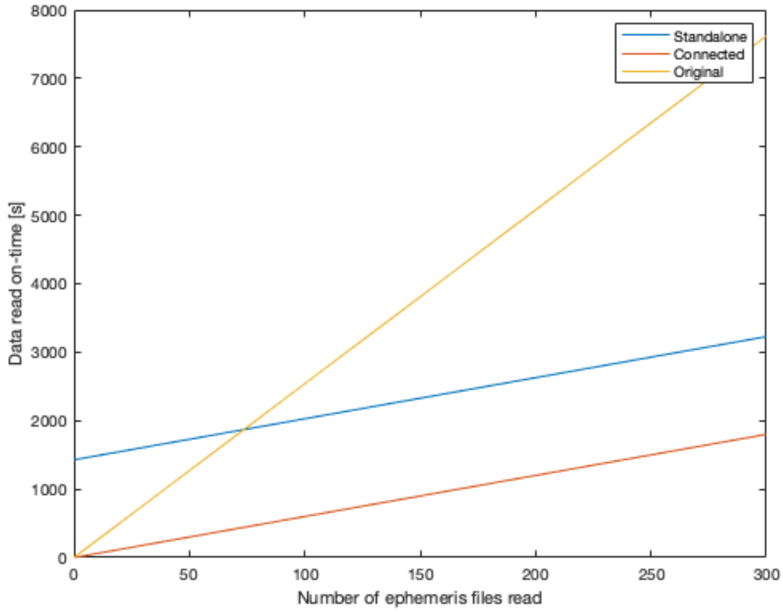

Figure 2.9: On-time versus read ephemerides for the original set, the standalone reduced set and the connected reduced set

2.5. Summary & conclusions

Part of the mass market GNSS users is interested in a faster fix rather than a more accurate position solution. This research therefore aimed to decrease the TTFF at the expense of position accuracy. The TTFF was decreased by focusing on its most dominant component: the TTFFD. In turn, the TTFFD was decreased by reducing the size of the CED and integrating the constructed reduced set into the existing Galileo I/NAV message while maintaining backward compatibility. Upon activation the receiver is assumed to have stored limited data only: the most recent almanac and an estimation of time held by the RTC. Within this work, three reduction strategies were presented to reduce the size of the CED. First, the relative expression of the CED parameters to the matching almanac parameters. This strategy requires the inclusion of an almanac marker such that the receiver is able to identify to which almanac the reduced set is referenced. Second, the absorption of t_{0c} and t_{0e} into related parameters by leveraging redundancies in the user algorithm to compute these parameters. Third, the truncation of the CED parameters, where the optimal parameter bit allocation per CED size was determined by means of a Monte Carlo simulation. The first and second strategy achieve a size reduction without a significant increase in SISRE. The third, in contrast, trades-off size for position accuracy. Subsequently, the constructed optimal reduced set was integrated into the existing Galileo I/NAV message, since it is not only size but also the location and repetition rate of the reduced CED in the navigation message that determine the final decrease in TTFFD.

Based on one year of broadcast navigation messages the effects of the proposed reduction strategies on the size of the CED and TTFFD were computed. As a measure for position accuracy the SISRE relative to original broadcast navigation messages was used. Starting off, the expression of the CED parameters relative to the almanac leads to a reduction of 76 bits. With the required 3 bit almanac marker, this corresponds to a net reduction of 73 bits. Thereafter, the absorption of t_{0c} and t_{0e} results in a further reduction of 15 and 10 bits respectively. Finally, the reduction in size that can be realized by truncating parameters depends on the required SISRE. When combining all three reduction strategies and the TTFFD target sizes, a reduced set can be constructed that occupies 132 bits, i.e. 31% of the original 428 bits, at a SISRE level of 10.04 meters. In this case 195 bits are saved by parameter truncation corresponding to 66% of the size reduction. When integrated in the reserved 1 and 2 fields of the I/NAV message this results in a 6 second average TTFFD. This is almost 20 seconds less than the current average TTFFD of 25.4 seconds. Moreover, the position accuracy is only initially degraded, since the receiver can use the original GNSS signal to improve the accuracy after obtaining a fast first fix.

The achieved decrease in TTFFD benefits fast fix GNSS applications. On the one hand, these applications are connected devices such as a mobile phone, sport watch or navigational device, that are switched into positioning mode after a period of time. On the other hand, these are standalone devices such as search & rescue beacons, freight management and stolen goods trackers that position at longer intervals. By positioning based on the reduced CED, these applications can decrease their waiting time nearly 20 seconds. Moreover, the receiver gains full independence of out-of-band channels for the computation of a fast position fix, which is attractive from a safety, privacy and redundancy perspective.

In addition, the reduced CED has several other characteristics that benefit GNSS users. The impact of a bit error on the TTFF becomes smaller when the repetition rate of the CED decreases from 30 to 6 seconds. Furthermore, at an equal bit error rate, the chance of receiving an error free CED is larger when the size is smaller. Moreover, the time the receiver has to be "on" to read the first fix data is found to decrease in certain situations. Assuming this on-time is proportional to the power usage, a reduced CED is not only interesting for fast fix applications desiring to decrease their waiting time but also for low-power applications that do not require a high accuracy, such as freight management, wildlife tracking and stolen goods trackers. Follow-up research should further research the reduction in on-time and the relation between the on-time and power usage of a receiver.

Another interesting follow-up is to research the effectiveness of the reduction strategies when applied to different parametrizations such as a Cartesian state vector, equinoctial elements or a set where additional parameters are introduced. For example, a Cartesian model would better match the Glonass navigation message. In this case, the parameters could still be expressed relative to the almanac by computing the Cartesian state vectors based on both the full CED and the almanac.

Finally, for the integration of the reduced CED into the existing Galileo I/NAV message, the spare and reserved bits were considered since they are specifically meant for future development. This allows to maintain backward compatibility and only requires receivers that want a faster position fix to change their functionality. For the broadcast of the reduced set, no changes in the Galileo infrastructure or satellite hardware are required. Upon integration it is recommended to further research the interchangeability of CED message blocks and the location of parameters within the subframe. To conclude, the constructed reduced CED provides multiple advantages for GNSS users and should therefore be considered by the management of the European GNSS program as a purpose for the spare and reserved bits of the Galileo I/NAV message. Alternatively, the reduced CED could be used for next generation Galileo or for integration into other GNSS navigation messages.

3
Conclusions & recommendations

In line with the research aim, this research successfully constructed a reduced set of clock correction and ephemeris data that ensures a faster position fix when integrated in the I/NAV navigation message while maintaining backward compatibility. The outcome of this research has the potential to play a pivotal role in the future development of the Galileo navigation message. This Chapter revisits the research questions identified in the Introduction of this thesis and outlines the conclusions that can be drawn from the obtained results. Next, the Chapter wraps up with recommendations for future research.

3.1. Conclusions

The conclusions that are drawn based on the results of this research are presented in the order of the identified research questions. We start off with the sub-questions and then combine all information to finally answer the main research question and expand the conclusions to a high generic level.

How much can the size of the CED be reduced by expressing broadcast CED parameters relative to the matching almanac parameters?

One year of broadcast navigation messages and almanacs were used to compute the effects of the proposed reduction strategies on the CED size, SISRE and TTFFD. The first reduction strategy, the relative expression of the CED parameters to the matching almanac parameters, was found to reduce the CED size with 76 bits from 428 to 352. With the inclusion of a required 3 bit almanac marker this corresponds to a net reduction of 73 bits, i.e. 17.1%, without increasing SISRE. The receiver needs the almanac marker to identify to which almanac the reduced set is referenced. When minimizing the size of the CED it is found that a 3 bit marker in the form of a modulus 8 day-of-year (DOY)-counter is most suitable. Moreover, the receiver has to download the most recent update of the almanac. If the user receiver uses an expired almanac issue to recover the relative CED to full state, the accuracy is degraded to a 100 km level SISRE. This is unacceptable for positioning and must be avoided at all times.

How much can the size of the CED be reduced by absorbing broadcast CED parameters through redundancies in the user algorithm?

The second reduction strategy leverages the redundancy in the Galileo user algorithm to absorb (and shift) the clock time reference, t_{0c}, and the ephemeris time reference, t_{0e}, into related parameters. This leads to a size reduction of 3.5% and 2.3% respectively. Since t_{0c} could not be fully decoupled from the time of interest, a_{f2} had to be neglected resulting in a SISRE contribution of 0.01 m. The exclusion of t_{0c} directly saves 14 bits and an additional bit is saved by a range decrease of a_{f0}. The absorption of t_{0c} thus yields a total size reduction of 15 bits.

The absorption of t_{0e} on the other hand requires an additional shift of the time reference from the beginning of the Galileo week to the beginning of the frame. This is due to the fact that the combination of the t_{0e} and time of interest determine whether a week rollover applies. Since they cannot be decoupled and neither neglected, the shift in time decreases the range such that the week rollover is known in advance. The exclusion of t_{0e} directly saves 14 bits. In parallel, the absorption leads to a 4 bit range increase of Ω_0. Overall, a net size reduction of 10 bits is achieved without an increase in SISRE.

Given the size of the reduced CED, which division of the total number of bits over the individual parameters yields the highest position accuracy?

The third reduction strategy trades-off size versus position accuracy, here expressed as SISRE. We have used a Monte Carlo simulation to determine the optimal set per CED size, i.e. the division of the total number of bits over the individual parameters that yields the lowest SISRE. A list that contains the optimal bit allocation and scale factors for all CED sizes ranging from 105 to 195 bits is presented in Appendix D. SISRE was found to be most sensitive to the bit allocation of m_0, Ω_0 and ω. This can be explained by the fact that these are all quickly changing angular parameters that vary over their entire range from $-\pi$ to π. On the other end of the spectrum, we found SISRE to be least sensitive to the bit allocation of $\dot{\Omega}$, i_{dot}, a_{f1}, a_{f2}, C_{uc}, C_{us} C_{ic} and C_{is}. The first four of these are all higher order parameters, logically having less influence than their first order counterparts. The last four have limited effect in radial direction, which is the direction SISRE is measured in. The remaining parameters: $\sqrt{a}$, e, i_0, C_{rc}, C_{rs}, and a_{f0} have an average influence on SISRE. Of these parameters, SISRE is clearly most sensitive to the bit allocation of a_{f0}. In general, the optimal bit allocation per size is the one that allocates most bits to the highly sensitive parameters and less bits to those that have marginal influence on SISRE.

Furthermore, we found a correlation between C_{rc}, C_{rs} and the clock bias a_{f0}. When the bit allocation to a_{f0} is reduced, from a certain bit allocation on wards, SISRE increases instead of decreases for an increasing number of bits allocated to either C_{rc} or C_{rs}. This behaviour is opposite to the common relation we notice between SISRE and the bit allocation. There is a possibility that more of these correlations exist. The existence of these correlations increases the chance of finding local rather than global optima in the division of bits over the parameters. To increase the chance of finding global maxima, we have run extensive Monte Carlo simulations that can be divided into two types. The first targets a range in size and a range in bit allocation per parameter that is likely to provide optimal results based on the parameter variation profiles. The second simulation targets a specific size but leaves the bit allocation ranges completely random. This way we efficiently find the optimal sets while including sufficient randomness to assure having found a global rather than a local maximum.

Lastly, to avoid overfitting the model on our specific data set, the input data set was divided into a train and test set with an 80/20 split. The difference in SISRE between the train set and the test set was found to be consistently below 1 m. This reinforces the assumption that the reduced set is not only optimal for the train data but that its characteristics are universal and have the same effect on a different set of Galileo I/NAV navigation messages.

How does the size of the reduced CED translate to the TTFFD when integrating this reduced set into the I/NAV navigation message while maintaining backward compatibility?

If the reduced CED is integrated in the reserved and spare bits of the existing Galileo I/NAV message, backward compatibility is maintained. In this case, only receivers that want to make use of the renewed signal are required to change their functionality. Due to the division of the available reserved and spare bit fields over the navigation message, we found that the TTFFD shows a step-wise behaviour. A reduction in size thus does not necessarily result in a decrease in TTFFD. Per TTFFD value we therefore choose the largest possible size as the TTFFD target size, since this results in the lowest SISRE. Depending on which fields are available for use in the I/NAV message, the TTFFD target sizes can be determined and the optimal set can be selected from Table D.2. In addition, the TTFFD is not only influenced by the repetition rate of the CED, but also by the repetition rate of the GST. If one can read the CED every 8 seconds, but the TOW (essential part of the GST) every 20 seconds, the functionality of the reduced set cannot be exploited.

In this research, we have proposed a method for the receiver to resolve the time within some tens of milliseconds based on the almanac, the time held by the RTC (accurate to within 2 seconds), and observation of the page-boundaries of the navigation message. Therefore, the full TOW-header does not necessarily have to be read. If, however, the RTC wanders beyond 2 seconds, additional TOW-headers are required to resolve the time-ambiguity. As such, a TOW repetition rate should be realized that is always equal to that of the CED thereby providing additional service to poorly synchronized receivers, and proving an additional level of redundancy to receivers that are well synchronized.

What is the effect of broadcasting the reduced CED within the I/NAV message on the receiver's availability and on-time?

Besides a faster position fix, the reduced CED has several other characteristics that benefit GNSS users. With regards to availability, the reduction of the CED allows for higher repetition rates. The impact of a bit error on the TTFF becomes smaller when the repetition rate of the CED increases. Moreover, it was shown that at an equal bit error rate, the chance of receiving an error free CED increases when the size of the CED decreases. Especially in low signal-to-noise environments this has a positive impact on the positioning capability of a receiver such as in an urban canyon or under foliage.

Furthermore, fast fix applications that require a high position accuracy can determine their fast, but less accurate first fix based on the reduced CED and can then continue reading the entire navigation message to improve their accuracy based on the full CED. In this case, the position accuracy is only initially degraded. Yet, applications that do not require a high position accuracy can choose to only use the reduced set for positioning and remain at the provided accuracy level. In this case, the research presented several situations in which the time the receiver had to be "on" to read the CED data was decreased. If we assume the on-time translates to a decrease in power usage of a receiver, the reduced CED becomes not only interesting for fast fix GNSS applications desiring to decrease their waiting time, but also for low-power applications that do not require a high accuracy, such as freight management, wildlife and stolen goods trackers. For these applications a sub-meter level accuracy is not necessary, neither does every second count, it is battery life that is crucial. A container at sea needs to be tracked for months consecutively, a wild animal cannot be caught every other week and you do not want to worry about charging your bicycle tracker. The internet of things is another segment that is focused on low-power applications and is becoming increasingly popular.

What is the optimal size of the CED in terms of TTFFD and position accuracy of a GNSS receiver when integrating this reduced set into the Galileo I/NAV message while maintaining backward compatibility?

Based on the answers to the preceding questions, we can conclude there is no straightforward answer to this main question. The optimal size depends on the desired TTFFD, the required SISRE and the available fields in the navigation message. Nevertheless, we opt to sketch a reasonable scenario. It is suspected that not all spare and reserved fields in the I/NAV message can be used for one initiative only. Based on the assumption that it is likely that both reserved fields 1 and 2 may be used, we can achieve a 6 second TTFFD with a 132 bit CED size and an 8 second TTFDD with a 180 bit CED size. The optimal 132 bit CED yields a SISRE of 10.04 m. In this case 66% of the size reduction is realized by truncation. The optimal 180 bit CED yields a SISRE of 1.51 m, of which 59% is realized by truncation. It is expected that users can accept an approximate initial position error of 10.04 m for an average TTFFD reduction from 25.4 to 6 seconds. If a user receiver would position only based on the reduced set to decrease the on-time and possibly power usage, it depends on the application whether a final position accuracy of 10.04 m suffices or that an 8 second TTFFD at 1.51 m is better suited.

In general, the realized decrease in TTFFD benefits fast fix GNSS applications that hold limited data upon activation. On the one hand, these applications are connected devices such as mobile phones, sport watches or navigational devices, that are switched to positioning mode after a period of time. On the other hand, these are standalone devices such as search & rescue beacons, freight management and stolen goods trackers that position at longer intervals. By positioning based on the reduced CED, these applications can decrease their waiting time nearly 20 seconds. Moreover, the receiver gains full independence of out-of-band channels for the computation of a fast position fix, which is attractive from a safety, privacy and redundancy perspective. The reduced CED also improves availability which is especially beneficial in low signal-to-noise environments. In addition, positioning based on the reduced CED was found to decrease receiver on-time and possibly power usage in certain situations. The reduced CED is therefore not only interesting for fast fix applications but also for low-power applications that do not require a high accuracy, such as freight management, wildlife and stolen goods trackers. The low-power GNSS market is growing and provides huge potential.

To conclude, the constructed reduced CED provides multiple advantages for GNSS users and should therefore be considered by the management of the European GNSS program as a candidate for the purpose of the spare and reserved bits of the Galileo I/NAV message. Alternatively, the reduced CED could be used for next generation Galileo or for integration into other GNSS navigation messages.

3.2. Recommendations

The research presented in this thesis has demonstrated a method to construct a reduced CED that upon proper integration into the Galileo I/NAV message leads to a faster first fix, a higher availability and possibly a lower power usage. Yet, before the GNSS user can actually benefit from this improved navigation message, additional research has to be carried out. This Section outlines recommendations for implementation and improvement of the software. Lastly, several recommendations are made for alternative research.

The first step upon implementation regards the integration of the reduced CED into the navigation message. The model this research uses to compute the TTFFD is simplified. It is important to reconsider this model and the assumptions it is based on. The model assumes the CED message blocks can be used interchangeably. In reality, it is suspected this leads to problems at message boundaries when a new reduced set is uploaded. It is recommendable to determine the effect on SISRE of using part of the parameters from a navigation message at upload interval n and part of those at interval $n+1$. If this effect is unacceptable, the addition of an upload marker could be considered. This marker is used to ensure the receiver positions based on a complete set and does not combine parts from different uploads. This would however require additional bits and thereby increase TTFFD, we therefore recommend an alternative approach.

At an average upload interval of 10 minutes and a 6 second repetition rate of the reduced CED, a message boundary occurs once every 100 reduced sets. Since the receiver knows the time, it also knows when a frame boundary occurs. The receiver can be instructed to wait with reading a CED when crossing a frame boundary. This means that 1 in 100 times the TTFFD on average increases to 9 seconds, which has a negligible effect on the overall average TTFFD.

Another assumption that is made in computing the TTFFD is that the reduced set is repeated constantly in a sequential order and that the receiver therefore knows what information it is reading. However, if the number of bits available per subframe is not exactly divisible by the size of the reduced CED, the location of the individual CED parameters within the subframe will change in a repeating pattern. It should thus be determined whether a constant location within the subframe is required for the receiver to know what information it is reading. If so, to make full use of the available fields, one should target a CED size of which the total availability per subframe is a multiple. Alternatively, one can assign a location to each parameter and leave the remainder of the available bits open if it does not fit an entire reduced CED. Alternatively, a page type marker could be used. All measures are expected to influence the TTFFD and the corresponding target size.

The in-depth integration study outlined in the preceding paragraphs, is likely to yield a new set of TTFFD target sizes. With this knowledge, one should use the list of optimal sets per CED size and the corresponding parameter bit allocations and scale factors provided in Appendix D to select a set matching the new TTFFD target size. Next it is required to collect more performance data for this newly selected optimal set. This research gives the performance of the reduced CED is terms of a relative SISRE. By simulating a network of user receivers that all determine their position based on the broadcast reduced set, the effects of satellite geometry, user equipment errors, bit errors, and other user receiver characteristics can be taken into account. We can then determine the impact of the reduced CED on the TTFFD, the TTFF, the availability, the non-relative SISRE and horizontal position error (HPE) in a situation that resembles reality more closely. It is recommended to use the same network of receivers to test how the performance improves if not only the Galileo satellites broadcast the reduced sets, but also the satellites of other GNSSs. Considering this possibility, the compatibility of the constructed reduced set with other GNSS navigation messages and their almanacs should be researched.

Subsequently, it is recommended to further research the effect of on-time on the power usage of a user receiver. Low-power GNSS applications are becoming increasingly popular, resulting in a substantial market potential. Think of freight management, wildlife and stolen good trackers, but also of your mobile phone and the internet of things. If we can prove the reduced set not only ensures a faster position fix but also reduces the power consumption of a user receiver, the attractiveness of including the reduced CED into the I/NAV message increases significantly.

Finally, with regards to implementation, the safety margins for the parameter ranges should be considered. The current bit allocation per parameter is based on the scale factor, the signedness and the maximum absolute value the parameter took on over the course of the researched period: October 2017 - September 2018. It should be researched to what extent it is desirable to be able to represent off-nominal orbits with the reduced set. This could lead to new parameter ranges, possibly increasing the CED size.

When considering the developed software, a Monte Carlo simulation is used to select the optimal set per CED size. This entails that still some form of luck is involved, and that there is a chance that we did not find the optimal sets yet. One could run additional Monte Carlo simulations to increase the chance of finding a global optimum, but a genetic algorithm might be more effective in selecting the optimal bit allocations. Moreover, this could benefit computation time, which is currently a serious limitation of the simulation. In addition, it is recommended to further research the discovered parameter correlations, this would also aid in improving the algorithm to find the optimal sets. Furthermore, this research uses a signed fixed-point binary format to represent the parameters and compute the number of bits. The up-link of the Galileo navigation messages is in a two's complement fixed-point binary format, which is slightly more efficient when presenting both positive and negative values. It is therefore recommended to use this format in follow-up research and in the final broadcast.

Finally, where this research focused on reducing the existing set of CED parameters in the Galileo I/NAV message, it is recommended to also research the inclusion of additional parameters and alternative parametrizations. In the modernized GPS navigation messages some parameters compatible with Keplerian elements were added, including these instead of increasing the bit allocation to other parameters could improve SISRE. The previously recommended research into parameter correlations could aid in selecting additional parameters to include. Next to the modification of the existing set, the benefits of using for example Cartesian or equinoctial elements should also be researched. A Cartesian model would better fit the current Glonass navigation message. Moreover, another parametrization might be able to express an equally accurate position with less parameters. This could lead to a smaller CED size. In case of Cartesian coordinates the almanac can still be leveraged. The receiver should then compute the state vector based on the almanac and the reduced navigation message should contain the satellite position expressed relative to this state vector. It is of interest to know to what extent the Cartesian state vectors overlap, how sensitive SISRE is to the truncation of this state vector, what the final size of this reduced set would be and which method of propagation should be used in the receiver.

A

Galileo I/NAV navigation message

Galileo, the European global navigation satellite system, is intended to be an independent satellite based positioning system providing worldwide service. All Galileo satellites broadcast several navigation messages that contain the necessary information for a user receiver to compute a position-velocity-time (PVT) solution (Teunissen and Montenbruck 2017). In this research we specifically focus on the Galileo I/NAV navigation message. This Appendix gives an overview of the I/NAV message structure and identifies if and where there is room to integrate the constructed reduced CED. Thereafter, the I/NAV message content is outlined and some practical remarks for change are made. The Appendix wraps up with a discussion on the opportunities for integration the Galileo I/NAV message provides.

A.1. Structure of the I/NAV navigation message

In general, the Galileo navigation messages are transmitted as a sequence of so-called frames. Each frame consist of several subframes, that in turn consist of several pages. Only the smallest building blocks, the pages, include a "type" marker with which the content can be identified. There is no way for the receiver to recognize frames or subframes. This "frame, subframe, page" structure allows for sending information at different rates. Data that needs to be instantly available, e.g. integrity data, is included entirely in one page. The clock correction and ephemeris data is contained within a subframe and thereby sent at a medium rate. Long lasting data such as the almanac is spread over the entire frame (European GNSS Open Service 2016) (Teunissen and Montenbruck 2017).

The duration of an I/NAV frame is 720 seconds. This frame consists of 24 subframes with a duration of 30 seconds, which in turn consist of 15 pages with a 2 second duration. The I/NAV message is broadcast on two frequency bands: E5b-I and E1-B. The general structure of the pages is the same for both signals, it is the page sequencing that differs. When using a dual-frequency receiver this allows for fast data reception. Nevertheless, the signal is designed such that it is also compatible with single-frequency receivers. On both frequencies data is sent at a rate of 125 bits per second (bps) (European GNSS Open Service 2016). Most low-cost GNSS receivers make use of the E1-B signal for positioning (Curran 2018).

Typically, each page is composed of a 10 bit synchronization pattern, a 114 bit I/NAV word and 6 tail bits. The synchronization pattern is always the same and allows the user to synchronize with the page boundary. The I/NAV word contains all the useful data. This data is interleaved and forward error correction (FEC) encoded to improve robustness. It consists of a page type marker to identify the page content, a navigation data field and a cyclic redundancy check (CRC) to detect corrupted data. The tail bits enable the completion of the FEC decoding. The two-second pages are split up in an even and odd part, called words. These words are broadcast one after another on the same data channel (Simsky and Boon 2010).

The bit allocation of a nominal I/NAV page is illustrated in Figure A.1. The meaning of the blocks is at this point of secondary importance. Yet, attention must be paid to the so-called spare bits that are meant for future evolution of the message and the reserved bits that are still to be defined in future ESA updates. Figure A.2 shows how the CED and time of week (TOW) information is divided over the I/NAV message subframe for the different channels. The CED is spread over four different words. All four of which have to be read before the user can compute the satellite position. The TOW is also present in four words of which at least one has to be read for a PVT solution. Moreover, the Figure shows the fields marked as reserved (European GNSS Open Service 2016).

A page transmitted on E5b-I has zero spare bits and 72 reserved bits in total, as can be seen in Figure A.1. On E1-B the page has 48 reserved bits. On top of that, the so-called "data" field also contains spare and reserved bits. Different words are sequentially broadcast in this field, as is illustrated in Figure A.2. An overview of the spare and reserved bits and their division over the subframe is presented in Table A.1a and A.1b for E5b-I and E1-B respectively (European GNSS Open Service 2016). Word type 7 is always combined with 8 and word type 9 is always combined with 10. In this overview we have included the word types marked "spare" that contain 88 spare bits each. To illustrate the bandwidth that spare or reserved fields could open up, the following example. Suppose we would use the "reserved 1" field of the I/NAV message nominal page broadcast on E1-B. This would provide 40 bits every odd page, i.e. 40 bits every 2 seconds. For the total subframe consisting of 15 pages this would translate to 600 available bits transmitted at a data rate of 20 bps (Hernández et al. 2014).

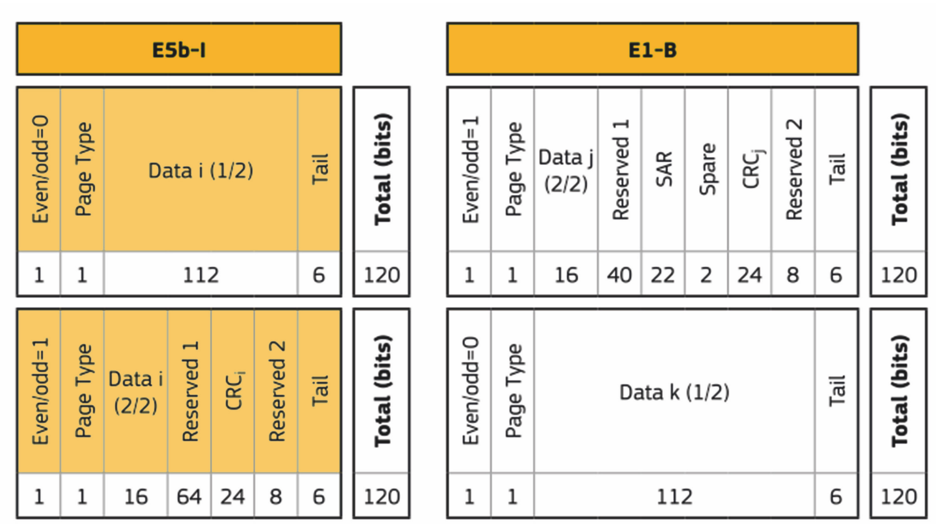

Figure A.1: Bits allocation for I/NAV even and odd nominal pages (European GNSS Open Service 2016)

I/NAV on E-1B

T_0 [s]	Word Type
1	2
3	4
5	6
7	7 or 9
9	8 or 10
11	Reserved
13	Reserved
15	Reserved
17	Reserved
19	Reserved
21	1
23	3
25	5
27	Spare
29	Spare

I/NAV on E5b-I

T_0 [s]	Word Type
0	1
2	3
4	5
6	7 or 9
8	8 or 10
10	Reserved
12	Reserved
14	Reserved
16	Reserved
18	Reserved
20	2
22	4
24	6
26	Spare
28	Spare

TOW
CED
Reserved

Figure A.2: Division of the TOW and CED over the I/NAV subframe on the E1-B and E5b-I channel (European GNSS Open Service 2016)

Table A.1: Division of the spare and reserved bits over the I/NAV subframe under nominal conditions

(a) On channel E5b-I

T_0 [s]	Reserved Bits	Spare Bits
0	74	0
2	72	0
4	72	23
6	If 7: 78, if 9: 72	0
8	72	If 8: 1, if 10: 0
10	200	20
12	200	20
14	200	20
16	200	20
18	200	20
20	74	0
22	72	2
24	72	3
26	72	88
28	72	88
Total if word 7+8	**1730**	**205**
Total if word 9+10	**1724**	**204**

(b) On channel E1-B

T_0 [s]	Reserved Bits	Spare Bits
1	50	2
3	48	4
5	48	5
7	If 7: 54, if 9: 48	2
9	48	If 8: 3, if 10: 2
11	176	2
13	176	2
15	176	2
17	176	2
19	176	2
21	50	2
23	48	2
25	48	25
27	48	90
29	48	90
Total if word 7+8	**1370**	**235**
Total if word 9+10	**1364**	**234**

A.2. Content of the I/NAV navigation message

Now the structure of the I/NAV message is clear, we continue with the content. The navigation message information is generated by the ground segment and is uploaded to the satellites generally at 10 minute intervals (Teunissen and Montenbruck 2017). In turn, the satellites broadcast the information to receivers worldwide. To compute a PVT solution four types of data are required, all of which are outlined below (European GNSS Open Service 2016). The satellite CED and almanac content are described more in depth as they are of specific importance to this research.

1. **Ephemeris parameters** - Used to express the position of the satellite.
2. **Time and clock correction parameters** - Used to compute the pseudorange, i.e. the pseudo distance between the satellite and the receiver.
3. **Service parameters** - Used to identify the set of navigation data and the satellites. These parameters also indicate the signal's health.
4. **Almanac parameters** - Used to calculate a rough estimate of the satellites' positions in the constellation.

The Galileo CED is composed of 16 ephemeris and 4 clock correction parameters. The ephemeris consists of 6 Keplerian parameters, 6 harmonic coefficients, 2 rate parameters, 1 correction parameter and 1 parameter indicating the time reference of the ephemeris. In addition, the message contains 3 clock correction parameters and 1 parameter indicating the time reference of the clock. Table A.2 shows the Galileo CED parameters and characteristics. With these parameters a receiver can compute the position of the satellite's antenna phase center in Earth-centered, Earth-fixed (ECEF) coordinates and the satellite clock correction. The total size of the CED is 428 bits (European GNSS Open Service 2016).

Table A.2: Galileo CED parameters (European GNSS Open Service 2016)

Parameter	Definition	Bits	Scale Factor	Unit
M_0	Mean anomaly at reference time	32*	2^{-31}	semi-circles
Δn	Mean motion difference from computed value	16*	2^{-43}	semi-circles/s
e	Eccentricity	32	2^{-33}	dimensionless
$\sqrt{a}$	Square root of the semi-major axis	32	2^{-19}	$\sqrt{m}$
Ω_0	Longitude of ascending node of orbit plane at weekly epoch	32*	2^{-31}	semi-circles
i_0	Inclination angle at reference time	32*	2^{-31}	semi-circles
ω	Argument of perigee	32*	2^{-31}	semi-circles
$\dot{\Omega}$	Rate of right ascension	24*	2^{-43}	semi-circles/s
i_{dot}	Rate of inclination angle	14*	2^{-43}	semi-circles/s
C_{uc}	Amplitude of the cosine harmonic correction term to the argument of latitude	16*	2^{-29}	radians
C_{us}	Amplitude of the sine harmonic correction term to the argument of latitude	16*	2^{-29}	radians
C_{rc}	Amplitude of the cosine harmonic correction term to the orbit radius	16*	2^{-5}	meters
C_{rs}	Amplitude of the sine harmonic correction term to the orbit radius	16*	2^{-5}	meters
C_{ic}	Amplitude of the cosine harmonic correction term to the angle of inclination	16*	2^{-29}	radians
C_{is}	Amplitude of the sine harmonic correction term to the angle of inclination	16*	2^{-29}	radians
t_{oe}	Reference time ephemeris	14	60	seconds
a_{f0}	SV clock bias correction coefficient	31*	2^{-34}	seconds
a_{f1}	SV clock drift correction coefficient	21*	2^{-46}	s/s
a_{f2}	SV clock drift rate correction coefficient	6*	2^{-59}	s/s^2
t_{0c}	Clock reference time	14	60	seconds

* Indicates the parameter is a two's complement, the sign bit (+ or -) occupies the most significant bit.

Using the almanac, a user receiver can compute the coarse locations of all active satellites in the Galileo constellation which originally aided signal acquisition. In essence, the almanac data is a reduced version of the CED. This commonality is leveraged by using the same algorithm to compute the satellite position independent of the ephemeris or almanac data as input. The parameters that do not overlap are set to zero. The almanac data consist of the following: 6 Keplerian parameters, a reduced set of clock correction parameters, the time of applicability referenced to the almanac week number, some parameters on the satellites' health status and an almanac issue of data to identify the almanac batch. These parameters, together with their assigned characteristics, are presented in Table A.3. For I/NAV the total almanac size including almanac reference is 149 bits (European GNSS Open Service 2016).

A.3. Practical remarks for change in the I/NAV navigation message

Based on ESA's specifications in the Galileo Interface Control Document (ICD), manufacturers have designed receivers capable of processing the Galileo signals for computing a PVT solution. Future changes to the signals and navigation messages should be such that these, by then, legacy receivers can continue to function. This constraint on change is called backward compatibility and is maintained in this research. In addition, it is desirable that the Galileo signals remain compatible and interoperable with other GNSS systems. Despite

Table A.3: Galileo almanac parameters (European GNSS Open Service 2016)

Parameter	Definition	Bits	Scale Factor	Unit
SVID	Satellite ID	6	1	dimensionless
$\Delta(\sqrt{a})$	Difference between the square root of the semi-major axis and the square root of the nominal semi-major axis (29600 km)	13*	2^{-9}	$\sqrt{m}$
e	Eccentricity	11	2^{-16}	dimensionless
δ_i	Inclination at reference time relative to $i_0 = 56°$	11*	2^{-14}	semi-circles
Ω_0	Longitude of ascending node of orbit plane at weekly epoch	16*	2^{-15}	semi-circles
$\dot{\Omega}$	Rate of change of right ascension	11*	2^{-33}	semi-circles/s
ω	Argument of perigee	16*	2^{-15}	semi-circles
M_0	Satellite mean anomaly at reference time	16*	2^{-15}	semi-circles
a_{f0}	Satellite clock correction bias 'truncated'	16*	2^{-19}	seconds
a_{f1}	Satellite clock correction linear 'truncated'	13*	2^{-38}	seconds/seconds
$E5b_{HS}**$	Satellite E5b signal health status	2	N/A	dimensionless
$E1-B_{HS}**$	Satellite E1-B/C signal health status	2	N/A	dimensionless
IOD_a	Almanac Issue of Data	4	N/A	dimensionless
t_{0a}	Almanac reference time	10	600	seconds
WN_a	Almanac reference Week Number	2	1	week

* Indicates the parameter is a two's complement, the sign bit (+ or -) occupies the most significant bit.
** The I/NAV almanac transmitted on the E5b-I and E1-B components contains both the $E5b_{HS}$ and $E1-B_{HS}$ signal health status.

these constraints, the Galileo message includes several degrees of freedom and spare room to allow for the introduction of new features. This potential change should be considered by the designers of receivers. For example, the following reservations are advisable for manufacturers to take into account:

- Only the individual pages of the navigation message contain a "type" marker to communicate the content of each page to the user. No information is supplied about higher-level structures like subframes or frames. It should be taken into account that the order of the different pages is subject to change. Moreover, new page types could be included in the future. A user receiver should therefore be designed such that it is capable of recognizing existing page types in whatever sequence. Additionally, it should respond adequately to page types unknown to the on-board software (European GNSS Open Service 2016).

- In case of I/NAV, the design should take into account that the relative timing between the pages on the different channels (E1-B and E5b-I) could change. For example, this could be caused by the addition of new pages (Teunissen and Montenbruck 2017).

- In the future, spare space within identifier value ranges could be used. For example, the almanac Space Vehicle Identification (SVID) parameter is now defined up to 36 in the ICD. Higher values could potentially be used to represent different data content (Teunissen and Montenbruck 2017) (European GNSS Open Service 2016).

Despite maintaining backward compatibility, the first suggestion would decrease the performance of the original navigation message in terms of TTFF. By adding additional pages the repetition rate of the original CED decreases. It is expected that the addition of pages leads to significant resistance and is therefore not considered for the integration of the reduced CED. The third remark concerns a very limited amount of available space. Compared to the expected size of the reduced CED this is negligible.

A.4. Opportunities for integration

Based on the information presented in this Appendix, we describe the opportunities for integrating the reduced set in the Galileo I/NAV message together with the limiting factors. The existence of spare and reserved bits play a central role. These bits are meant for future evolution of the signal and could thus be put to use to integrate the reduced set. Subsection A.1 identifies a minimum of 1724 reserved and 204 spare bits per I/NAV subframe broadcast on E5b-I. On E1-B this amounts to 1364 reserved and 234 spare bits. To target the majority of the GNSS receivers, we take the availability in the E1-B signal as a reference.

To give an indication of how many bits might be needed, we look at the size of the CED and almanac. As described in Section A.2 the entire CED of one satellite takes up 428 bits. For I/NAV, the less accurate almanac consist of 149 bits. A CED with reduced data size, but somewhat better accuracy than the almanac, probably ends up somewhere between 149 and 428 bits. This means that the spare bits alone do not provide enough space to include several copies of the reduced CED, the reserved fields have to be used for integration as well.

As indicated in Section A.3, when changing a navigation message it is an unquestioned baseline that backward compatibility is ensured such that legacy receivers are not disabled. When only using the spare and reserved bits as previously discussed, this would indeed be the case. Moreover, the signal would then remain compatible with other GNSS systems. Adding new page types is a possibility for integration, but is deemed to have a low chance of actual implementation. To conclude, any change in the Galileo navigation message is finally dictated by the market. A change in the navigation message will only see through when it is strongly believed that it is useful for current and future users.

B
Measures of performance

This Appendix provides background information about three measures of performance that are central to this research: the TTFF, size of the CED and SISRE; discussed in the same order. This Appendix is especially of value for readers that are less familiar with the topic of GNSS and the broadcast navigation message.

B.1. Time to first fix

As mentioned previously, the TTFF is the time it takes a user receiver to compute a first position fix after activation. This study considers a situation which resembles a cold start, i.e. there is no valid navigation data stored in the receiver yet. The only difference with a cold start is that the receiver does already contain the most recent almanac and an estimation of time held by the RTC. More specifically, we focus on the contribution that is in this case most dominant to the TTFF: the TTFFD. Several factors influence the TTFFD. Firstly, the size of the data, i.e. the amount of bits that has to be read. Secondly, the rate at which this data is then broadcast. If the navigation message would only contain first fix data, these two aspects would be decisive (next to robustness). However, the first fix data is only a portion of the navigation message, other information is also broadcast. Therefore, the manner of division of the first fix data over the entire repeating navigation message is also of importance (Anghileri et al. 2012).

To understand the influence of the manner of division of the first fix data on the TTFFD, some explanation is required. Figure B.1 shows the TTFFD of the I/NAV message versus the reading epoch of the first available symbol. The maximum TTFFD is 32 seconds and occurs if the first symbol of a word containing information about the CED is skipped. In this case the receiver has to finish the incomplete word (about 2 seconds) and has to read an entire new subframe (30 seconds). The TTFFD curve reflects that the I/NAV message has four words containing CED parameters, since it contains four peaks. The TTFFD decreases when words are skipped that are not part of the first fix data. For I/NAV, the minimum TTFFD is 14 seconds. As indicated previously the TTFFD does not only depend on the CED but also on the GST. In contrast to the CED, the GST is repeated four times per subframe (including spare words). Since there are several opportunities to obtain the time reference per subframe cycle, it does not cause any peaks in the TTFFD curve (Anghileri et al. 2013).

It is possible to create similar TTFFD curves for other navigation messages. Their behaviour is dictated by the repeat intervals of the CED and GST presented in Table B.1 (Paonni et al. 2010). It is interesting to take a look at how these repeat intervals influence the final TTFFD performance. Anghileri et al. (2013) assessed the TTFFD performance of all six civil GPS and Galileo signals. The results are shown in Table B.2. We can judge that the main factor influencing the TTFFD is the maximum interval between the broadcast of two CED or GST sets. Minimizing only one of them, does not improve the overall TTFFD performance.

The GPS L1C signal has the shortest maximum repetition interval and therefore outperforms the other signals with regards to timeliness. The low repetition intervals are made possible by designing the CED messages such that they are invariant over a known period of time and use an overlay code on the pilot component for frame synchronization. This enables the user to combine the data from different frames in the navigation message (Betz et al. 2006). When looking at the other signals, we see that the TTFFD is penalized for adding

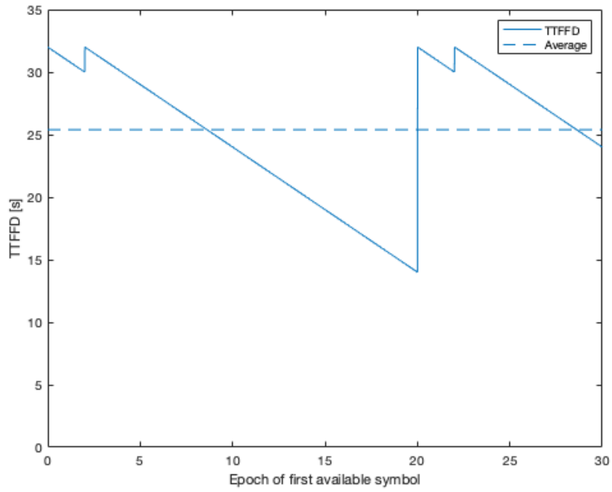

Figure B.1: Galileo I/NAV navigation message TTFFD versus the epoch of the first available symbol in case of error free data and the average TTFFD (Anghileri et al. 2013)

information other than the first fix data. Especially for the Galileo E1-B and E5b signals this is the case. These signals have by far the highest data rate, at least more than twice all the other data rates. If only broadcasting the first fix data this signal would be quickest. Yet, for Galileo it has been decided to incorporate a lot of extra information to the navigation message. On the one hand, this adds useful features to the signal, on the other hand it results in relatively long intervals between the separate CED sets. Consequently, the high data rate cannot be properly exploited to realize the desired low TTFFD (Anghileri et al. 2013) (Zhou et al. 2014).

Finally, the previously described TTFFD performance assumed the reception of error free data. In reality, the signal is subject to errors. A user receiver discards an entire message block if, after decoding, these errors remain. This means the receiver has to wait for that information until it is repeated. The effect of the introduction of bit errors is illustrated in Figure B.2. It shows the cumulative distribution function of the Galileo I/NAV message broadcast on E1-B. The introduction of bit errors results, as expected, in a jump of 30 seconds in the TTFFD. This jump corresponds to the time it takes to read an entire new subframe. The error probability can be reduced by designing a robust navigation message. The higher the message robustness, the lower the number of discarded message blocks is and finally the average TTFFD (Anghileri et al. 2013).

Table B.1: Repetition intervals of CED and GST for GPS and Galileo signals. Adapted from Paonni et al. (2010) with information from Global Positioning Systems Directorate (2015)

GNSS	Signal	Navigation Message	GST Interval [s]	CED Interval [s]
GPS	L1 C/A	NAV	6	30
GPS	L2C	CNAV	12	48
GPS	L5	CNAV	6	24
GPS	L1C	CNAV-2	18	18
Galileo	E1-B/E5b	I/NAV	20	30
Galileo	E5a	F/NAV	50	50

Table B.2: TTFFD performance of GPS and Galileo signals (Anghileri et al. 2013)

Navigation System	GPS				Galileo	
Channel	L1 C/A	L2C	L5	L1C	E1 OS/E5b	E5a
Message	NAV	CNAV	CNAV	CNAV-2	I/NAV	F/NAV
Average [s]	29.4	51.0	25.5	18.0	25.4	53.0
95% [s]	35.5	59.2	29.6	18.0	31.6	59.4
Worst case [s]	36.0	60.0	30.0	18.5	32.0	60.0

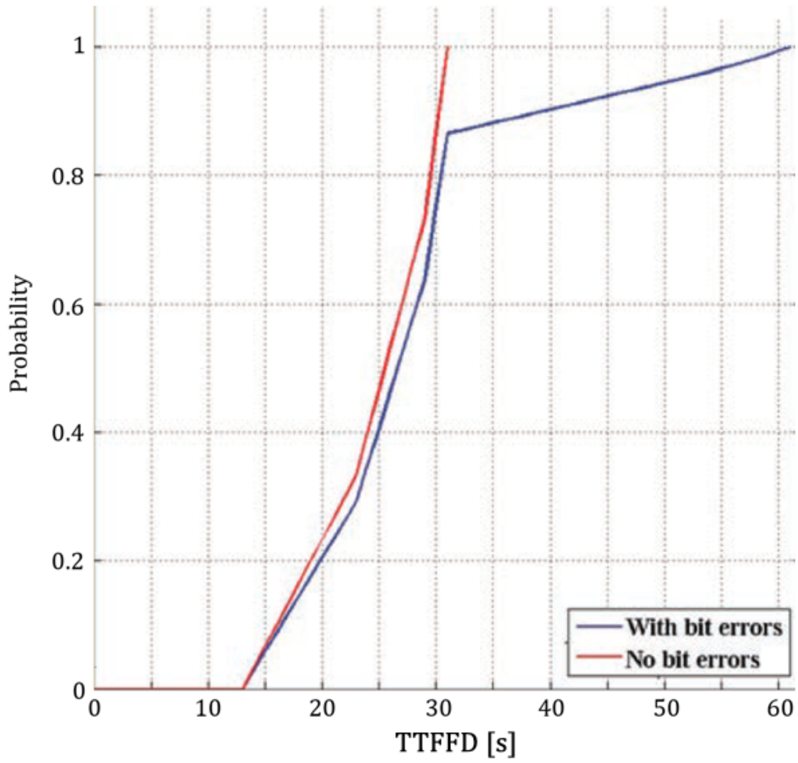

Figure B.2: Cumulative distribution function of the TTFFD of the Galileo E1-B I/NAV message with the introduction of bit errors in the CED blocks (Anghileri et al. 2013)

B.2. Size of the CED

The second measure of performance we discuss, is the size of the CED. This size is the sum of the individual bit allocations per parameter. The CED is broadcast by the Galileo satellites in a fixed-point binary representation (Anghileri et al. 2012). In this research we use a signed format to represent both positive and negative values. In this format the number of bits allocated per parameter depends on three factors: the range, scale factor and signedness. To illustrate this concept, a ruler analogy is used. If we would have unlimited bits we could represent any number with infinite precision. However, we want to minimize the size of the CED and are therefore limited by two constraints. First, we should make sure the values of the parameters do not fall out of range. In other words, if the satellite is at 20000 km, but the selected ruler can measure only up to 10000 km. The satellite's position cannot be represented and accuracy is degraded heavily. Secondly, we want to be able to know the satellite's position at a certain resolution. If the marks on the ruler are selected to be 1 meter apart, the satellite's position cannot be indicated at centimeter resolution. The scale factor is thereby simply the distance between two marks. The larger the required range and resolution, the more bits are necessary. The combination of range, scale factor and signedness finally determines the number of bits transmitted per parameter, and consequently the total size of the CED and level of accuracy with which the user can determine its position. In equation form the number of bits per parameter can be computed as follows:

$$\text{range} = \max(\text{abs}[\text{lower limit}, \text{upper limit}]) \tag{B.1}$$

$$\text{number of bits} = \text{ceil}(\log_2(\text{range}/\text{scale factor}) + \text{signedness}) \tag{B.2}$$

Here the range is the maximum absolute value the parameter should be able to represent, the scale factor is a power of two and signedness can be either 0 or 1 depending on whether the parameter can have a negative value (Parhami 1999).

B.3. Signal-in-space ranging error

The final measure of performance that is outlined is SISRE. SISRE accounts for the accuracy of the broadcast navigation message, including ephemeris and satellite clock errors (Warren and Raquet 2003). Montenbruck et al. (2015) point out SISRE is a key performance indicator for the comparison of different GNSSs. It also serves the purpose of this research to compare the accuracy of the reduced CED with the original CED. This thesis uses the definition of SISRE as outlined by Montenbruck et al. (2018):

$$SISRE = \sqrt{(w_R * R - \Delta cdt)^2 + w_{A,C}^2(A^2 + C^2)} \tag{B.3}$$

Here w_R and $w_{A,C}$ are constellation-specific weight factors. For Galileo they are found to be $w_R = 0.98$ and $w_{A,C}^2 = 1/61$ (Montenbruck et al. 2015). R, A and C represent the radial, along-track and cross-track components of the position error vector. Lastly, Δcdt denotes the error in the broadcast clock offset multiplied by the speed of light. It is emphasized that this research uses SISRE as a relative measure of accuracy. It expresses the accuracy of the reduced set with respect to the original set. The original set thus serves as the "true" orbit and corresponds to a SISRE of 0 m. In reality this is not the case. According to Montenbruck et al. (2018) the 2017 root mean square (rms) SISRE value of the Galileo original broadcast ephemeris is generally at the 0.2 m level with respect to the precise orbit, which serves as the "true" orbit here. However, since we trade-off position accuracy for TTFF, the computed relative SISRE values are expected to be at least one order of magnitude larger than the 0.2 m level. The contribution of the original set is therefore deemed negligible.

As indicated, the radial, along-track and cross-track components of the position error vector are required to compute SISRE. We now elaborate on acquiring these components. The user algorithm provides the state vector in the ECEF coordinate system. To convert the satellite state vectors to the relative RAC system, we define a target and a chaser. The RAC system is centered at the target. Next, the chaser's position and motion are expressed relative to this moving target. We define the state vector based on the original broadcast ephemeris as our target and the state vector based on the reduced ephemeris as our chaser. To obtain the position error vector in RAC, we start by computing the inertial velocity vector of the target:

$$\mathbf{v}_{target,I} = \mathbf{v}_{target,ECEF} + \dot{\omega}_e[-y \quad x \quad 0]^T \tag{B.4}$$

Here x and y refer to the target position vector. $\dot{\omega}_e$ is the Earth's rotational speed in rad/s. Next, we obtain the position error vector in ECEF, $\mathbf{r}_{error,ECEF}$, by subtracting the target position vector from the chaser position vector. The ECEF position error vector can then by transformed to RAC with the following transformation matrix, $M_{ECEF->RAC}$ (Vallado 2003):

$$\hat{R} = \frac{\mathbf{r}}{|\mathbf{r}|}, \quad \hat{C} = \frac{\mathbf{r} \times \mathbf{v}}{|\mathbf{r} \times \mathbf{v}|}, \quad \hat{A} = \hat{C} \times \hat{R}, \quad M_{ECEF->RAC} = [\hat{R}\hat{A}\hat{C}]^T \tag{B.5}$$

Where $\mathbf{r}$ and $\mathbf{v}$ are respectively the ECEF position and inertial velocity vector of the target body. Finally, the RAC position error vector is computed as:

$$\mathbf{r}_{error,RAC} = M_{ECEF->RAC} * \mathbf{r}_{error,ECEF} \tag{B.6}$$

Together with the error in the clock offset, the components of this RAC position error vector form the input to the SISRE computation.

C
Verification

When developing software, verification and validation are paramount. These processes let themselves be described respectively as: "are we building the product right?" and "are we building the right product?" More specifically, with verification we ensure the software is free of bugs and other errors. With validation we check whether the right problem is solved. This Appendix describes the verification steps that were executed to make sure the simulation works as it is supposed to. Since the proposed method is completely new, we cannot validate the "product", i.e. the performance of the reduced set, by reconstructing the results of other researches. In fact, the simulation itself is a series of experiments based on historical data to find out the properties of the product. We therefore consider the simulation as the validation of the product of which the outcome is presented and discussed in Section 2.4 and Appendix D.

On the basis of Figure C.1, we go through the verification steps in more or less sequential order. This Figure is a software flow chart showing the input data, the processing steps and the created output data of the simulation. Only the more elaborate steps or steps with a surprising outcome are discussed. The simple tests and/or comparisons with analytic results are disregarded in this Appendix for reasons of conciseness.

C.1. Construction of the relative CED and recovery of the full state

The first step in the simulation process is the construction of the relative CED, which is a straightforward procedure. The almanac parameters are simply subtracted from the matching original CED parameters. To check whether this procedure works the way it is supposed to, we undo it by adding the parameters of the reference almanac again. This is equivalent to the module: "convert back to full state". In theory, the original CED and the recovered CED should be exactly equal when no truncation nor absorption is applied. SISRE should be zero. Yet, it turns out SISRE is at a 10^{-9} m level. When studying the mean and standard deviations of the difference between the original and recovered parameters, it is found the differences are due to Matlab rounding errors. Nevertheless, the SISRE contribution is deemed negligible compared to the expected overall SISRE budget. The modules are thus confirmed verified.

C.2. Truncation and absorption

The truncation module is verified based on the test set provided by Anghileri et al. (2012). Here the number 0.00987536064349115 is truncated from 32 to 22 bits through a scale factor increase from 2^{-31} to 2^{-21}. After truncation the value should become 0.00987541675567627. This is indeed the case. The difference between the verification value and the module outcome is zero. Subsequently, the absorption modules are verified by checking if the clock correction Δ_{SV}, the mean anomaly M, the inclination i and the right ascension Ω have an equal value with and without application of the absorption modules. Since the t_{0c} absorption module neglects a_{f2}, its contribution has to be added as well. Except for some negligible rounding errors, all values match. The modules thus work as they are intended to.

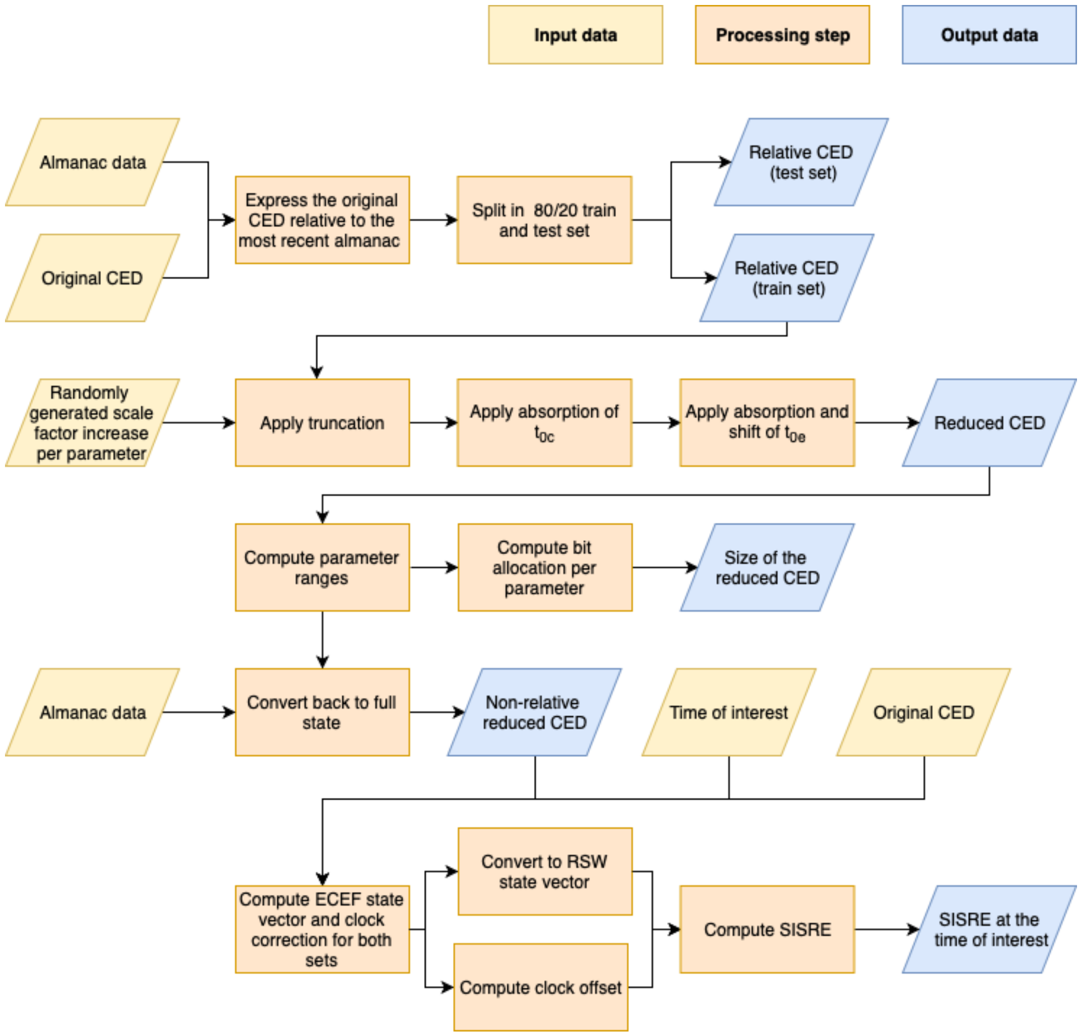

Figure C.1: Software flowchart of the developed simulation

C.3. ECEF state vector computation

The module that computes the ECEF state vector is based on the user algorithm presented in the Galileo ICD (European GNSS Open Service 2016). The ICD does not provide any examples for verification, so a GPS example by Remondi (2004) is used. This example is suitable for comparison since the working principle of both user algorithms is the same. When using the input set represented in Table C.1, the results presented in Table C.2 are computed. We can see there is a negligible difference between the verification value and the computed value. The minor differences can be attributed to the use of a limited precision machine (Remondi 2004). The module is deemed verified.

Table C.1: Input values for the verification of the state vector computation (Remondi 2004)

Parameter	**Value**	**Unit**
$\sqrt{a}$	5153.79589081	$\sqrt{m}$
m_0	1.05827953357	rad
e	0.00223578442819	-
i_0	0.961685061380	rad
Ω_0	1.64046615454	rad
ω	2.06374037770	rad
Δn	0.465376527657e-08	rad/s
i_{dot}	0.342514267094e-09	rad/s
Ω_{dot}	-0.856928551657e-08	rad/s
C_{us}	0.177137553692e-05	rad
C_{uc}	0.457651913166e-05	rad
C_{rs}	88.6875000000	m
C_{rc}	344.968750000	m
C_{is}	-0.856816768646e-07	rad
C_{ic}	0.651925802231e-07	rad
t_{oe}	93600.0	s
t	86400.00	s

Table C.2: Comparison of the verified and computed state vector

Parameter	**Verification value**	**Computed value**
x [m]	-12611434.19782218519	-12611434.19782219
y [m]	-13413103.97797041226	-13413103.97797042
z [m]	19062913.07357876760	19062913.07357876
$\dot{x}$ [m/s]	266.2803795674	266.28037957
$\dot{y}$ [m/s]	-2424.7683468482	- 2424.76834685
$\dot{z}$ [m/s]	-1529.7620784616	- 1529.76207846

C.4. Conversion ECEF to RAC coordinate system

For the computation of SISRE the position based on the reduced set must be expressed relative to the position based on the original set, i.e. the true set. This is done by converting the position error vector from the ECEF coordinate system to the radial, along-track, cross-track (RAC) coordinate system where the position based on the original set serves as the origin. The transformation from ECEF to RAC is verified based on data from Williams (2014). Here, the transformation from ECEF to local vertical, local horizontal (LVLH) is explained. Vectors in LVLH and RAC are equal in magnitude but differ in direction. They are related to the components in Equation B.5 as follows: $\hat{\mathbf{e}}_x = \hat{A}$, $\hat{\mathbf{e}}_y = -\hat{C}$ and $\hat{\mathbf{e}}_z = -\hat{R}$ (Vallado 2001). Table C.3 shows the input values as used by Williams (2014). Table C.4 then compares the verification with the computed values. We can see the values are equal, thereby verifying the module.

Table C.3: Input ECEF state vectors based on the 'true' and reduced set for the verification of the ECEF to RAC transformation (Williams 2014)

Parameter	Verification value
x_{true} [m]	-2301672.24489839
y_{true} [m]	-5371076.10250925
z_{true} [m]	-3421146.71530212
$\dot{x}_{true}$ [m/s]	6133.8624555516
$\dot{y}_{true}$ [m/s]	306.265184163608
$\dot{z}_{true}$ [m/s]	-4597.13439017524
x_{red} [m]	-2255213.51862763
y_{red} [m]	-5366553.94133467
z_{red} [m]	-3453871.15040494
$\dot{x}_{red}$ [m/s]	6156.89588163809
$\dot{y}_{red}$ [m/s]	356.79933181917
$\dot{z}_{red}$ [m/s]	-4565.88915429063

Table C.4: Comparison of the verified and computed RAC error vector

Parameter	Verification value	Computed value
x [m]	56935.52933486611	56935.52933486611
y [m]	38.16029598938621	38.16029598939
z [m]	2845.326754409645	2845.32675440964
$\dot{x}$ [m/s]	4.890395234717321	4.89039523472
$\dot{y}$ [m/s]	-0.09759947085768417	-0.09759947086
$\dot{z}$ [m/s]	-0.8044815052666578	-0.80448150527

C.5. SISRE computation

The computation of SISRE is difficult to verify due to the lack of input-output examples. Many researches use SISRE as a measure of accuracy but do not disclose their exact input data. Moreover, these researches mostly use SISRE as an absolute measure in which the true orbit is a precise one. In this case there are many more things to take into account than when computing a relative SISRE where the true orbit is based on broadcast ephemerides. Among others, the antenna off-set should be included, since the precise ephemerides are referenced to the center of mass and the broadcast ephemerides are referenced to the antenna (Montenbruck et al. 2018).

An exception is the research published by Anghileri et al. (2012), it also uses SISRE to compare a reduced navigation message to the original navigation message. Although they use a different method and GPS data, we can use their parameter settings and outcome to verify if the SISRE module yields a value in that agrees to reasonable extent. Where Anghileri et al. (2012) reports an average 3D rms position error of 85.9 m and an average SISRE of 50.3 m, the computation module yields an average 3D rms position error of 111.2 m and an average SISRE of 70.1 m. The verification and computed values are not the same but agree to a reasonable level. Moreover, the average SISRE is in both cases about 60% of the average 3D rms position error. The module is therefore deemed partially verified.

In addition, the computed SISRE values match the expectations. For example, a higher level of truncation yields a higher SISRE. It thus satisfies sanity checks. Lastly, since SISRE is computed relative a computational error affects the reference value in the same way as it affects the evaluated value. This limits the effects of errors in the computation of the input values and finally on SISRE.

D

Additional results

This Appendix provides results in addition to those presented in Section 2.4. These could not be included in the article for reasons of conciseness. It is likely that this Appendix is included to the article as well. First, the elaborate results of the almanac analysis are presented. Second, we detail the outcomes with regards to the optimal set. An overview of the size reduction based on the first reduction strategy is given, the full list of parameter bit allocations per size is presented and the universality of the optimal set is validated.

D.1. Almanac analysis

This Section presents the variation of the almanac parameters over time for all Galileo satellites considered in this research, except for satellite E04 which has already been shown in Figure 2.1. The almanacs of satellite E01, E07, E08, E22 presented in Figure D.2, D.6, D.7 and D.12 contain no outliers that affect the range of the relative ephemeris parameters. In contrast, the almanacs of satellites E02, E03, E05, E09, E11, E12, E19, E24, E26 and E30 presented in Figure D.3, D.4, D.5, D.8, D.9, D.10, D.11, D.13, D.14 and D.15 do contain these types of outliers.

As was discussed in Section 2.3.3 the anomalous almanac issues that were indicated in Table 2.3 are not used for constructing a reduced CED. The source of the anomalies has not been established. They might originate at computation by the ground segment or at the upload of the parameters to the website. If the reduced CED is implemented, it is expected that these anomalous parameters are no longer broadcast, since the range of the reduced parameters will not suffice. The ground segment is therefore obliged to correct the parameters to fit the range before broadcast.

D.2. Optimal reduced sets

One of the main outcomes of this research is the constructed reduced set about which we now present some more elaborate results. First the achieved size reduction per parameter is provided based on the first reduction strategy. Next, an overview is presented of all optimal sets that we found and their corresponding bit allocation and scale factor per parameter. Lastly, we discuss the universality of the reduced set.

By expressing the CED parameters relative to the matching almanac parameters, the reductions presented in Table D.1 are realized. In total a size reduction of 76 bits is achieved without an increase in SISRE. However, since the inclusion of a 3 bit almanac marker is required, the net reduction comes down to 73 bits. Upon analyzing the individual reductions per parameter, we see that the quickly changing angular parameters: Ω_0, ω and m_0, experience a limited range decrease. This makes sense since they vary between -π and π within one almanac issue, thereby needing their entire range and leaving no lasting overlap. The more slowly changing parameters allow for a larger reduction, since the almanac basically has "time" to keep up, ensuring a large continuous overlap in parameter value.

Next, Table D.2 lists the optimal reduced sets that were constructed with their corresponding parameter bit allocation and scale factor ranging from a CED size of 105 to 195 bits. C_{ic}, C_{is}, a_{f2}, t_{0e} and t_{0c} were not included in this list as they are assigned zero bits in each set. The size without absorption of t_{0c} and t_{0e} and can be computed by adding 15 and 10 bits to the CED size respectively. The bit allocation then no longer holds, since the absorption also has an influence on the parameter ranges. If another TTFFD target size is determined, the presented table can be used to find the corresponding optimal set.

Lastly, a Monte Carlo simulation is used to find the optimal set per CED size. We want to avoid overfitting the model and reinforce the assumption that this set is not only optimal for the input data, but that it is also likely to be optimal for another set of Galileo navigation messages. In other words, we want to validate that we found a universal characteristic, rather than a specific characteristic of the input data. For this purpose, the input to the Monte Carlo simulation is divided into a train and test set with an 80/20 per cent split. First, the optimal sets per CED size are determined based on the training data only. Next, the found bit allocation of these optimal sets is applied to the test data and the difference between the test and train SISRE levels is computed.

Figure D.1 shows SISRE per optimal set for both the train and test data. Both curves follow each other closely. The largest difference between the two sets is 0.7827 m, which is a 6.6% difference with respect to the SISRE of the test set. This difference is deemed small enough to state the optimal sets are not only optimal for the data the model trained on, but also for an entirely new set of Galileo I/NAV messages. It thereby validates the universality of the characteristics of the optimal set. Of course this is no complete guarantee, but it does provide an important reinforcement.

Table D.1: Size reduction per parameter realized by relative expression

Parameter	**Original size [bits]**	**Relative size [bits]**
$\sqrt{a}$	32	15
e	32	20
i_0	32	19
Ω_0	32	28
ω	32	31
m_0	32	32
$\dot{\Omega}$	24	13
a_{f0}	31	24
a_{f1}	21	10

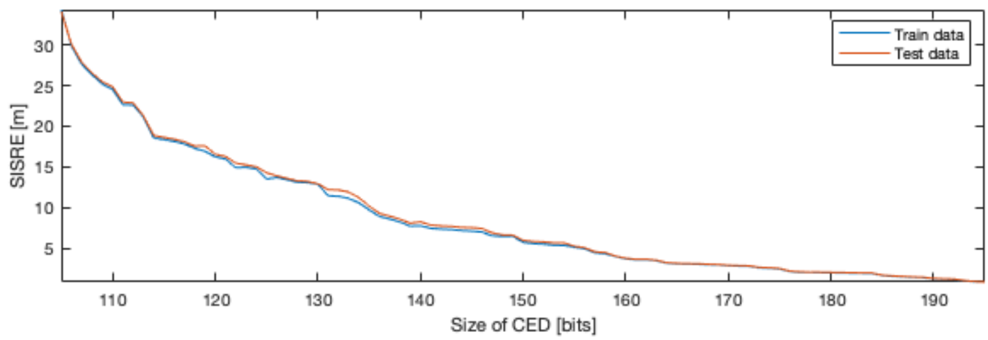

Figure D.1: Comparison of SISRE with the optimal set applied to test and train data

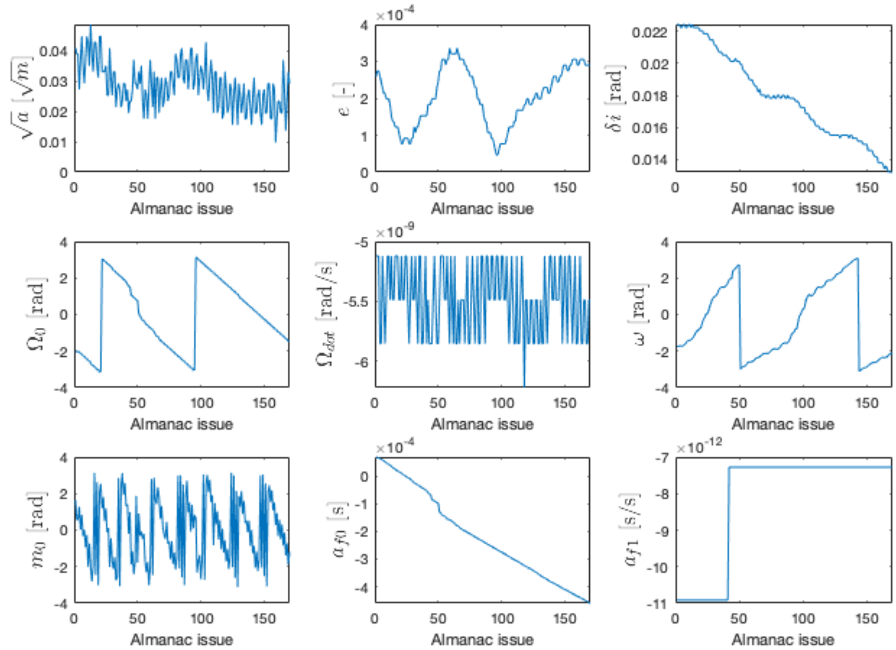

Figure D.2: Variation over time of the almanac parameters for SVID E01

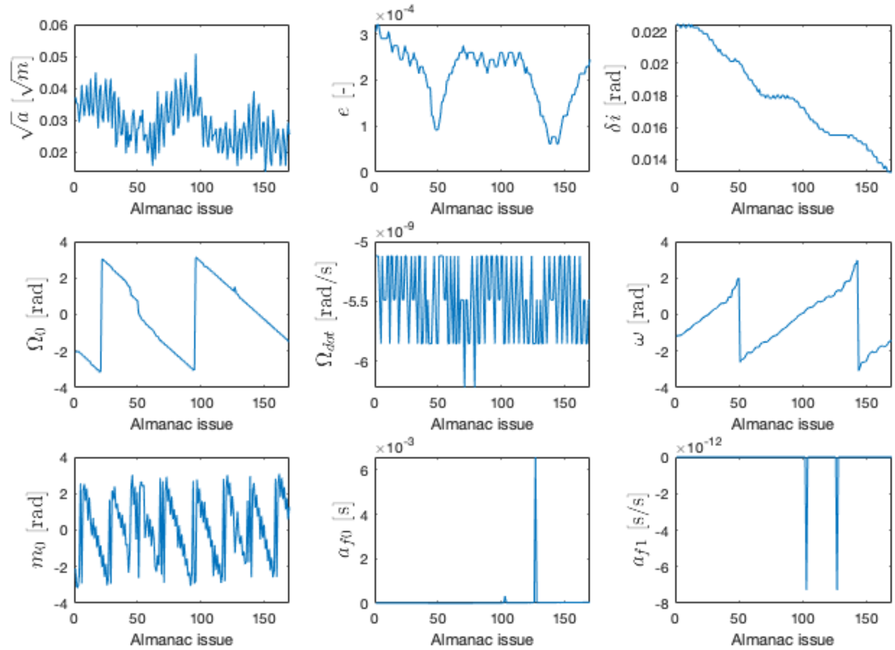

Figure D.3: Variation over time of the almanac parameters for SVID E02

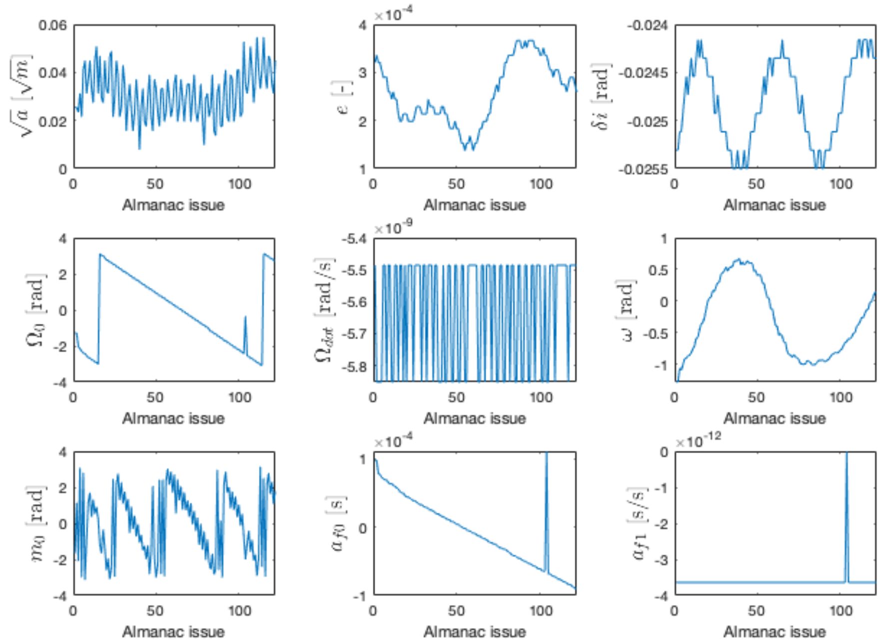

Figure D.4: Variation over time of the almanac parameters for SVID E03

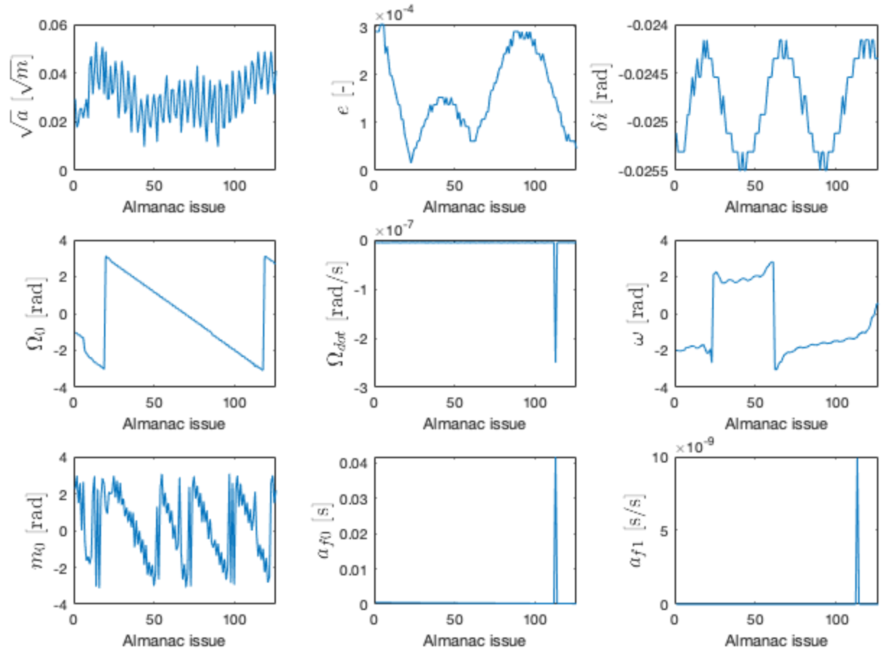

Figure D.5: Variation over time of the almanac parameters for SVID E05

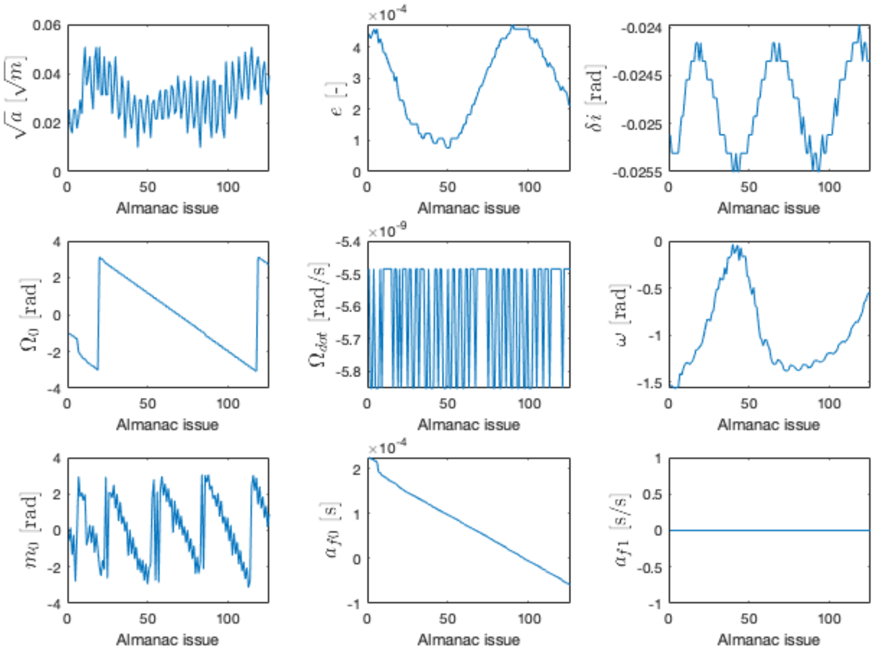

Figure D.6: Variation over time of the almanac parameters for SVID E07

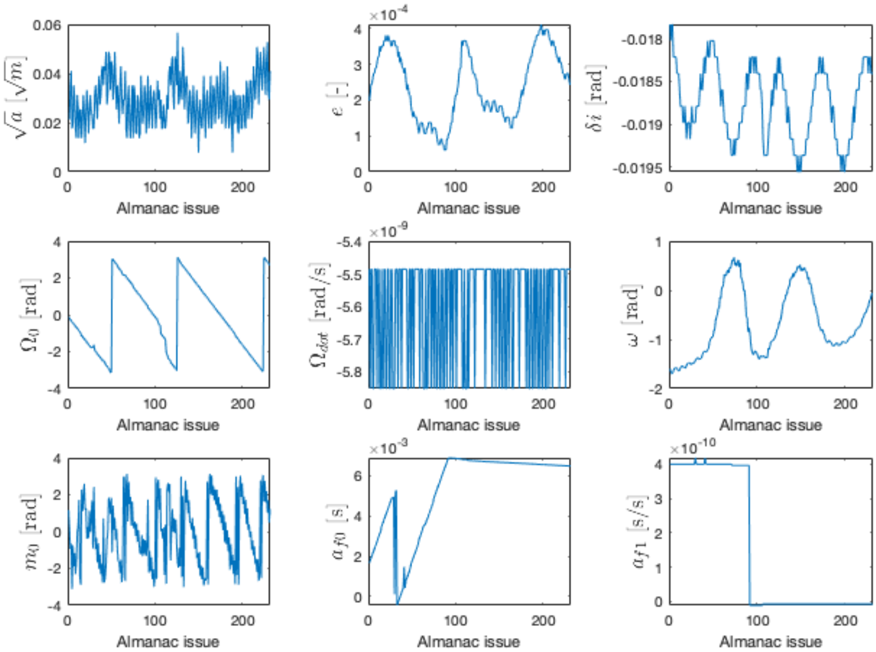

Figure D.7: Variation over time of the almanac parameters for SVID E08

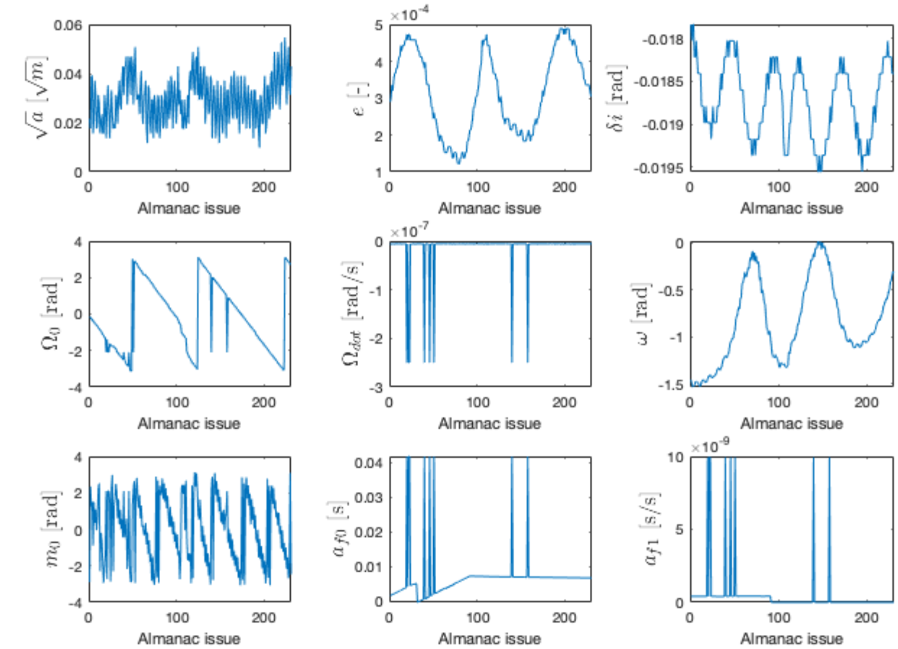

Figure D.8: Variation over time of the almanac parameters for SVID E09

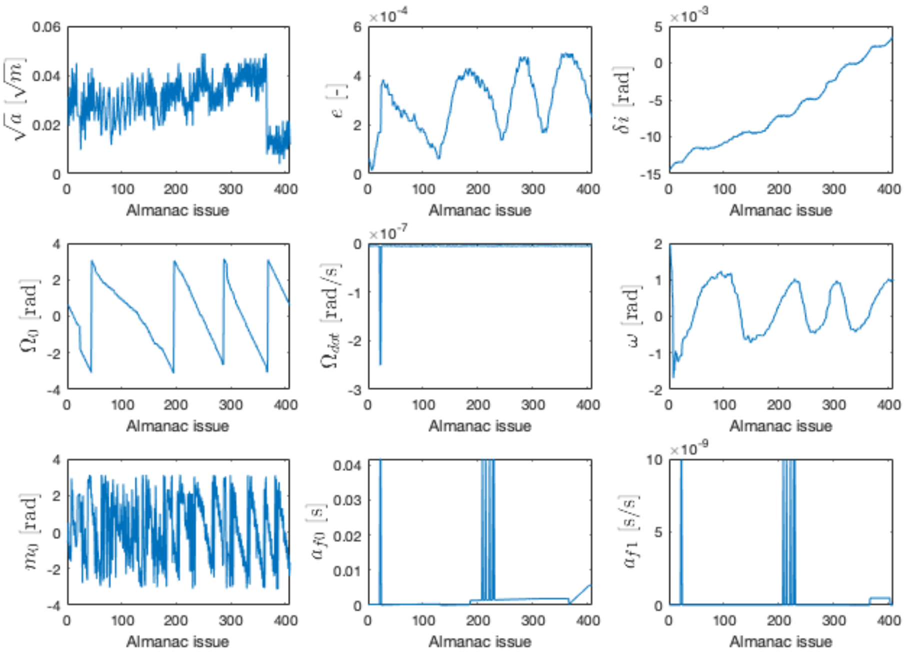

Figure D.9: Variation over time of the almanac parameters for SVID E11

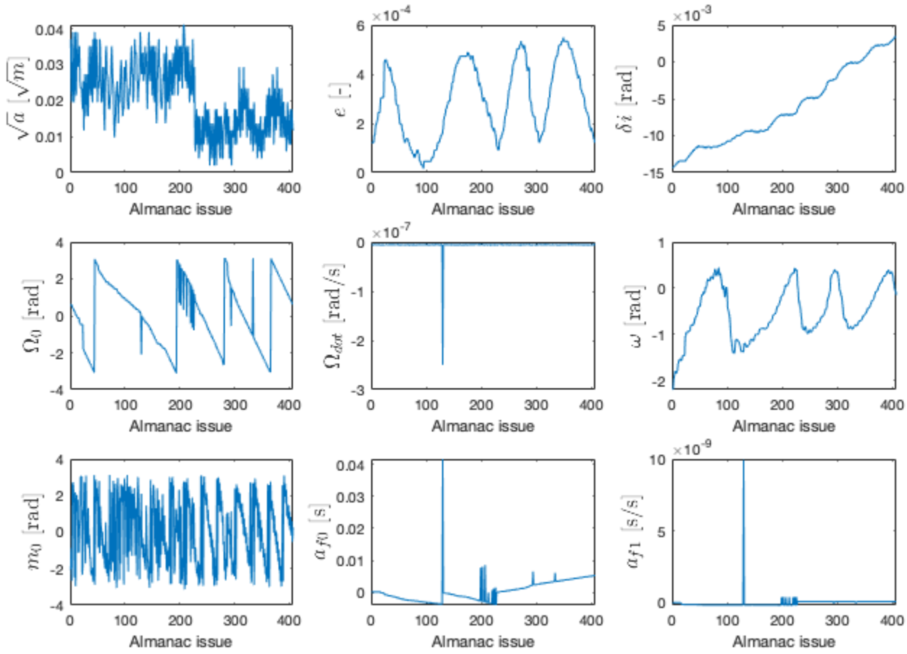

Figure D.10: Variation over time of the almanac parameters for SVID E12

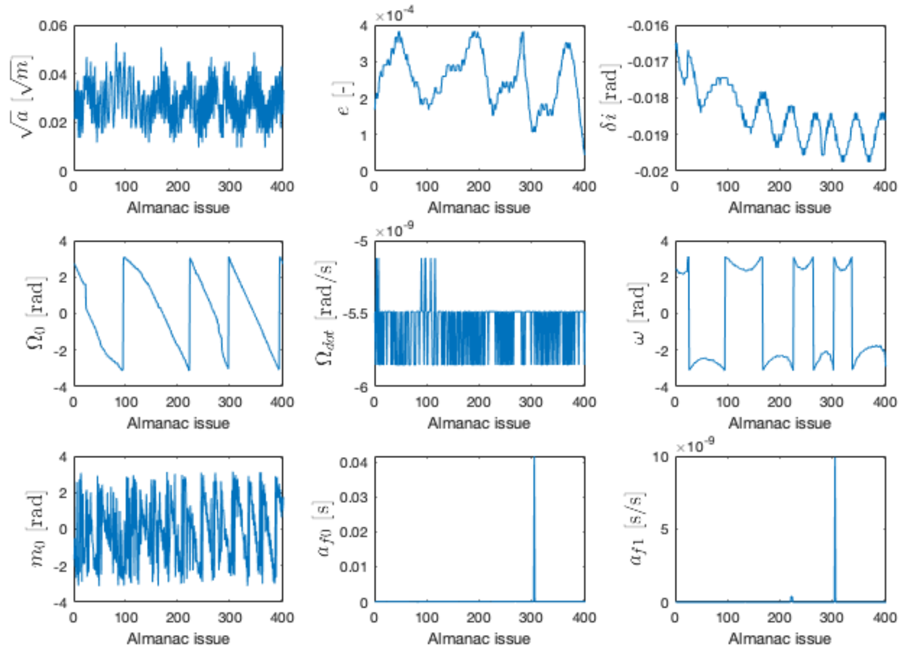

Figure D.11: Variation over time of the almanac parameters for SVID E19

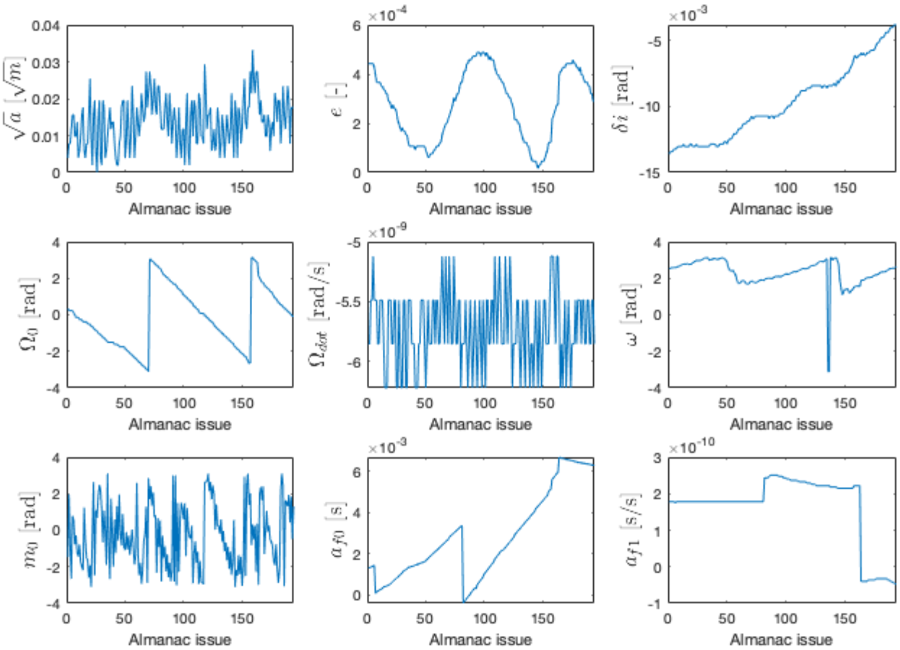

Figure D.12: Variation over time of the almanac parameters for SVID E22

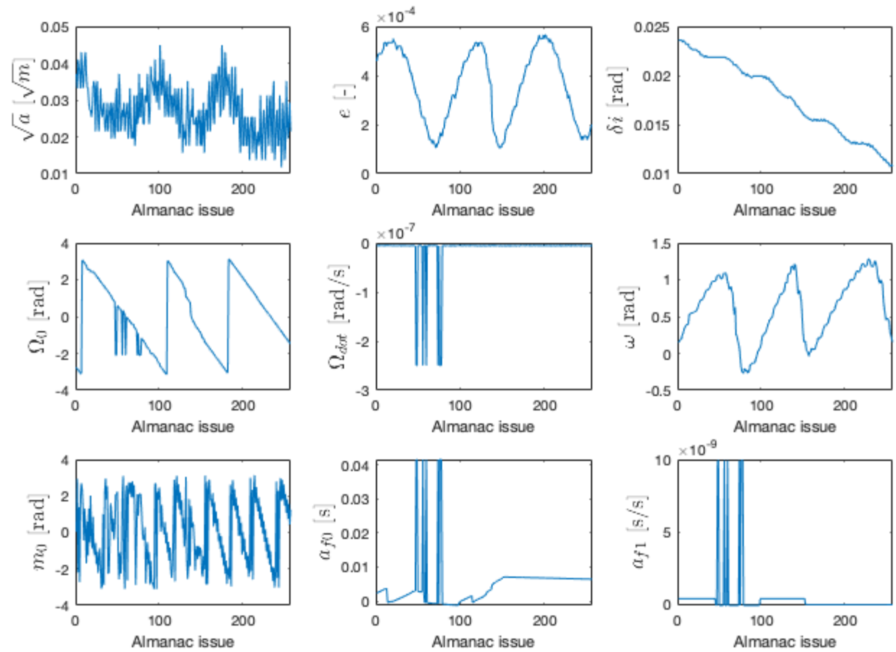

Figure D.13: Variation over time of the almanac parameters for SVID E24

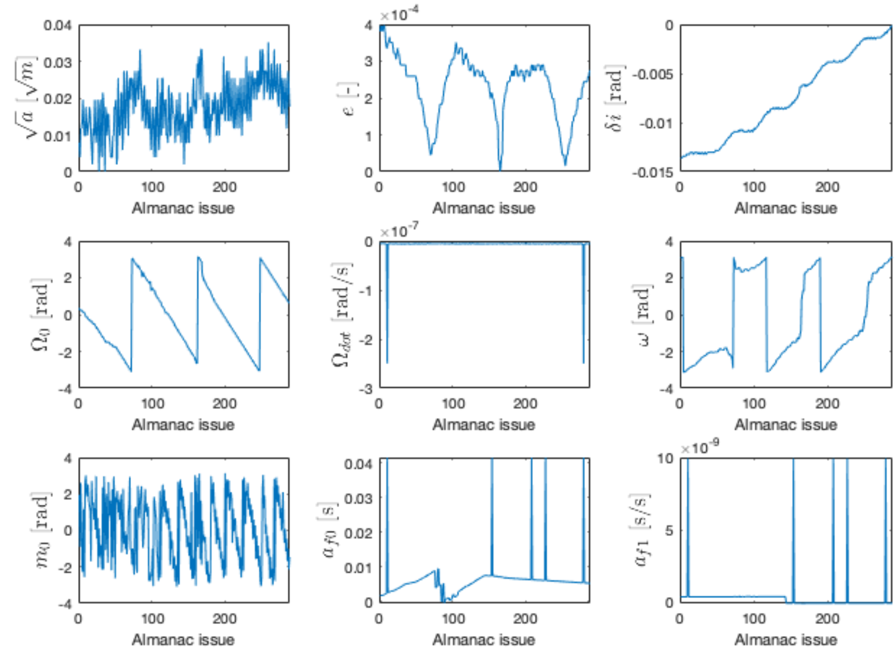

Figure D.14: Variation over time of the almanac parameters for SVID E26

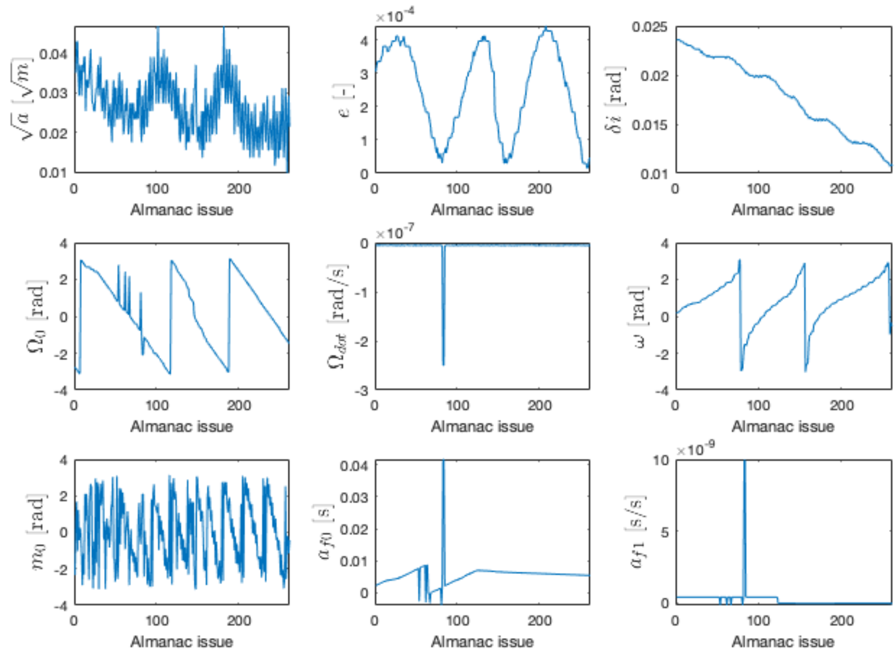

Figure D.15: Variation over time of the almanac parameters for SVID E30

Table D.2: Overview of the constructed optimal sets in terms of size, SISRE and parameter bit allocation

Size	SISRE	$\sqrt{a}$	e	i_0	Ω_0	ω	m_0	Δn	$\dot{\Omega}$	i_{dot}	C_{rc}	C_{rs}	C_{uc}	C_{us}	a_{f0}	a_{f1}
[bits]	[m]	**Allocated bits/Scale factor**														
105	33.96	$3/2^{-7}$	$6/2^{-19}$	$7/2^{-19}$	$16/2^{-19}$	$20/2^{-20}$	$23/2^{-22}$	$4/2^{-31}$	0/-	0/-	$4/2^{7}$	$4/2^{7}$	0/-	$4/2^{-17}$	$11/2^{-21}$	0/-
106	28.89	$4/2^{-8}$	$6/2^{-19}$	$7/2^{-19}$	$16/2^{-19}$	$19/2^{-19}$	$21/2^{-20}$	$4/2^{-31}$	0/-	0/-	$5/2^{6}$	$5/2^{6}$	0/-	$4/2^{-17}$	$12/2^{-22}$	0/-
107	27.50	$4/2^{-8}$	$6/2^{-19}$	$7/2^{-19}$	$16/2^{-19}$	$20/2^{-20}$	$21/2^{-20}$	$4/2^{-31}$	0/-	0/-	$5/2^{6}$	$5/2^{6}$	0/-	$4/2^{-17}$	$12/2^{-22}$	0/-
108	26.35	$4/2^{-8}$	$6/2^{-19}$	$8/2^{-20}$	$16/2^{-19}$	$20/2^{-20}$	$21/2^{-20}$	$4/2^{-31}$	0/-	0/-	$5/2^{6}$	$5/2^{6}$	0/-	$4/2^{-17}$	$12/2^{-22}$	0/-
109	24.94	$4/2^{-8}$	$6/2^{-19}$	$8/2^{-20}$	$16/2^{-19}$	$20/2^{-20}$	$21/2^{-20}$	$5/2^{-32}$	0/-	0/-	$5/2^{6}$	$5/2^{6}$	0/-	$4/2^{-17}$	$12/2^{-22}$	0/-
110	22.79	$4/2^{-8}$	$6/2^{-19}$	$8/2^{-20}$	$16/2^{-19}$	$20/2^{-20}$	$21/2^{-20}$	$5/2^{-32}$	0/-	0/-	$5/2^{6}$	$5/2^{6}$	0/-	$5/2^{-18}$	$12/2^{-22}$	0/-
111	22.75	$4/2^{-8}$	$7/2^{-20}$	$8/2^{-20}$	$16/2^{-19}$	$20/2^{-20}$	$21/2^{-20}$	$4/2^{-31}$	0/-	0/-	$5/2^{6}$	$5/2^{6}$	0/-	$6/2^{-19}$	$12/2^{-22}$	0/-
112	22.64	$4/2^{-8}$	$6/2^{-19}$	$7/2^{-19}$	$16/2^{-19}$	$21/2^{-21}$	$21/2^{-20}$	$5/2^{-32}$	0/-	0/-	$6/2^{5}$	$5/2^{6}$	0/-	$6/2^{-19}$	$12/2^{-22}$	0/-
113	21.16	$4/2^{-8}$	$7/2^{-20}$	$8/2^{-20}$	$17/2^{-20}$	$21/2^{-21}$	$22/2^{-21}$	$5/2^{-32}$	0/-	0/-	$5/2^{6}$	$5/2^{6}$	0/-	$4/2^{-17}$	$12/2^{-22}$	0/-
114	18.58	$4/2^{-8}$	$7/2^{-20}$	$8/2^{-20}$	$17/2^{-20}$	$21/2^{-21}$	$22/2^{-21}$	$5/2^{-32}$	0/-	0/-	$5/2^{6}$	$5/2^{6}$	0/-	$5/2^{-18}$	$12/2^{-22}$	0/-
115	18.33	$4/2^{-8}$	$8/2^{-21}$	$8/2^{-20}$	$17/2^{-20}$	$21/2^{-21}$	$22/2^{-21}$	$5/2^{-32}$	0/-	0/-	$5/2^{6}$	$5/2^{6}$	0/-	$5/2^{-18}$	$12/2^{-22}$	0/-
116	17.52	$4/2^{-8}$	$7/2^{-20}$	$8/2^{-20}$	$17/2^{-20}$	$22/2^{-22}$	$22/2^{-21}$	$5/2^{-32}$	0/-	0/-	$5/2^{6}$	$5/2^{6}$	0/-	$6/2^{-19}$	$12/2^{-22}$	0/-
117	17.40	$4/2^{-8}$	$7/2^{-20}$	$8/2^{-20}$	$17/2^{-20}$	$22/2^{-22}$	$23/2^{-22}$	$5/2^{-32}$	0/-	0/-	$5/2^{6}$	$5/2^{6}$	0/-	$6/2^{-19}$	$12/2^{-22}$	0/-
118	16.86	$4/2^{-8}$	$7/2^{-20}$	$8/2^{-20}$	$17/2^{-20}$	$22/2^{-22}$	$23/2^{-22}$	$6/2^{-33}$	0/-	0/-	$5/2^{6}$	$5/2^{6}$	0/-	$6/2^{-19}$	$12/2^{-22}$	0/-
119	16.41	$4/2^{-8}$	$7/2^{-20}$	$8/2^{-20}$	$18/2^{-21}$	$22/2^{-22}$	$23/2^{-22}$	$6/2^{-33}$	0/-	0/-	$5/2^{6}$	$5/2^{6}$	0/-	$6/2^{-19}$	$12/2^{-22}$	0/-
120	16.33	$5/2^{-9}$	$7/2^{-20}$	$9/2^{-21}$	$18/2^{-21}$	$21/2^{-21}$	$22/2^{-21}$	$6/2^{-33}$	0/-	0/-	$5/2^{6}$	$5/2^{6}$	0/-	$7/2^{-20}$	$12/2^{-22}$	0/-
121	15.23	$5/2^{-9}$	$7/2^{-20}$	$9/2^{-21}$	$17/2^{-20}$	$21/2^{-21}$	$22/2^{-21}$	$6/2^{-33}$	0/-	0/-	$6/2^{5}$	$6/2^{5}$	0/-	$6/2^{-19}$	$13/2^{-23}$	0/-
122	15.13	$5/2^{-9}$	$7/2^{-20}$	$9/2^{-21}$	$17/2^{-20}$	$21/2^{-21}$	$23/2^{-22}$	$6/2^{-33}$	0/-	0/-	$6/2^{5}$	$6/2^{5}$	0/-	$6/2^{-19}$	$13/2^{-23}$	0/-
123	15.02	$5/2^{-9}$	$8/2^{-21}$	$10/2^{-22}$	$17/2^{-20}$	$21/2^{-21}$	$22/2^{-21}$	$5/2^{-32}$	0/-	0/-	$6/2^{5}$	$6/2^{5}$	0/-	$7/2^{-20}$	$13/2^{-23}$	0/-
124	14.19	$4/2^{-8}$	$7/2^{-20}$	$9/2^{-21}$	$18/2^{-21}$	$22/2^{-22}$	$23/2^{-22}$	$5/2^{-32}$	0/-	0/-	$5/2^{6}$	$5/2^{6}$	$5/2^{-18}$	$6/2^{-19}$	$12/2^{-22}$	0/-
125	13.79	$5/2^{-9}$	$7/2^{-20}$	$9/2^{-21}$	$17/2^{-20}$	$21/2^{-21}$	$22/2^{-21}$	$5/2^{-32}$	0/-	0/-	$6/2^{5}$	$6/2^{5}$	$5/2^{-18}$	$6/2^{-19}$	$13/2^{-23}$	0/-
126	13.75	$4/2^{-8}$	$7/2^{-20}$	$10/2^{-22}$	$18/2^{-21}$	$21/2^{-21}$	$22/2^{-21}$	$5/2^{-32}$	0/-	0/-	$5/2^{6}$	$5/2^{6}$	$7/2^{-20}$	$7/2^{-20}$	$12/2^{-22}$	0/-
127	12.79	$4/2^{-8}$	$7/2^{-20}$	$9/2^{-21}$	$18/2^{-21}$	$21/2^{-21}$	$23/2^{-22}$	$7/2^{-34}$	0/-	0/-	$5/2^{6}$	$5/2^{6}$	$7/2^{-20}$	$6/2^{-19}$	$12/2^{-22}$	0/-
128	12.74	$4/2^{-8}$	$7/2^{-20}$	$9/2^{-21}$	$18/2^{-21}$	$21/2^{-21}$	$23/2^{-22}$	$7/2^{-34}$	0/-	0/-	$5/2^{6}$	$5/2^{6}$	$7/2^{-20}$	$7/2^{-20}$	$12/2^{-22}$	0/-
129	12.26	$5/2^{-9}$	$7/2^{-20}$	$9/2^{-21}$	$18/2^{-21}$	$21/2^{-21}$	$22/2^{-21}$	$7/2^{-34}$	0/-	0/-	$6/2^{5}$	$6/2^{5}$	$7/2^{-20}$	$5/2^{-18}$	$13/2^{-23}$	0/-

Continued on next page

Table D.2 – continued from previous page

Size	SISRE	$\sqrt{a}$	e	i_0	Ω_0	ω	m_0	Δn	$\dot{\Omega}$	i_{dot}	C_{rc}	C_{rs}	C_{uc}	C_{us}	a_{f0}	a_{f1}
130	12.06	$4/2^{-8}$	$8/2^{-21}$	$10/2^{-22}$	$18/2^{-21}$	$21/2^{-21}$	$23/2^{-22}$	$6/2^{-33}$	0/-	0/-	$5/2^{6}$	$5/2^{6}$	$6/2^{-19}$	$6/2^{-19}$	$12/2^{-22}$	$3/2^{-40}$
131	10.80	$5/2^{-9}$	$7/2^{-20}$	$9/2^{-21}$	$18/2^{-21}$	$22/2^{-22}$	$22/2^{-21}$	$7/2^{-34}$	0/-	0/-	$6/2^{5}$	$6/2^{5}$	$6/2^{-19}$	$7/2^{-20}$	$13/2^{-23}$	0/-
132	10.04	$5/2^{-9}$	$8/2^{-21}$	$9/2^{-21}$	$18/2^{-21}$	$22/2^{-22}$	$23/2^{-22}$	$6/2^{-33}$	0/-	0/-	$6/2^{5}$	$6/2^{5}$	$6/2^{-19}$	$7/2^{-20}$	$13/2^{-23}$	0/-
133	9.67	$5/2^{-9}$	$8/2^{-21}$	$9/2^{-21}$	$18/2^{-21}$	$22/2^{-22}$	$23/2^{-22}$	$6/2^{-33}$	0/-	0/-	$6/2^{5}$	$6/2^{5}$	$5/2^{-18}$	$6/2^{-19}$	$13/2^{-23}$	$3/2^{-40}$
134	9.55	$5/2^{-9}$	$7/2^{-20}$	$9/2^{-21}$	$18/2^{-21}$	$21/2^{-21}$	$24/2^{-23}$	$6/2^{-33}$	0/-	0/-	$6/2^{5}$	$7/2^{4}$	$6/2^{-19}$	$6/2^{-19}$	$13/2^{-23}$	$3/2^{-40}$
135	9.25	$6/2^{-10}$	$7/2^{-20}$	$10/2^{-22}$	$18/2^{-21}$	$21/2^{-21}$	$23/2^{-22}$	$6/2^{-33}$	0/-	0/-	$6/2^{5}$	$6/2^{5}$	$7/2^{-20}$	$6/2^{-19}$	$13/2^{-23}$	$3/2^{-40}$
136	8.60	$5/2^{-9}$	$8/2^{-21}$	$9/2^{-21}$	$18/2^{-21}$	$22/2^{-22}$	$22/2^{-21}$	$7/2^{-34}$	0/-	0/-	$6/2^{5}$	$6/2^{5}$	$7/2^{-20}$	$7/2^{-20}$	$13/2^{-23}$	$3/2^{-40}$
137	8.48	$5/2^{-9}$	$8/2^{-21}$	$10/2^{-22}$	$18/2^{-21}$	$21/2^{-21}$	$23/2^{-22}$	$8/2^{-35}$	0/-	0/-	$6/2^{5}$	$6/2^{5}$	$6/2^{-19}$	$7/2^{-20}$	$13/2^{-23}$	$3/2^{-40}$
138	8.28	$5/2^{-9}$	$8/2^{-21}$	$10/2^{-22}$	$18/2^{-21}$	$22/2^{-22}$	$22/2^{-21}$	$7/2^{-34}$	0/-	0/-	$6/2^{5}$	$7/2^{4}$	$7/2^{-20}$	$7/2^{-20}$	$13/2^{-23}$	$3/2^{-40}$
139	7.86	$5/2^{-9}$	$8/2^{-21}$	$10/2^{-22}$	$18/2^{-21}$	$22/2^{-22}$	$23/2^{-22}$	$7/2^{-34}$	0/-	0/-	$6/2^{5}$	$7/2^{4}$	$7/2^{-20}$	$7/2^{-20}$	$13/2^{-23}$	$3/2^{-40}$
140	7.82	$5/2^{-9}$	$8/2^{-21}$	$10/2^{-22}$	$18/2^{-21}$	$22/2^{-22}$	$23/2^{-22}$	$7/2^{-34}$	0/-	0/-	$7/2^{4}$	$6/2^{5}$	$7/2^{-20}$	$8/2^{-21}$	$13/2^{-23}$	$3/2^{-40}$
141	7.44	$5/2^{-9}$	$8/2^{-21}$	$10/2^{-22}$	$19/2^{-22}$	$22/2^{-22}$	$24/2^{-23}$	$6/2^{-33}$	0/-	0/-	$6/2^{5}$	$6/2^{5}$	$7/2^{-20}$	$7/2^{-20}$	$13/2^{-23}$	$5/2^{-41}$
142	7.41	$5/2^{-9}$	$8/2^{-21}$	$10/2^{-22}$	$18/2^{-21}$	$22/2^{-22}$	$23/2^{-22}$	$7/2^{-34}$	0/-	0/-	$7/2^{4}$	$6/2^{5}$	$7/2^{-20}$	$8/2^{-21}$	$13/2^{-23}$	$5/2^{-41}$
143	7.27	$5/2^{-9}$	$8/2^{-21}$	$10/2^{-22}$	$18/2^{-21}$	$22/2^{-22}$	$23/2^{-22}$	$7/2^{-34}$	0/-	0/-	$7/2^{4}$	$6/2^{5}$	$7/2^{-20}$	$8/2^{-21}$	$13/2^{-23}$	$6/2^{-42}$
144	6.88	$5/2^{-9}$	$8/2^{-21}$	$10/2^{-22}$	$18/2^{-21}$	$22/2^{-22}$	$24/2^{-23}$	$7/2^{-34}$	$2/2^{-33}$	0/-	$6/2^{5}$	$6/2^{5}$	$8/2^{-21}$	$7/2^{-20}$	$13/2^{-23}$	$5/2^{-41}$
145	6.73	$5/2^{-9}$	$9/2^{-22}$	$10/2^{-22}$	$20/2^{-23}$	$22/2^{-22}$	$23/2^{-22}$	$8/2^{-35}$	0/-	0/-	$6/2^{5}$	$6/2^{5}$	$7/2^{-20}$	$7/2^{-20}$	$13/2^{-23}$	$6/2^{-42}$
146	6.60	$5/2^{-9}$	$8/2^{-21}$	$9/2^{-21}$	$19/2^{-22}$	$22/2^{-22}$	$24/2^{-23}$	$7/2^{-34}$	0/-	$4/2^{-33}$	$6/2^{5}$	$6/2^{5}$	$7/2^{-20}$	$7/2^{-20}$	$13/2^{-23}$	$6/2^{-42}$
147	6.39	$6/2^{-10}$	$8/2^{-21}$	$10/2^{-22}$	$19/2^{-22}$	$23/2^{-23}$	$23/2^{-22}$	$6/2^{-33}$	0/-	0/-	$7/2^{4}$	$7/2^{4}$	$8/2^{-21}$	$8/2^{-21}$	$14/2^{-24}$	$5/2^{-41}$
148	6.33	$5/2^{-9}$	$8/2^{-21}$	$10/2^{-22}$	$18/2^{-21}$	$23/2^{-23}$	$23/2^{-22}$	$7/2^{-34}$	0/-	$5/2^{-34}$	$7/2^{4}$	$6/2^{5}$	$7/2^{-20}$	$8/2^{-21}$	$13/2^{-23}$	$5/2^{-41}$
149	5.83	$5/2^{-9}$	$8/2^{-21}$	$10/2^{-22}$	$19/2^{-22}$	$22/2^{-22}$	$24/2^{-23}$	$7/2^{-34}$	0/-	$5/2^{-34}$	$6/2^{5}$	$7/2^{4}$	$7/2^{-20}$	$8/2^{-21}$	$13/2^{-23}$	$5/2^{-41}$
150	5.61	$6/2^{-10}$	$9/2^{-22}$	$10/2^{-22}$	$19/2^{-22}$	$23/2^{-23}$	$23/2^{-22}$	$7/2^{-34}$	$2/2^{-33}$	0/-	$7/2^{4}$	$7/2^{4}$	$7/2^{-20}$	$7/2^{-20}$	$14/2^{-24}$	$6/2^{-42}$
151	5.25	$6/2^{-10}$	$9/2^{-22}$	$10/2^{-22}$	$19/2^{-22}$	$22/2^{-22}$	$23/2^{-22}$	$7/2^{-34}$	0/-	$4/2^{-33}$	$7/2^{4}$	$7/2^{4}$	$7/2^{-20}$	$7/2^{-20}$	$14/2^{-24}$	$6/2^{-42}$
152	4.99	$6/2^{-10}$	$8/2^{-21}$	$10/2^{-22}$	$19/2^{-22}$	$22/2^{-22}$	$24/2^{-23}$	$7/2^{-34}$	0/-	$5/2^{-34}$	$7/2^{4}$	$7/2^{4}$	$8/2^{-21}$	$7/2^{-20}$	$14/2^{-24}$	$5/2^{-41}$
153	4.85	$6/2^{-10}$	$8/2^{-21}$	$10/2^{-22}$	$19/2^{-22}$	$22/2^{-22}$	$24/2^{-23}$	$7/2^{-34}$	0/-	$5/2^{-34}$	$8/2^{3}$	$7/2^{4}$	$8/2^{-21}$	$7/2^{-20}$	$14/2^{-24}$	$5/2^{-41}$
154	4.76	$6/2^{-10}$	$8/2^{-21}$	$10/2^{-22}$	$19/2^{-22}$	$23/2^{-23}$	$24/2^{-23}$	$7/2^{-34}$	$2/2^{-33}$	$4/2^{-33}$	$8/2^{3}$	$7/2^{4}$	$7/2^{-20}$	$7/2^{-20}$	$14/2^{-24}$	$5/2^{-41}$
155	4.29	$6/2^{-10}$	$9/2^{-22}$	$10/2^{-22}$	$20/2^{-23}$	$23/2^{-23}$	$24/2^{-23}$	$7/2^{-34}$	0/-	$5/2^{-34}$	$7/2^{4}$	$7/2^{4}$	$7/2^{-20}$	$8/2^{-21}$	$14/2^{-24}$	$5/2^{-41}$
156	4.17	$6/2^{-10}$	$9/2^{-22}$	$10/2^{-22}$	$20/2^{-23}$	$23/2^{-23}$	$24/2^{-23}$	$8/2^{-35}$	0/-	$5/2^{-34}$	$7/2^{4}$	$7/2^{4}$	$7/2^{-20}$	$8/2^{-21}$	$14/2^{-24}$	$5/2^{-41}$

Continued on next page

Table D.2 – continued from previous page

Size	SISRE	$\sqrt{a}$	e	i_0	Ω_0	ω	m_0	Δn	$\dot{\Omega}$	i_{dot}	C_{rc}	C_{rs}	C_{uc}	C_{us}	a_{f0}	a_{f1}
157	4.15	$6/2^{-10}$	$9/2^{-22}$	$11/2^{-23}$	$20/2^{-23}$	$22/2^{-22}$	$24/2^{-23}$	$7/2^{-34}$	0/-	$5/2^{-34}$	$7/2^{4}$	$7/2^{4}$	$8/2^{-21}$	$8/2^{-21}$	$14/2^{-24}$	$6/2^{-42}$
158	4.04	$6/2^{-10}$	$9/2^{-22}$	$11/2^{-23}$	$20/2^{-23}$	$22/2^{-22}$	$24/2^{-23}$	$8/2^{-35}$	0/-	$5/2^{-34}$	$7/2^{4}$	$7/2^{4}$	$8/2^{-21}$	$8/2^{-21}$	$14/2^{-24}$	$6/2^{-42}$
159	3.95	$7/2^{-11}$	$8/2^{-21}$	$10/2^{-22}$	$19/2^{-22}$	$23/2^{-23}$	$25/2^{-24}$	$9/2^{-36}$	$3/2^{-34}$	$5/2^{-34}$	$7/2^{4}$	$7/2^{4}$	$7/2^{-20}$	$7/2^{-20}$	$14/2^{-24}$	$5/2^{-41}$
160	3.72	$6/2^{-10}$	$9/2^{-22}$	$10/2^{-22}$	$20/2^{-23}$	$23/2^{-23}$	$23/2^{-22}$	$8/2^{-35}$	$3/2^{-34}$	$5/2^{-34}$	$7/2^{4}$	$8/2^{3}$	$7/2^{-20}$	$8/2^{-21}$	$14/2^{-24}$	$6/2^{-42}$
161	3.27	$6/2^{-10}$	$9/2^{-22}$	$11/2^{-23}$	$19/2^{-22}$	$23/2^{-23}$	$25/2^{-24}$	$7/2^{-34}$	$3/2^{-34}$	$5/2^{-34}$	$7/2^{4}$	$7/2^{4}$	$9/2^{-22}$	$8/2^{-21}$	$14/2^{-24}$	$5/2^{-41}$
162	3.09	$6/2^{-10}$	$9/2^{-22}$	$11/2^{-23}$	$19/2^{-22}$	$23/2^{-23}$	$25/2^{-24}$	$8/2^{-35}$	$3/2^{-34}$	$5/2^{-34}$	$7/2^{4}$	$7/2^{4}$	$9/2^{-22}$	$8/2^{-21}$	$14/2^{-24}$	$5/2^{-41}$
163	3.04	$6/2^{-10}$	$9/2^{-22}$	$11/2^{-23}$	$19/2^{-22}$	$23/2^{-23}$	$24/2^{-23}$	$8/2^{-35}$	$5/2^{-35}$	$5/2^{-34}$	$7/2^{4}$	$7/2^{4}$	$9/2^{-22}$	$8/2^{-21}$	$14/2^{-24}$	$5/2^{-41}$
164	2.89	$6/2^{-10}$	$9/2^{-22}$	$11/2^{-23}$	$20/2^{-23}$	$23/2^{-23}$	$24/2^{-23}$	$8/2^{-35}$	$5/2^{-35}$	$5/2^{-34}$	$7/2^{4}$	$7/2^{4}$	$9/2^{-22}$	$8/2^{-21}$	$14/2^{-24}$	$5/2^{-41}$
165	2.84	$6/2^{-10}$	$9/2^{-22}$	$11/2^{-23}$	$20/2^{-23}$	$23/2^{-23}$	$24/2^{-23}$	$8/2^{-35}$	$5/2^{-35}$	$5/2^{-34}$	$7/2^{4}$	$7/2^{4}$	$9/2^{-22}$	$9/2^{-22}$	$14/2^{-24}$	$5/2^{-41}$
166	2.79	$6/2^{-10}$	$9/2^{-22}$	$11/2^{-23}$	$20/2^{-23}$	$23/2^{-23}$	$24/2^{-23}$	$9/2^{-36}$	$5/2^{-35}$	$5/2^{-34}$	$7/2^{4}$	$7/2^{4}$	$9/2^{-22}$	$9/2^{-22}$	$14/2^{-24}$	$5/2^{-41}$
167	2.68	$6/2^{-10}$	$9/2^{-22}$	$11/2^{-23}$	$20/2^{-23}$	$23/2^{-23}$	$24/2^{-23}$	$9/2^{-36}$	$5/2^{-35}$	$5/2^{-34}$	$7/2^{4}$	$7/2^{4}$	$9/2^{-22}$	$9/2^{-22}$	$14/2^{-24}$	$6/2^{-42}$
168	2.61	$6/2^{-10}$	$9/2^{-22}$	$12/2^{-24}$	$20/2^{-23}$	$23/2^{-23}$	$24/2^{-23}$	$9/2^{-36}$	$5/2^{-35}$	$5/2^{-34}$	$7/2^{4}$	$7/2^{4}$	$9/2^{-22}$	$9/2^{-22}$	$14/2^{-24}$	$6/2^{-42}$
169	2.37	$6/2^{-10}$	$10/2^{-23}$	$12/2^{-24}$	$20/2^{-23}$	$23/2^{-23}$	$25/2^{-24}$	$9/2^{-36}$	$3/2^{-34}$	$6/2^{-35}$	$7/2^{4}$	$7/2^{4}$	$9/2^{-22}$	$9/2^{-22}$	$14/2^{-24}$	$6/2^{-42}$
170	2.25	$6/2^{-10}$	$10/2^{-23}$	$12/2^{-24}$	$20/2^{-23}$	$24/2^{-24}$	$25/2^{-24}$	$9/2^{-36}$	$3/2^{-34}$	$6/2^{-35}$	$7/2^{4}$	$7/2^{4}$	$9/2^{-22}$	$9/2^{-22}$	$14/2^{-24}$	$6/2^{-42}$
171	2.24	$6/2^{-10}$	$9/2^{-22}$	$12/2^{-24}$	$20/2^{-23}$	$24/2^{-24}$	$25/2^{-24}$	$9/2^{-36}$	$5/2^{-35}$	$6/2^{-35}$	$7/2^{4}$	$7/2^{4}$	$9/2^{-22}$	$9/2^{-22}$	$14/2^{-24}$	$6/2^{-42}$
172	2.09	$6/2^{-10}$	$10/2^{-23}$	$12/2^{-24}$	$20/2^{-23}$	$24/2^{-24}$	$25/2^{-24}$	$9/2^{-36}$	$5/2^{-35}$	$6/2^{-35}$	$7/2^{4}$	$7/2^{4}$	$9/2^{-22}$	$9/2^{-22}$	$14/2^{-24}$	$6/2^{-42}$
173	2.04	$6/2^{-10}$	$10/2^{-23}$	$12/2^{-24}$	$20/2^{-23}$	$24/2^{-24}$	$25/2^{-24}$	$9/2^{-36}$	$6/2^{-36}$	$6/2^{-35}$	$7/2^{4}$	$7/2^{4}$	$9/2^{-22}$	$9/2^{-22}$	$14/2^{-24}$	$6/2^{-42}$
174	1.99	$6/2^{-10}$	$10/2^{-23}$	$12/2^{-24}$	$21/2^{-24}$	$24/2^{-24}$	$25/2^{-24}$	$9/2^{-36}$	$6/2^{-36}$	$6/2^{-35}$	$7/2^{4}$	$7/2^{4}$	$9/2^{-22}$	$9/2^{-22}$	$14/2^{-24}$	$6/2^{-42}$
175	1.97	$6/2^{-10}$	$10/2^{-23}$	$12/2^{-24}$	$21/2^{-24}$	$24/2^{-24}$	$25/2^{-24}$	$9/2^{-36}$	$6/2^{-36}$	$6/2^{-35}$	$7/2^{4}$	$7/2^{4}$	$9/2^{-22}$	$9/2^{-22}$	$14/2^{-24}$	$7/2^{-43}$
176	1.95	$6/2^{-10}$	$10/2^{-23}$	$12/2^{-24}$	$21/2^{-24}$	$25/2^{-25}$	$25/2^{-24}$	$9/2^{-36}$	$6/2^{-36}$	$6/2^{-35}$	$7/2^{4}$	$7/2^{4}$	$9/2^{-22}$	$9/2^{-22}$	$14/2^{-24}$	$7/2^{-43}$
177	1.82	$9/2^{-13}$	$9/2^{-22}$	$11/2^{-23}$	$21/2^{-24}$	$24/2^{-24}$	$25/2^{-24}$	$8/2^{-35}$	$5/2^{-35}$	$7/2^{-36}$	$8/2^{3}$	$8/2^{3}$	$8/2^{-21}$	$9/2^{-22}$	$15/2^{-25}$	$7/2^{-43}$
178	1.79	$9/2^{-13}$	$9/2^{-22}$	$11/2^{-23}$	$21/2^{-24}$	$24/2^{-24}$	$25/2^{-24}$	$8/2^{-35}$	$5/2^{-35}$	$7/2^{-36}$	$8/2^{3}$	$8/2^{3}$	$8/2^{-21}$	$10/2^{-23}$	$15/2^{-25}$	$7/2^{-43}$
179	1.77	$9/2^{-13}$	$10/2^{-23}$	$12/2^{-24}$	$20/2^{-23}$	$25/2^{-25}$	$24/2^{-23}$	$8/2^{-35}$	$6/2^{-36}$	$6/2^{-35}$	$8/2^{3}$	$8/2^{3}$	$8/2^{-21}$	$10/2^{-23}$	$15/2^{-25}$	$7/2^{-43}$
180	1.51	$7/2^{-11}$	$10/2^{-23}$	$13/2^{-25}$	$20/2^{-23}$	$25/2^{-25}$	$25/2^{-24}$	$10/2^{-37}$	$5/2^{-35}$	$6/2^{-35}$	$8/2^{3}$	$8/2^{3}$	$10/2^{-23}$	$9/2^{-22}$	$15/2^{-25}$	$6/2^{-42}$
181	1.45	$7/2^{-11}$	$10/2^{-23}$	$13/2^{-25}$	$20/2^{-23}$	$25/2^{-25}$	$25/2^{-24}$	$10/2^{-37}$	$5/2^{-35}$	$7/2^{-36}$	$8/2^{3}$	$8/2^{3}$	$10/2^{-23}$	$9/2^{-22}$	$15/2^{-25}$	$6/2^{-42}$
182	1.39	$7/2^{-11}$	$11/2^{-24}$	$13/2^{-25}$	$20/2^{-23}$	$25/2^{-25}$	$25/2^{-24}$	$10/2^{-37}$	$5/2^{-35}$	$7/2^{-36}$	$8/2^{3}$	$8/2^{3}$	$10/2^{-23}$	$9/2^{-22}$	$15/2^{-25}$	$6/2^{-42}$
183	1.37	$7/2^{-11}$	$12/2^{-25}$	$13/2^{-25}$	$20/2^{-23}$	$25/2^{-25}$	$25/2^{-24}$	$10/2^{-37}$	$5/2^{-35}$	$7/2^{-36}$	$8/2^{3}$	$8/2^{3}$	$10/2^{-23}$	$9/2^{-22}$	$15/2^{-25}$	$6/2^{-42}$

Continued on next page

Table D.2 – continued from previous page

Size	SISRE	$\sqrt{a}$	e	i_0	Ω_0	ω	m_0	Δn	$\dot{\Omega}$	i_{dot}	C_{rc}	C_{rs}	C_{uc}	C_{us}	a_{f0}	a_{f1}
184	1.31	$7/2^{-11}$	$12/2^{-25}$	$13/2^{-25}$	$20/2^{-23}$	$25/2^{-25}$	$25/2^{-24}$	$10/2^{-37}$	$6/2^{-36}$	$7/2^{-36}$	$8/2^{3}$	$8/2^{3}$	$10/2^{-23}$	$9/2^{-22}$	$15/2^{-25}$	$6/2^{-42}$
185	1.29	$8/2^{-12}$	$12/2^{-25}$	$12/2^{-24}$	$20/2^{-23}$	$24/2^{-24}$	$25/2^{-24}$	$10/2^{-37}$	$6/2^{-36}$	$8/2^{-37}$	$8/2^{3}$	$8/2^{3}$	$9/2^{-22}$	$10/2^{-23}$	$15/2^{-25}$	$7/2^{-43}$
186	1.26	$8/2^{-12}$	$12/2^{-25}$	$13/2^{-25}$	$20/2^{-23}$	$24/2^{-24}$	$25/2^{-24}$	$10/2^{-37}$	$6/2^{-36}$	$8/2^{-37}$	$8/2^{3}$	$8/2^{3}$	$9/2^{-22}$	$10/2^{-23}$	$15/2^{-25}$	$7/2^{-43}$
187	1.22	$8/2^{-12}$	$12/2^{-25}$	$13/2^{-25}$	$20/2^{-23}$	$25/2^{-25}$	$25/2^{-24}$	$10/2^{-37}$	$6/2^{-36}$	$8/2^{-37}$	$8/2^{3}$	$8/2^{3}$	$9/2^{-22}$	$10/2^{-23}$	$15/2^{-25}$	$7/2^{-43}$
188	1.16	$9/2^{-13}$	$10/2^{-23}$	$14/2^{-26}$	$21/2^{-24}$	$25/2^{-25}$	$25/2^{-24}$	$10/2^{-37}$	$7/2^{-37}$	$7/2^{-36}$	$8/2^{3}$	$8/2^{3}$	$9/2^{-22}$	$9/2^{-22}$	$15/2^{-25}$	$8/2^{-44}$
189	1.13	$9/2^{-13}$	$10/2^{-23}$	$14/2^{-26}$	$21/2^{-24}$	$25/2^{-25}$	$25/2^{-24}$	$10/2^{-37}$	$7/2^{-37}$	$8/2^{-37}$	$8/2^{3}$	$8/2^{3}$	$9/2^{-22}$	$9/2^{-22}$	$15/2^{-25}$	$8/2^{-44}$
190	1.12	$9/2^{-13}$	$11/2^{-24}$	$14/2^{-26}$	$21/2^{-24}$	$25/2^{-25}$	$26/2^{-25}$	$8/2^{-35}$	$6/2^{-36}$	$8/2^{-37}$	$9/2^{2}$	$9/2^{2}$	$9/2^{-22}$	$9/2^{-22}$	$16/2^{-26}$	$7/2^{-43}$
191	1.01	$8/2^{-12}$	$11/2^{-24}$	$14/2^{-26}$	$21/2^{-24}$	$24/2^{-24}$	$26/2^{-25}$	$10/2^{-37}$	$6/2^{-36}$	$6/2^{-35}$	$9/2^{2}$	$10/2^{1}$	$10/2^{-23}$	$9/2^{-22}$	$16/2^{-26}$	$8/2^{-44}$
192	0.91	$8/2^{-12}$	$11/2^{-24}$	$14/2^{-26}$	$21/2^{-24}$	$24/2^{-24}$	$26/2^{-25}$	$10/2^{-37}$	$6/2^{-36}$	$7/2^{-36}$	$9/2^{2}$	$10/2^{1}$	$10/2^{-23}$	$9/2^{-22}$	$16/2^{-26}$	$8/2^{-44}$
193	0.85	$8/2^{-12}$	$11/2^{-24}$	$14/2^{-26}$	$21/2^{-24}$	$25/2^{-25}$	$26/2^{-25}$	$10/2^{-37}$	$6/2^{-36}$	$7/2^{-36}$	$9/2^{2}$	$10/2^{1}$	$10/2^{-23}$	$9/2^{-22}$	$16/2^{-26}$	$8/2^{-44}$
194	0.81	$8/2^{-12}$	$11/2^{-24}$	$14/2^{-26}$	$21/2^{-24}$	$25/2^{-25}$	$26/2^{-25}$	$10/2^{-37}$	$6/2^{-36}$	$8/2^{-37}$	$9/2^{2}$	$10/2^{1}$	$10/2^{-23}$	$9/2^{-22}$	$16/2^{-26}$	$8/2^{-44}$
195	0.80	$8/2^{-12}$	$11/2^{-24}$	$14/2^{-26}$	$21/2^{-24}$	$26/2^{-26}$	$26/2^{-25}$	$10/2^{-37}$	$6/2^{-36}$	$8/2^{-37}$	$9/2^{2}$	$10/2^{1}$	$10/2^{-23}$	$9/2^{-22}$	$16/2^{-26}$	$8/2^{-44}$

Bibliography

Abracon. Standalone real time clocks (rtc), 2019. URL `https://abracon.com/product-lineup/timing-synchronization/standalone-real-time-clocks-rtc`. Last accessed: 2019-01-12.

David W Affens, Roy Dreibelbis, James E Mentall, and George Theodorakos. The distress alerting satellite system. *GPS World*, 2011.

M Anghileri, M Paonni, E Gkougkas, and B Eissfeller. Reduced navigation data for a fast first fix. In *Satellite Navigation Technologies and European Workshop on GNSS Signals and Signal Processing,(NAVITEC), 2012 6th ESA Workshop on*, pages 1–7. IEEE, 2012.

M Anghileri, M Paonni, D Fontanella, et al. Assessing gnss data message performance. *Inside GNSS*, (March/April):60–71, 2013.

Baseband Technologies. 28-day extended ephemeris, 2018. URL `http://basebandtech.com/wp-content/uploads/28-Day-Extended-Ephemeris.pdf`. Last accessed: 2018-12-12.

A Bensky. *Wireless positioning technologies and applications.* Artech House, 2016.

J W Betz, C R Cahn, P A Dafesh, C J Hegarty, K W Hudnut, A J Jones, R Keegan, K Kovach, L S Lenahan, and H H Ma. L1c signal design options. Technical report, MITRE CORP BEDFORD MA, 2006.

B Bhatta. *Global navigation satellite systems: insights into GPS, GLONASS, Galileo, Compass, and others.* BS Publications, 2010.

D Braunschvig, R L Garwin, and J C Marwell. Space diplomacy. *Foreign Affairs*, pages 156–164, 2003.

B Chan, O Al-Fanek, and K Van Dierendonck. Method and apparatus for providing a compact extended ephemeris package for gnss processing, March 6 2018. US Patent 9,910,159.

J T Curran. Personal conversations, 2018.

J Dow, R Neilan, and C Rizos. The international gnss service in a changing landscape of global navigation satellite systems. *Journal of geodesy*, 83(3-4):191–198, 2009.

European GNSS Agency. GNSS Market Report. Technical Report 4, European GNSS Agency, 2015.

European GNSS Agency. GNSS Market Report. Technical Report 5, European GNSS Agency, 2017.

European GNSS Open Service. Signal-in-Space Interface Control Document. Technical report, European GNSS Open Service, 2016.

EGCS European GNSS Service Centre. Almanac data, 2018. URL `https://www.gsc-europa.eu/system-status/almanac-data`. Last accessed: 2018-12-09.

M Forin-Wiart, P Hubert, P Sirguey, and M Poulle. Performance and accuracy of lightweight and low-cost gps data loggers according to antenna positions, fix intervals, habitats and animal movements. *PLoS One*, 10 (6):e0129271, 2015.

L Garin. Ephemeris extension method for gnss applications, June 16 2009. US Patent 7,548,200.

Global Positioning Systems Directorate. NAVSTAR GPS Space Segment/Navigation User Segment Interfaces. Technical Report H, Global Positioning Systems Directorate, 2015.

T Grelier and L Ries. Gnss radio signal with an improved navigation message, March 1 2016. US Patent 9,274,227.

W He, E L Tan, E W Lee, and T Li. A solution for integrated track and trace in supply chain based on rfid & gps. In *Emerging Technologies & Factory Automation, 2009. ETFA 2009. IEEE Conference on*, pages 1–6. IEEE, 2009.

I F Hernández, V Rijmen, G S Granados, J Simón, I Rodríguez, and J D Calle. Design drivers, solutions and robustness assessment of navigation message authentication for the galileo open service. In *Proceedings of the ION IEEE+ meeting*, 2014.

E Kaplan and C Hegarty. *Understanding GPS: principles and applications*. Artech house, 2005.

Maxim Integrated. ±5ppm, i2c real-time clock, 2019. URL `https://www.maximintegrated.com/en/products/digital/real-time-clocks/DS3231M.html`. Last accessed: 2019-01-12.

O Montenbruck, P Steigenberger, R Khachikyan, G Weber, RB Langley, L Mervart, and U Hugentobler. Igs-mgex: preparing the ground for multi-constellation gnss science. *Inside Gnss*, 9(1):42–49, 2014.

O Montenbruck, P Steigenberger, and A Hauschild. Broadcast versus precise ephemerides: a multi-gnss perspective. *GPS solutions*, 19(2):321–333, 2015.

O Montenbruck, P Steigenberger, and A Hauschild. Multi-gnss signal-in-space range error assessment - methodology and results. *Advances in Space Research*, 61(12):3020–3038, 2018.

Network Time Foundation. Ntp: the network time protocol, 2018. URL `http://www.ntp.org`. Last accessed: 2019-01-12.

OECD. *Information Technology Outlook 2000: ICTs, E-commerce and the Information Economy*. Organisation for Economic Co-operation and Development, 2000.

M Paonni, M Anghileri, S Wallner, J Avila-Rodriguez, and B Eissfeller. Performance assessment of gnss signals in terms of time to first fix for cold, warm and hot start. In *Proceedings of the international technical meeting of the institute of navigation ION-ITM*, pages 25–27, 2010.

B Parhami. *Computer arithmetic*. Oxford university press, 1999.

Jun-jie Peng. A survey of location based service for galileo system. In *Computer Science and Computational Technology, 2008. ISCSCT'08. International Symposium on*, volume 1, pages 737–741. IEEE, 2008.

B W Remondi. Computing satellite velocity using the broadcast ephemeris. *GPS solutions*, 8(3):181–183, 2004.

Jochen Schiller and Agnès Voisard. *Location-based services*. Elsevier, 2004.

A Simsky and F Boon. Galileo integrity concept-user level. *The Technical University of Munich, Septentrio, Munich*, 2010.

Statista. Euro (eur) to u.s. dollar (usd) annual average exchange rate from 1999 to 2017, 2018. URL `https://www.statista.com/statistics/412794/euro-to-u-s-dollar-annual-average-exchange-rate/`. Last accessed: 2018-05-30.

STMicroelectronics. Serial i2c bus real-time clock (rtc) with battery switch over, 2018. URL `https://www.st.com/en/clocks-and-timers/m41t83.html`. Last accessed: 2019-01-12.

P Teunissen and O Montenbruck. *Springer handbook of global navigation satellite systems*. Springer, 2017.

H L Trautenberg. Method for the transmission of additional data along with navigation messages in a satellite navigation system, June 25 2013. US Patent 8,473,210.

U-blox. Neo-m8 u-blox m8 concurrent gnss modules – data sheet, 2018. URL `https://www.u-blox.com/sites/default/files/NEO-M8-FW3_DataSheet_28UBX-1503108629.pdf`. Last accessed: 2019-01-12.

D A Vallado. *Fundamentals of astrodynamics and applications*, volume 12. Springer Science & Business Media, 2001.

D A Vallado. Covariance transformations for satellite flight dynamics operations. *AAS/AIAA Astrodynamics Specialist Conference*, 03(526), 2003.

D Warren and J Raquet. Broadcast vs. precise gps ephemerides: a historical perspective. *GPS Solutions*, 7(3): 151–156, 2003.

IGS RINEX WG and RTCM-SC104. Rinex – the receiver independent exchange format, version 3.03, 14 july 2015., 2015. URL `ftp://igs.org/pub/data/format/rinex303.pdf`. Last accessed: 2018-05-30.

J Williams. Lvlh transformations. 2014.

Y Zhou, Y Meng, X Tao, L Wang, and Z Su. Gnss message structure optimization. In *China Satellite Navigation Conference (CSNC) 2014 Proceedings: Volume II*, pages 15–24. Springer, 2014.